



FHV
Vorarlberg University
of Applied Sciences

Near-Real-Time Demand Side Management of Battery-electric Vehicle Charging Stations in Residential Complexes of Vorarlberg using Methods of linear and stochastic Optimization

Master Thesis

Submitted in Fulfillment of the Degree

Master of Science in Engineering

Vorarlberg University of Applied Sciences
Sustainable Energy Systems

Submitted to

Dr. Klaus Rheinberger

Handed in by

Dipl.-Ing. (FH) Albert Ulmer, BSc, MA

Dornbirn, August 11th 2022

Statuary Declaration

I declare that I have developed and written the enclosed work completely by myself, and have not used sources or means without declaration in the text. Any thoughts from others or literal quotations are clearly marked. This Master Thesis was not used in the same or in a similar version to achieve an academic degree nor has it been published elsewhere.

Dornbirn, August 11th 2022 Dipl.-Ing. (FH) Albert Ulmer, BSc, MA

Abstract

Near-Real-Time Demand Side Management of Battery-electric Vehicle Charging Stations in Residential Complexes of Vorarlberg using Methods of linear and stochastic Optimization

The number of electric vehicles will increase rapidly in the coming years. Studies suggest that most owners prefer to charge their electric vehicle at home, which will fuel the need for charging stations in residential complexes where vehicles can be charged overnight. Currently, there already are over 100 such residential complexes, with another 70 added every year in Vorarlberg alone.

In most existing residential complexes, however, the grid connections are not sufficient to charge all vehicles at the same time with maximum power. In addition, it is also desirable for grid operators and electricity producers that the power demand be as smooth and predictable as possible. To achieve this, ways to manage flexible loads need to be found, which can operate within the technical constraints.

Therefore, the most common scenarios how the load can be made grid-friendly with the help of optional battery storage and/or photovoltaics using optimization methods of linear and stochastic programming were examined. At the same time, the needs of the vehicle owners for charging comfort - namely to find their vehicles reliably charged at the time of their respective departure - were addressed by combining both objectives using suitable weights.

The algorithms determined were verified in practice on an existing Vlotte prototype installation. For this purpose, the necessary programs were implemented in Python, so that the data obtained during the test operation, which lasted one month, could be subjected to a well-founded analysis. In addition, simulation studies helped to further reveal the influence of PV and BESS sizing on the achievable optimums and confirm that advanced optimization algorithms such as the ones discussed are a vital contribution in reducing the charging stations' peak load while at the same time maintaining high satisfaction levels.

Keywords: Demand Side Management, Vorarlberg, Residential Complex, Charging Station, Linear Optimization, Stochastic Optimization, Peak Shaving, Charging Comfort, Computation Time

Kurzreferat

Quasi-Echtzeit Lastmanagement von Ladestationen für elektrische Fahrzeuge in Wohnanlagen Vorarlbergs mit Methoden der linearen und stochastischen Optimierung

Der Anteil von E-Autos wird in den kommenden Jahren rasant zunehmen. Damit einher geht der Bedarf an Ladestationen in Wohnanlagen, an welchen die Fahrzeuge über Nacht aufgeladen werden können.

Die vorhandenen Anschlussleistungen reichen in den meisten Bestandsanlagen jedoch nicht aus, um alle Fahrzeuge gleichzeitig mit maximaler Leistung aufzuladen. Für Netzbetreiber und Stromproduzenten ist es zudem wünschenswert, dass die Last möglichst gleichmäßig und vorhersehbar ist. Mögliche Lösungsansätze bestehen vor allem darin, flexible Lasten zeitlich so zu planen, dass die vorhandene Anschlussleistung ausreicht.

Es wurde daher mit Optimierungsmethoden der linearen und stochastischen Programmierung für die häufigsten Szenarien untersucht, wie sich unter Zuhilfenahme von optionalen Batteriespeichern und/oder Photovoltaik die Last netzfreundlich gestalten lässt. Gleichzeitig wird das Bedürfnis der Fahrzeugeigner nach Komfort befriedigt werden, morgens verlässlich ein aufgeladenes Auto vorzufinden.

Die ermittelten Algorithmen wurden in der Praxis an einer bestehenden Prototyp-Anlage der Flotte verifiziert. Hierzu wurden die nötigen Programme in Python implementiert und anschließend die während des einmonatigen Testbetriebs gewonnenen Daten einer fundierten Analyse unterzogen. Zusätzlich wurde in einer Simulation der Einfluss der Photovoltaik- und Batteriespeicher-Dimensionierung auf die erreichbaren Optimalwerte untersucht, wodurch bestätigt werden konnte, dass fortgeschrittene Optimierungsmethoden ein zentrales Laststeuerungselement sind, mit dem einerseits die Spitzenlasten reduziert und andererseits die Kundenzufriedenheit berücksichtigt werden kann.

Schlagwörter: Lastmanagement, Vorarlberg, Wohnanlagen, Ladestation, Lineare Optimierung, Stochastische Optimierung, Spitzenlastreduktion, Ladekomfort, Rechenzeit

Table of Contents

1	Introduction	1
1.1	Initial Situation	1
1.2	Research Problem & Objective	1
1.2.1	Research Question	2
1.2.2	Hypotheses	2
1.2.3	Objective	3
1.3	Methodology	3
1.4	Structure of the Thesis	4
1.4.1	Theoretical Foundation	4
1.4.2	Available Literature	5
2	Basic Concepts and Definitions	7
2.1	Demand-Side Management	7
2.2	Deterministic & Stochastic Optimization	7
2.3	Optimization Goals & Metrics	7
2.3.1	Peak shaving	8
2.3.2	Charging comfort	9
2.3.3	Computation Time	9
2.3.4	SSR & SCR	9
3	Energy System Model	10
3.1	System Configurations	10
3.1.1	LVG + PV + BESS	10
3.1.2	LVG + PV	15
3.1.3	LVG + BESS	15
3.1.4	LVG only	16
3.2	Charging Strategies	17
3.2.1	Direct Charging	17
3.2.2	Rule-based Charging	18
3.2.3	Predictive Charging	19
3.2.4	Stochastic Charging	20
4	Field Test	22
4.1	Hardware Setup	22
4.1.1	Components	22
4.1.2	Implementation	26
4.2	Software Setup	27
4.2.1	Design Goals	27

4.2.2	Components	28
4.2.3	Implementation	29
4.3	Results	32
4.3.1	Data quality	32
4.3.2	Driving Profiles	34
4.3.3	Optimization Runs	35
4.3.4	Peak Shaving	40
4.3.5	Charging Comfort	42
4.3.6	Computation Time	43
4.4	Discussion	44
5	Simulation Studies	46
5.1	Setup	46
5.1.1	Data	46
5.1.2	Simulation planning	47
5.2	Results	48
5.2.1	Optimization Runs	49
5.2.2	Peak Shaving	53
5.2.3	Charging Comfort	58
5.2.4	Computation Time	61
5.2.5	Self-Sufficiency- & Self-Consumption-Rate	63
5.3	Discussion	66
6	Conclusion	69
7	Outlook	71
	References	72
	List of Abbreviations and Symbols	77
	List of Figures	78
	List of Tables	80

1 Introduction

1.1 Initial Situation

Vorarlberg was Austria's first model region for electromobility and already has extensive experience in this area with internationally recognized pilot projects such as Vlotte [1]. Newly built apartment buildings and residential complexes are equipped with sufficiently sized power grid connections, so that every parking space can be equipped with charging infrastructure if required [1], while there are subsidies for retrofitting the cabling that meets the new requirements for existing buildings. However, it must be taken into account that the one-off subsidy for upgrading the supply line is offset by significantly higher running costs if the power requirement exceeds the threshold of about 35 kW and thus ongoing power measurement by the local network operator becomes mandatory[2].

The shift to electromobility itself is already presenting local grid operators with major challenges. The demand for electricity and, in particular, the requirements for power output are increasing [1], while at the same time, as part of the process towards energy autonomy, massive investments are being made in the expansion of decentralized renewable energies for power generation [1], in the hope of making a meaningful contribution to relieving the power grid [3].

On the one hand, this requires practical possibilities for load shifting of large consumers such as electric car charging stations in times of lower demand and, on the other hand, for grid stabilization through inexpensive, stationary electricity storage [1], as they are being investigated by Vlotte in the 'LiLa' prototype plant, among others.

There is therefore a two-fold motivation to keep the power requirements of existing residential complexes for electromobility below the limit of 35 kW: On the one hand on the part of the network operator, who can possibly postpone a complex and costly expansion of capacity, and on the other hand on the part of the residents of residential complexes, who can avoid unnecessarily high electricity costs by means of load shifting through optimization.

1.2 Research Problem & Objective

The number of electric vehicles will increase rapidly in the coming years. Studies [4] suggest that most owners prefer to charge their electric vehicle at home, which will fuel the need for charging stations in residential complexes where vehicles can be charged overnight. According to the experts at Vlotte, there already are over 100 such residential complexes, with another 70 added every year in Vorarlberg alone.

In most existing residential complexes, however, the grid connections are not sufficient to charge all vehicles at the same time with maximum power. In addition, it is also desirable for grid operators and electricity producers that the power demand be as smooth and predictable as possible. To achieve this, ways to manage flexible loads need to be found, which can operate within the technical constraints.

It is therefore to be examined for the most common scenarios how the load can be made grid-friendly with the help of optional battery storage and/or photovoltaics using optimization methods of linear and stochastic programming. At the same time, the needs of the vehicle owners for charging comfort should be addressed, i.e. to find a reliably charged car at the time of their respective departure.

The algorithms determined are to be verified in practice on an existing Vlotte prototype installation. For this purpose, the necessary programs will be implemented in Python using software engineering, so that the data obtained during the test operation, which is expected to last one month, can be subjected to a well-founded analysis. In addition, simulation studies will help to further quantify the influence of PV and BESS sizing on the achievable optimums.

1.2.1 Research Question

The main research question this thesis aims to answer is:

- To which extent can the peak load be reduced by autonomous demand side management using linear and stochastic optimization in residential complexes?

Secondary research questions include:

- How can loads be managed in order to minimize and smoothen grid draw?
- How can the vehicle owners' desires regarding a sufficiently charged vehicle be adequately considered?
- What added value regarding charging management is generated by extra data?
- What added value does stochastic optimization have compared to deterministic optimization and perfect information?
- What is the effect of BESS and PV sizing regarding the achievable optimum?

1.2.2 Hypotheses

The following hypotheses are assumed for the scope of this thesis:

1. Historical load profiles are suitable for the prediction of future loads.
2. The more sophisticated the optimization algorithm, the higher the added value.
3. Additional data used for the prediction of loads and PV production lead to an improved optimization result.
4. Peak shaving and charging comfort can be combined in one optimization model.
5. Even advanced optimization algorithms can successfully be run on modest single-board computers.

1.2.3 Objective

The main goal of this thesis is the quantitative evaluation and practical application of well-known optimization algorithms to electric car charging stations in residential complexes. At the heart of the energy system under consideration is the charging station itself, which, in addition to the grid connection, can optionally be equipped with a battery storage system and/or a photovoltaic power generator. This results in 4 possible basic configurations, for each of which a separate mathematical model is to be set up and examined. The main power consumers of the energy system are the vehicles to be charged, whose charging behavior should be controlled in such a way that on the one hand the grid-side load is as smooth as possible and remains below the threshold of 35 kW of maximum allowable power, while at the same time ensuring that the vehicles themselves are charged sufficiently by the time their respective owners want to start driving..

Of particular interest in the context of modeling is the determination of the quantitative advantages and disadvantages of the system configurations considered, in order to subsequently form a decision-making basis for practical application. Starting with trivial charging strategies such as directly charging with maximum power, we explore more advanced strategies like predictive charging all the way up to complex modeling approaches like stochastic optimization. In addition, we attempt to quantify what added value can result from the additional modeling and computational effort and to what extent advanced optimization algorithms can be run in a decentralized fashion modest computer infrastructure (e.g. a Raspberry Pi single-board computer).

1.3 Methodology

Informed by the relevant topic matter literature, the central concepts of optimization are briefly introduced in order to subsequently describe the energy system "residential complex with charging station" in more detail and define the input and target variables to be examined. The specification of the energy system configuration informs the acquisition of necessary simulation data, most importantly load and production profiles, as well as the formulation of the optimization models used both in the field test as well as the simulation studies.

Based on the theoretical foundation, all components of the scientific arc are executed, consisting of the following steps:

- Initial situation
- Research question
- Methodology
- Data
- Execution
- Results
- Discussion and conclusions, including critical reflection

1.4 Structure of the Thesis

Following the general pattern of funneling from general concepts to specific data and ideas, this thesis has been structured accordingly. The introduction gives a short overview of the topic and concepts involved, including the motivation and goals as well as methodology and underlying hypotheses. The basic concepts and definitions are approached in more detail in the second chapter, mainly focusing on demand-side management, optimization techniques and suitable metrics to be used going forward. Building upon this foundation, the third chapter zooms in on the energy system model that is the foundation of chapters four and five, namely the field test and the simulation studies, each of which conclude with a discussion of the results. Chapter six draws the conclusions from the results discussed previously, while the seventh and final chapter offers an outlook to future trends and possibilities.

1.4.1 Theoretical Foundation

In order to arrive at a scientific result, the theoretical foundation has to be sound and as comprehensive as necessary. Hence, we thoroughly evaluated available literature by leading authors in the field and combined the insights gained with scientific articles from current and relevant journals.

1.4.1.1 Demand-side management

The main goal of DSM is to avoid peak loads and implement load management without loss of comfort for the consumer [5]. DSM strategies typically include a combination of increasing energy efficiency, reducing consumption, shifting consumption and demand-response programs.

1.4.1.2 Grid friendliness

Grid operators specify rules for equipment that consumes electric power, like i.e. charging stations. These rules depend on the power consumption of the system and include, in particular, specifications regarding interruptibility, reactive power control capability and active power behavior [6]. Energy suppliers also define grid-friendliness as the smoothness and predictability of the consumer load, which allows for better planning and utilization of existing power plants.

1.4.1.3 Charging comfort

Depending on their driving profile, owners of electric vehicles have certain expectations of the charging speed of charging stations. For the charging process at home, the focus is primarily on efficiency, while when charging on the go, fast charging has top priority [7]. In residential contexts, however, experts agree that there is a strong connection between satisfaction and the vehicle's SOC.

1.4.1.4 Linear programming

Optimization problems in which there are only linear relationships between the variables can be solved with linear programming [8]. The target function specifies the optimization goal, while the other conditions are formulated as linear (in)equation systems. In practice, mixed-integer linear programming is particularly relevant, since it allows variables to be restricted to integers (or booleans) which is a necessity when for example implementing anti-concurrency constraints or special ordered sets.

1.4.1.5 Stochastic optimization

Stochastic optimization takes into account the fact that today's decisions have to be made under uncertainty [9]. The risks regarding the future development of decision variables are mapped by formulating suitable probabilities of occurrence and the resulting problem is solved using linear programming.

1.4.2 Available Literature

The basics of the linear optimization of energy systems have been sufficiently researched in the standard works by Grimme and Bossek [8], Schellong [10], Diwekar [11] and Kallrath [12]. In the context of flexibilities that are difficult to predict, such as those of electric vehicles, works such as those by Marti [13] and Powell [14] are of great importance.

Richardson, Flynn, and Keane [15] already recognized 10 years ago, that widespread adoption of electric vehicles and uncontrolled charging processes could have adverse effects on the power grid and thus recommended to use linear programming to determine the optimal charging rate for each vehicle.

Elamin and Shaaban [16] describe a new real-time DSM system for switchable flexibilities in the household, which, however, has comparatively high hardware requirements for daily operation.

Yang, Li, Foley, *et al.* [17] review state-of-the-art optimization methods suitable for scheduling charging processes of electric vehicles (i.e. MILP), recognizing the need for powerful commercial solver software as well as the high computational complexity as major concerns.

Nguyen, Tran-Quoc, Bacha, *et al.* [18] present an interesting method for distributing peak loads, which, however, does without the integration of battery storage and renewable energies.

Amoasi Acquah, Kodaira, and Han [19] present a highly interesting approach to the stochastic optimization of an energy system similar to the one described in this thesis, but do not provide any information about the (probably quite high) computing power required for their extensive distribution estimates and dimensional reductions.

Meer, Chandra Mouli, Morales-Espana Mouli, *et al.* [20] also consider an energy system very similar to that of this thesis, but focus on charging processes at the workplace and cost reduction through time series forecasting of PV production.

Sundstrom and Binding [21] already used grid-operator signals 12 years ago to optimize EV charging, but they depend on expensive software to create their charging schedules.

Wu and Sioshansi [22] mathematically impressively model a comparable energy system for stochastic optimization, but their elevated hardware and software requirements are also out of reach for use in private residential complexes.

Gong, Cao, Liu, *et al.* [23] also deal with the limitations of the grid connection power, but formulate their energy system as a non-linear model, which subsequently can only be solved using genetic algorithms and is therefore far removed from the objectives of this thesis.

Mehta, Srinivasan, Khambadkone, *et al.* [24] focus primarily on the comparison of charging strategies in large parking areas in terms of costs versus peak loads, which again requires a relatively complex model that is solved with a genetic algorithm.

Chrysanidis, Kosmanos, Argyriou, *et al.* [25] present various algorithms for the stochastic control of charging processes at a public charging station, but also do not provide any information about the required computing power.

Judging from the research described above, we conclude that many exciting approaches in current research are hardly suitable for practical application in residential complexes, since powerful hardware and/or expensive software is often required.

2 Basic Concepts and Definitions

2.1 Demand-Side Management

The term demand-side management (DSM) was coined in the early 1980s by EPRI (Electric Power Research Institute) and it is defined as “the planning, implementation and monitoring of those utility activities designed to influence customer use of electricity in ways that will produce desired changes in the utility’s load shape, i.e. changes in the pattern and magnitude of a utility’s load.” [26]

Shewale, Mokhade, Funde, *et al.* [27] go on to explain that DSM is a key feature of energy management in that it “reduces the peak load instead of having to install new generating capacities”. In our case, the problem is actually less one of needing new power generation capacities, but rather one of limited power transportation capacities, which can be solved using the same DSM techniques.

2.2 Deterministic & Stochastic Optimization

According to Shewale, Mokhade, Funde, *et al.* [27], classical deterministic optimization techniques like mixed integer linear programming can be applied to solve DSM problems like the one outlined above deterministically and with great computational efficiency. Cavazzuti [28] goes on to explain that deterministic optimization methods are intrinsically single-objective, while stochastic ones have the ability to overcome local optimums.

In order to evaluate the benefits of either approach, Birge and Louveaux [29] recommend using metrics like the VSS and EVPI, defined as follows:

$$\begin{aligned} VSS &= \text{Value of Stochastic solution} - \text{Value of Deterministic solution} \\ EVPI &= \text{Value of Perfect information} - \text{Value of Stochastic solution} \end{aligned}$$

2.3 Optimization Goals & Metrics

As the title of this thesis already suggests, we will attempt to implement DSM by taking advantage of the fact that the load generated by the charging process of the EVs is potentially flexible, as suggested by Martin, Feron, De Jaeger, *et al.* [30]. At the same time, residents charging their EVs have certain expectations as to how much their vehicle should be charged at their typical times of departure.

2.3.1 Peak shaving

According to Next Kraftwerke [31], peak shaving in the energy industry refers to the process of 'leveling out peaks in electricity use by [...] power consumers'. They go on to clarify the difference between actual peak shaving and load shifting: While peak shaving actually means that the overall power consumption is reduced, mere load shifting tries to move peak consumption to other times of the day (see Figure 2.1). While actual peak shaving requires extra energy sources like a PV as well as a BESS, load shifting can already be achieved by optimizing the charging time slots of the EVs.

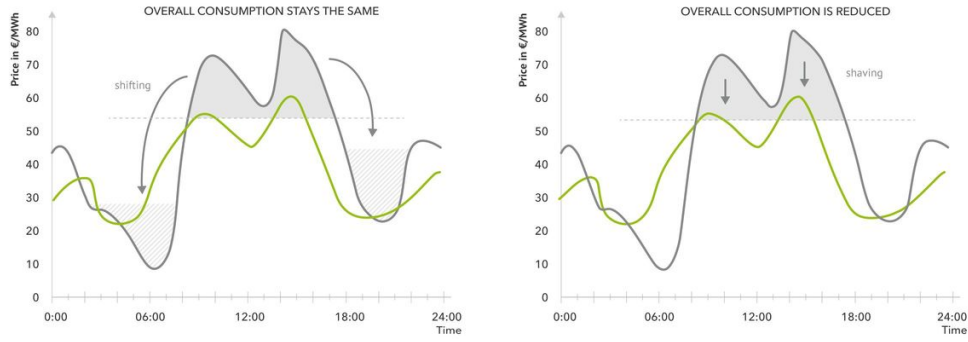


Figure 2.1: Load shifting vs. Peak shaving
Source: Next Kraftwerke [31]

There are numerous references in literature [32], [33] that propose to use the peak/average power ratio (PAPR) as an indicator of the achieved smoothness of the load curve (see Equation (2.3)). However, for configurations that potentially introduce extra energy from a PV, thus changing the average value in the denominator, we find the application of a metric that is relative to the average like the standard deviation (see Equation (2.2)) to be more suitable and will therefore add this metric alongside the PAPR for comparison.

$$\mu = E[X] = \frac{1}{N} \sum_{i=1}^N x_i \quad (2.1)$$

$$\sigma = \sqrt{E[(X - \mu)^2]} \quad (2.2)$$

$$PAPR = \frac{\max(X)}{\mu} \quad (2.3)$$

Directly minimizing the PAPR or the standard deviation in an optimization problem's objective function makes the problem non-linear and thus much more difficult to solve. For this reason, both peak shaving as well as load shifting are typically formulated as so-called Minimax problems [34] by introducing an additional decision variable y which is minimized in the objective function and is defined to be the maximum of all values x_i [35]:

$$\begin{aligned} \min. & y \\ \text{s.t. } & y \geq x_i, \forall i \end{aligned} \quad (2.4)$$

In practice, vector X will accumulate the respective first period values of each optimization run, since those were the actual values that were actually measured or set, while all later period values are just predictions. All metrics are then evaluated against this vector of result values in order to answer the main research question of this thesis.

2.3.2 Charging comfort

As a consequence of the load shifting approach described in the previous section, EVs will typically not be charged with maximal power right after they have been connected to the wallbox. For non-residential settings, the length of the charging process until the vehicle is fully charged is often cited as a good indicator for drivers' preferences [36]. Similarly, some DSM approaches suggest using the waiting time until power is actually delivered to the consumer as an indicator of user satisfaction with the process [27].

We feel that neither of which are a good fit in a residential setting, since drivers expect to find a fully charged EV by the time they want to depart for their daily activities the next day. From an optimization point of view, this is formulated by maximizing the SOC at those time periods where the EV is expected to depart. Thus, we propose using the EV's SOC in percent at the time of departure on a given day as quality metric.

2.3.3 Computation Time

Considering that we want to regulate charging power in near-real-time, it is important that the optimization process be complete within a reasonable amount of time. In contrast to simple systems that just divide and distribute the available power among all electric vehicles for charging, more complex approaches like the ones discussed in the following chapters require more computation time in order to arrive at a result. Nonetheless, we feel that an optimization run should take no longer than 600 seconds, in order for a quarter-hour resolution to be possible.

Thus, we propose to record the computation time needed for the solution of the optimization problem in seconds and report the maximum, average and standard deviation of that measure for comparison.

2.3.4 SSR & SCR

While not explicit optimization goals in our context, we feel that including metrics like self-sufficiency rate and self-consumption rate is helpful in evaluating energy systems that contain PV components.

Markstaler [37] defines these metrics as follows:

$$SSR = \frac{W_{consumed} - W_{grid}}{W_{consumed}} \quad (2.5)$$

$$SCR = \frac{W_{consumed} - W_{grid}}{W_{produced}} \quad (2.6)$$

3 Energy System Model

Considering the context given in the introduction, our energy system model consists of the following main components, as depicted in Figure 3.1:

- Electric vehicles (EV)
- Wallboxes (WB)
- Battery-electric storage system (BESS)
- Photovoltaic power generator (PV)
- Low-voltage grid (LVG)

For the sake of simplicity and interpretability, electrical details like power form (AC or DC) or number of phases (1 to 3) are ignored, since only power and energy are the relevant quantities for the research question. In addition, electricity prices are assumed to be constant, as is usually the case for residential power consumers. Lastly, we only consider the load from the charging of the EVs, household load is ignored.

3.1 System Configurations

While the a complete energy system would contain a BESS and PV, most existing residential complexes will probably have to do without one or both of them. For this reason, in addition to the model with all components (see Figure 3.1) we also consider reduced system configurations (see Table 3.1) in which either of PV or BESS or both are missing.

		BESS available	
		yes	no
PV available	yes	LVG + PV + BESS (1)	LVG + PV (2)
	no	LVG + BESS (3)	LVG only (4)

Table 3.1: Possible System Configurations Overview

3.1.1 LVG + PV + BESS

This configuration, containing both PV and BESS components (see Figure 3.1), is the most desirable from a DSM point of view, as it offers the most flexibility and self-generation. As such, it should be the default for newly planned residential complexes, considering the foreseeable rapid adoption of EVs.

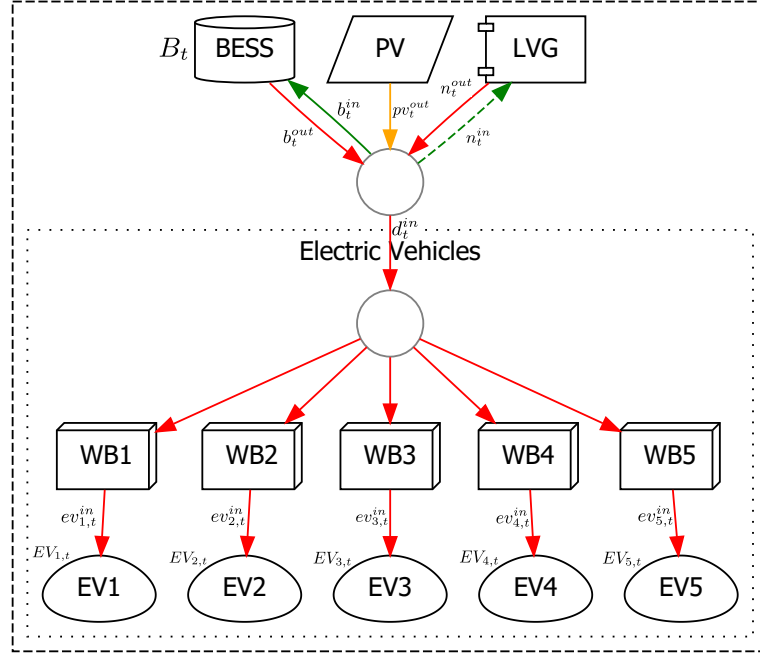


Figure 3.1: Energy System Model consisting of LVG, PV, BESS, EV & WB

We proceed to formulate the model constraints of this configuration as depicted in Figure 3.1 in the following, with a list of all symbols and units used given in Table 3.2. As a general convention, the direction of flow for each variable is denoted by a “in” or “out” in superscript in reference to the perspective of the respective entity. As an example, n_t^{out} denotes the power coming *out* of the LVG for time period t , while d_t^{in} resembles the power going *into* the EVs for time period t .

First, we combine the sum of all power consumed by the EVs for all time periods \mathcal{P} :

$$d_t^{in} = \sum_{v \in \mathcal{V}} ev_{v,t}^{in} \quad \forall t \in \mathcal{P} \quad (3.1)$$

We define the maximum power drawn from the LVG as follows:

$$n_{ceil}^{out} = \max_{t \in \mathcal{P}}(n_t^{out}) \quad (3.2)$$

Next, we require power conservation at the junction between power sources (LHS of Equation (3.3)) and power sinks (RHS of Equation (3.3)):

$$n_t^{out} + b_t^{out} + pv_t^{out} = n_t^{in} + b_t^{in} + d_t^{in} \quad \forall t \in \mathcal{P} \quad (3.3)$$

In order not to draw power from and feed excess power into the LVG, we introduce anti-concurrency constraints by means of binary decision variables ν_t^{out} and ν_t^{in} while also limiting power to the allowable maximum. This classifies the problem as a so-called MILP [11]:

$$\forall t \in \mathcal{P} :$$

$$\nu_t^{out} + \nu_t^{in} \leq 1 \quad (3.4)$$

$$n_t^{out} \leq \nu_t^{out} * n_{max}^{out} \quad (3.5)$$

$$n_t^{in} \leq \nu_t^{in} * n_{max}^{in} \quad (3.6)$$

$$n_t^{out} \geq 0 \quad (3.7)$$

$$n_t^{in} \geq 0 \quad (3.8)$$

As with the LVG, it makes no sense to charge and discharge the BESS at the same time, so analogous anti-concurrency constraints are put in place using binary decision variables β_t^{out} and β_t^{in} which also set the minimum and maximum allowed charging power:

$$\forall t \in \mathcal{P} :$$

$$\beta_t^{out} + \beta_t^{in} \leq 1 \quad (3.9)$$

$$b_t^{out} \leq \beta_t^{out} * b_{max}^{out} \quad (3.10)$$

$$b_t^{in} \leq \beta_t^{in} * b_{max}^{in} \quad (3.11)$$

$$b_t^{out} \geq \beta_t^{out} * b_{min}^{out} \quad (3.12)$$

$$b_t^{in} \geq \beta_t^{in} * b_{min}^{in} \quad (3.13)$$

Realistically, charging and discharging the BESS will not be 100 % efficient. In addition, there will be a certain degree of self-discharge over time. Based on the proposal of Ven, Hegde, Massoulie, *et al.* [38], we model this behavior as follows in the BESS SOC-tracking Equation (3.14). The amount of energy stored in the BESS of the next time period B_{t+1} is based on the current SOC B_t reduced by the self-discharging factor ξ_B , to which the energy put into the BESS by charging $\eta_B^{in} * b_t^{in} * \Delta t$ is added and from which the energy taken out by discharging $\frac{b_t^{out}}{\eta_B^{out}} * \Delta t$ is subtracted respectively:

$$\forall t \in \mathcal{T} :$$

$$B_{t+1} = B_t * \xi_B + (\eta_B^{in} * b_t^{in} - \frac{b_t^{out}}{\eta_B^{out}}) * \Delta t \quad (3.14)$$

$$B_t \leq B_{max} \quad (3.15)$$

$$B_t \geq 0 \quad (3.16)$$

The EVs can only be charged when they are loadable, which means they are connected to their assigned wallbox. In addition, there are lower and upper bounds to the charging power, which we model as follows:

$$\forall v \in \mathcal{V}, t \in \mathcal{P} :$$

$$ev_{v,t}^{in} \leq \varepsilon_t^{in} * \lambda_{v,t} * ev_{v,max}^{in} \quad (3.17)$$

$$ev_{v,t}^{in} \geq \varepsilon_t^{in} * \lambda_{v,t} * ev_{v,min}^{in} \quad (3.18)$$

Similar to the BESS, the EVs' charging processes will not be 100 % efficient nor will they fully retain their SOC over time. The amount of energy stored in each EV of the next time period $EV_{v,t+1}$ is based on the current SOC $EV_{v,t}$ reduced by the self-discharging factor ξ_{EV} , to which the energy put into the EV by charging $\eta_{EV}^{in} * ev_{v,t}^{in} * \Delta t$ is added and from which the energy taken out by discharging $\frac{ev_{v,t}^{out}}{\eta_{EV}^{out}} * \Delta t$ is subtracted respectively, leading to Equation (3.19). As a safeguard, we allow discharging of an EV only while it is driving, which is why we add the appropriate constraint as shown in Equation (3.22).

$$\forall v \in \mathcal{V}, t \in \mathcal{T} :$$

$$EV_{v,t+1} = EV_{v,t} * \xi_{EV} + (\eta_{EV}^{in} * ev_{v,t}^{in} - \frac{ev_{v,t}^{out}}{\eta_{EV}^{out}}) * \Delta t \quad (3.19)$$

$$EV_{v,t} \leq EV_{v,max} \quad (3.20)$$

$$EV_{v,t} \geq 0 \quad (3.21)$$

$$ev_{v,t}^{out} \leq \delta_{v,t} * ev_{v,max}^{out} \quad (3.22)$$

To accommodate for EV owners' expectations of never finding their vehicle less than 50 % charged, we introduce a trickle-charge constraint that ensures charging is always attempted until the EV's SOC has reached 50 %. We implement this in Equation (3.23) by subtracting the dimensionless ratio of $\frac{EV_{v,t}}{EV_{v,max}}$ (which is the EV's SOC in percent) from the threshold of $\frac{1}{2}$ (which is the same as 50 %) on the right hand side and requiring that the binary variable $\varepsilon_{v,t}^{in}$ be greater or equal to the result on the left hand side. If the EV's SOC in percent is lower than 50 %, the result is greater than zero, thus forcing the binary variable to become one:

$$\varepsilon_{v,t}^{in} \geq \frac{1}{2} - \frac{EV_{v,t}}{EV_{v,max}} \quad \forall v \in \mathcal{V}, t \in \mathcal{P} \quad (3.23)$$

As for initial conditions, the BESS should have the same SOC at the beginning and at the end of the time period considered:

$$B_0 = B_{T*\Delta t} \quad (3.24)$$

Finally, all decision variables are constrained to be non-negative, while the efficiency factors are set to reasonable values. The actual values chosen for the field test and simulation studies are described in Chapter 4 and Chapter 5 respectively.

Symbol	Quantity	Unit	Decision Variable
t	Index of time periods		
s	Index of scenarios		
Δt	time step	h	
T	number of time periods		
S	number of scenarios		
\mathcal{P}	set of time periods := $\{1, \dots, T\}$		
\mathcal{T}	set of time instants := $\{0, \dots, T\}$		
\mathcal{S}	set of scenarios := $\{0, \dots, S\}$		
\mathcal{D}_v	set of departure time periods $\subset \mathcal{P}$ of EV v		
\mathcal{V}	set of vehicles		
$EV_{v,t}$	SOC of EV v at period t	kWh	✓
$EV_{v,max}$	maximum SOC of EV v	kWh	
$ev_{v,t}^{in}$	EV v charging power during period t	kW	✓
$ev_{v,t}^{out}$	EV v discharging power during period t	kW	
$ev_{v,min}^{in}$	minimum allowable EV v charging power	kW	
$ev_{v,max}^{in}$	maximum allowable EV v charging power	kW	
η_{EV}^{in}	efficiency factor for charging of EV		
η_{EV}^{out}	efficiency factor for discharging of EV		
ξ_{EV}	self-discharging factor of EV		
$\varepsilon_{v,t}^{in}$	switch for charging EV v , 0 if open, 1 if closed	binary	✓
$\lambda_{v,t}$	EV v loadability during period t	binary	
$\delta_{v,t}$	EV v driving during period t	binary	
B_t	SOC of BESS at period t	kWh	✓
B_{max}	maximum SOC of BESS	kWh	
b_t^{in}	BESS charging power during period t	kW	✓
b_t^{out}	BESS discharging power during period t	kW	✓
b_{min}^{in}	minimum allowable BESS charging power	kW	
b_{min}^{out}	minimum allowable BESS discharging power	kW	
b_{max}^{in}	maximum allowable BESS charging power	kW	
b_{max}^{out}	maximum allowable BESS discharging power	kW	
η_B^{in}	efficiency factor for charging of BESS		
η_B^{out}	efficiency factor for discharging of BESS		
ξ_B	self-discharging factor of BESS		
β_t^{out}	switch for discharging BESS, 0 if open, 1 if closed	binary	✓
β_t^{in}	switch for charging BESS, 0 if open, 1 if closed	binary	✓
n_t^{in}	power fed into LVG during period t	kW	✓
n_t^{out}	power drawn from LVG during period t	kW	✓
n_{ceil}^{out}	maximum power drawn from LVG	kW	✓
n_{max}^{out}	maximum allowable power draw from LVG	kW	
n_{max}^{in}	maximum allowable power feed into LVG	kW	
ν_t^{out}	switch for LVG power draw, 0 if open, 1 if closed	binary	✓
ν_t^{in}	switch for LVG power feed, 0 if open, 1 if closed	binary	✓
d_t^{in}	total EV charging power demand during period t	kW	✓
pv_t^{out}	power output of PV during period t	kW	
pv_{peak}^{out}	peak power output of PV generator	kWp	

Table 3.2: Symbols and units used to describe the energy system model

3.1.2 LVG + PV

The LVG + PV configuration as depicted in Figure 3.2 is currently the most popular choice for existing residential complexes which want to offset their total electricity costs consisting of household and EV charging by installing PV panels on their roofs and/or walls. Since solar power has its peak power output typically around noon, this configuration will therefore be most useful in cases where the residents charge their vehicles during the day, otherwise the excess solar power from the PV will be fed into the LVG.

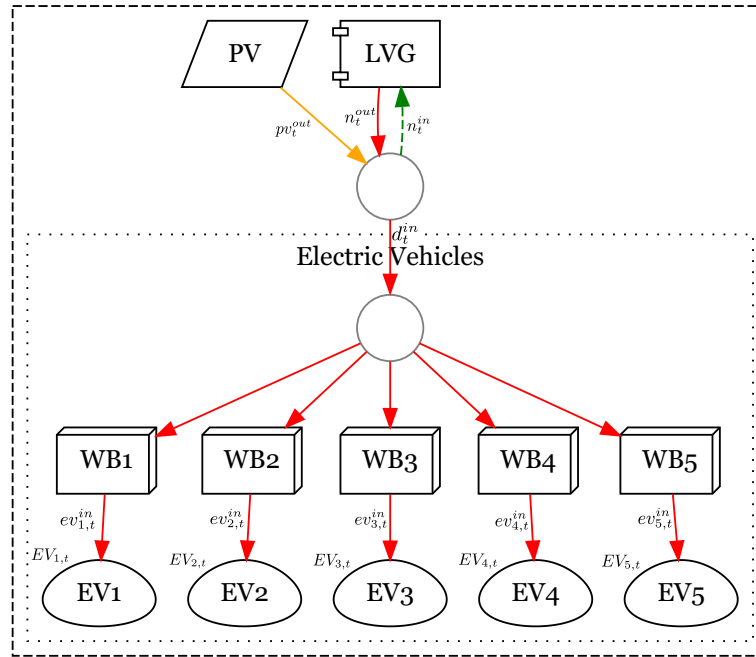


Figure 3.2: Energy System Model consisting of LVG, PV, EV & WB

The degrees of freedom for DSM in this configuration stem exclusively from load shifting of the individual EVs. Due to the extra power of the PV introduced during daytime, we expect to see the optimized charging strategies shift EV charging load from night to day where possible.

We model the missing BESS component by adding the following constraint to the base model put forward in section 3.1.1:

$$B_{max} = 0 \quad (3.25)$$

3.1.3 LVG + BESS

The LVG + BESS configuration (see figure 3.3) is probably one of the rarer configurations one can think of. This is because BESS capacity has been and still is expensive, which - combined with the effort of installing and maintaining the infrastructure - makes it less desirable from a cost perspective. However, a BESS provides flexibility for DSM by load shifting, making this still a relevant configuration.

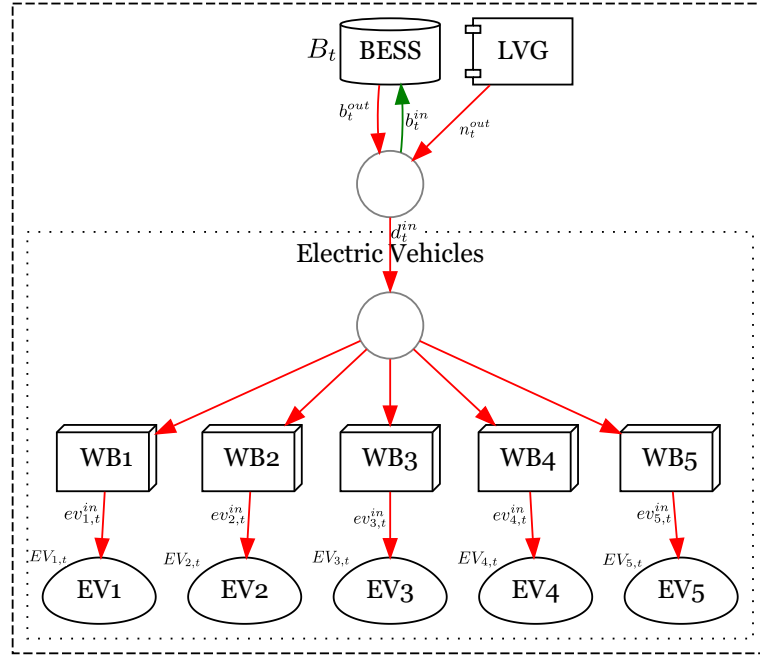


Figure 3.3: Energy System Model consisting of LVG, BESS, EV & WB

As such, it will be interesting to see which influence the capacity of the BESS has on the optimization results in terms of peak shaving.

We model the missing PV component by adding the following constraint to the base model put forward in section 3.1.1:

$$pv_t^{out} = 0 \quad \forall t \in \mathcal{P} \quad (3.26)$$

3.1.4 LVG only

The LVG only configuration is the most minimalistic of all possible configurations, since there is no PV or BESS available (see Figure 3.4). This configuration is included to resemble the large number of old residential complexes which were built without renewable energy sources and/or peak shaving considerations in mind.

It goes without saying that this configuration possesses the least degrees of freedom when it comes to DSM, since the only flexibility lies in the possibility to delay the charging processes of the individual EVs.

We model the missing PV and BESS components by combining the constraints from the previous two configurations, adding both Equation (3.25) and Equation (3.26) to this configuration's constraints.

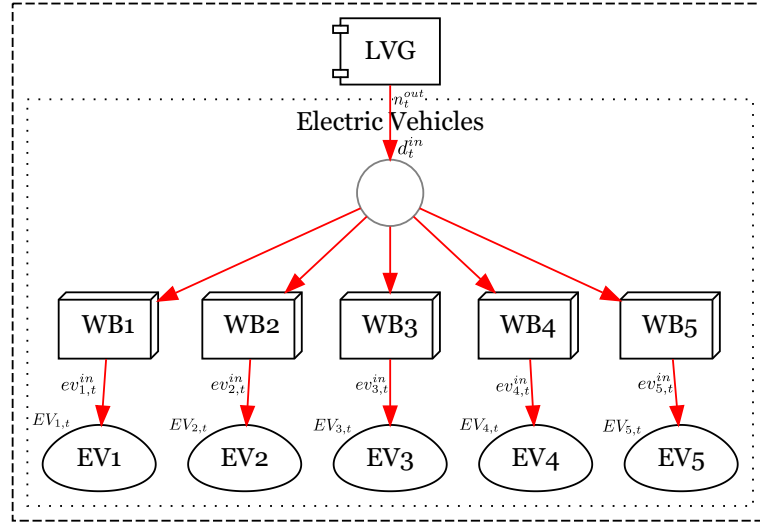


Figure 3.4: Energy System Model consisting of LVG, EV & WB

3.2 Charging Strategies

In the following section we explore some of the possible ways the charging process of EVs can be controlled. We do this by starting with the simplest method and working our way up the hierarchy to the computationally most expensive. In addition, all strategies described are based on the same ESMs described above, adding the effective objective function to complete the optimization model.

3.2.1 Direct Charging

The most well known charging strategy is the one we refer to as 'direct charging'. Here, the EV is connected to the wallbox and the charging process begins immediately, with the maximum allowable power as negotiated between EV and wallbox.

This behavior is what EV drivers usually expect when plugging in their EV, since it leads to the shortest charging time. The drawback, however, is that when this strategy is used by multiple vehicles at the same time, the allowable maximum power that can be drawn from the LVG might not suffice to satisfy their charging power demands. In addition, this is the kind of behavior that leads to huge load peaks in the LVG, which is exactly what we are trying to avoid.

We implement the direct charging strategy in our ESM by using the time period index as a pseudo-price-function and minimizing the price of the optimization problem:

$$\min. \sum_{t=1}^T n_t^{out} * t \quad (3.27)$$

3.2.2 Rule-based Charging

To improve upon the direct charging strategy and avoid load peaks by all EVs trying to charge at maximum power, one possibility is to introduce rules that govern how much power each EV is allowed to draw for charging. In its simplest form, the maximum available power is simply divided between all connected vehicles, which, however, can lead to problems if the individual share allocated to a vehicle is below its minimum power requirements for charging. For such cases, queuing systems resolving such concurrency issues [25] can be envisioned, but are beyond of the scope of this thesis.

To introduce an element of fairness, we implement a rule-based charging strategy in our ESM by coupling charging power with the SOC as depicted in Figure 3.5. The idea is that the higher the SOC the lower the charging power will be. This should ensure that vehicles needing a recharge the most urgently also get the highest amount of power.

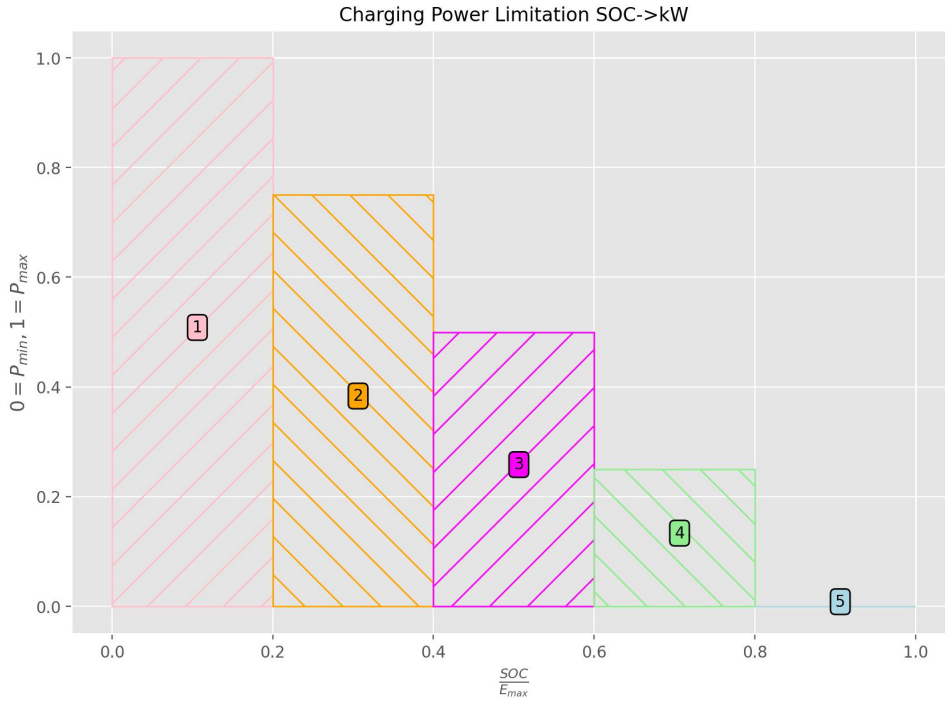


Figure 3.5: Charging power limit based on EV SOC

While the objective remains identical to that of the direct charging strategy described above, we have to add 4 additional constraints to the optimization model to implement this special ordered set of type 1 [12]:

$$\sum I_{i,v,t} = 1 \quad \forall i \in \{1, 2, 3, 4, 5\}, v \in \mathcal{V}, t \in \mathcal{P} \quad (3.28)$$

$$EV_{v,t} \leq EV_{v,max} * \left(\frac{5}{5} - \frac{4}{5}I_{1,v,t} - \frac{3}{5}I_{2,v,t} - \frac{2}{5}I_{3,v,t} - \frac{1}{5}I_{4,v,t} \right) \quad (3.29)$$

$$EV_{v,t} \geq EV_{v,max} * \left(\frac{0}{5} + \frac{1}{5}I_{2,v,t} + \frac{2}{5}I_{3,v,t} + \frac{3}{5}I_{4,v,t} + \frac{4}{5}I_{5,v,t} \right) \quad (3.30)$$

$$ev_{v,t}^{in} \leq ev_{v,max}^{in} - (ev_{v,max}^{in} - ev_{v,min}^{in}) * \left(\frac{1}{4}I_{2,v,t} + \frac{1}{2}I_{3,v,t} + \frac{3}{4}I_{4,v,t} + \frac{4}{4}I_{5,v,t} \right) \quad (3.31)$$

First, we define five indicators, referring to the respective area as depicted in Figure 3.5. In Equation (3.28), we require that one (and only one) of the five indicators is set to one for each time period and vehicle. In Equations 3.29 and 3.30, we couple the actual EV SOC to the five areas by creating appropriate inequality boundaries. For example, if $EV_{v,t}$ were to be $\frac{1}{2}EV_{v,max}$, indicator $I_{3,v,t}$ would have to become one, giving us $.5 \leq (\frac{5}{5} - \frac{4}{5} * 0 - \frac{3}{5} * 0 - \frac{2}{5} * 1 - \frac{1}{5} * 0)$ and $.5 \geq (\frac{0}{5} + \frac{1}{5} * 0 + \frac{2}{5} * 1 + \frac{3}{5} * 0 + \frac{4}{5} * 0)$, both of which being true statements. With the indicator coupled to the EV SOC, Equation (3.31) allows us to set the upper bound of the EV charging power to the desired limit. Again, assuming $I_{3,v,t}$ being set to one as an example, we limit $ev_{v,t}^{in}$ to be less or equal than $ev_{v,max}^{in} - (ev_{v,max}^{in} - ev_{v,min}^{in}) * (\frac{1}{4} * 0 + \frac{1}{2} * 1 + \frac{3}{4} * 0 + \frac{4}{4} * 0)$ or 50 % of the allowed maximum charging power.

3.2.3 Predictive Charging

For the predictive charging strategy, we replace the objective function from the previously discussed strategies with one that takes into consideration the goals of peak shaving and charging comfort, as described in section §2.3. Regarding charging comfort, we need to consider that it is not guaranteed that all vehicles depart at least once per day, which is why we split this goal into two sub goals. The first sub goal is to maximize the SOC of the electric vehicle at departure time, if any. The second sub goal is to maximize the SOC at the end of the 24 hour look ahead period, which ensures that a given vehicle is fully charged within one day at the least. Thus, we will be combining three objectives into one objective function: Firstly, minimize grid draw peaks. Secondly, maximize EV SOC at departure times. Thirdly, maximize EV SOC at the end of the look ahead horizon.

Since we are trying to combine entities that differ in their unit of measure (i.e. grid draw is measured in kW while SOC is measured in kWh) as well as their numerical range in a unified objective function, we adopt the advice of [12] and will scale the entities to a common unit and numerical range, preventing either of the three objectives to dominate the optimization result [39].

We begin the formulation of our objective function by adding a constraint to implement n_{ceil}^{out} based on the time periods considered as described in equation (2.4). By minimizing n_{ceil}^{out} , we lay the foundation for the desired peak shaving behavior:

$$n_{ceil}^{out} \geq n_t^{out} \quad \forall t \in \mathcal{P} \quad (3.32)$$

The first term of our objective function is $\frac{1}{n_{max}^{out}} n_{ceil}^{out}$. As we pointed out earlier, dividing n_{ceil}^{out} by the maximum allowable value n_{max}^{out} effectively gives us a percentage, which not only removes the unit, but also scales the result to values between zero and one.

The second term of our objective function is $\frac{1}{len(\mathcal{V})} \sum_{t \in \mathcal{D}_v, v \in \mathcal{V}} \frac{1}{len(\mathcal{D}_v)} \frac{1}{EV_{v,max}} EV_{v,t}$, which aims to maximize the EV SOC at the predicted departure times \mathcal{D}_v . This is achieved by adding all the EV SOC at those departure times and dividing them by the maximum EV SOC per vehicle $EV_{v,max}$ to get rid of the unit, while dividing the value further by the number of departure times $len(\mathcal{D}_v)$ and the number of vehicles $len(\mathcal{V})$ will scale this part of the objective function down to a percentage as well.

The last term of our objective function is $\frac{1}{len(\mathcal{V})} \sum_{t=T, v \in \mathcal{V}} \frac{1}{EV_{v,max}} EV_{v,t}$, which aims to maximize the EV SOC by the end of the 24 hour look ahead horizon. Similar to the previous term, we divide the EV SOC by the EV battery capacity to remove the unit and divide by the number of vehicles to scale the result to a percentage.

As we decided to give equal weight to peak shaving as well as charging comfort, with equal weight to be given to both charging comfort sub goals, we determine the weights of the three objectives to be 1, .5 and .5 respectively. Since objectives two and three are to be maximized, we will multiply the terms with -1 in order combine them with objective one. Thus, we formulate the objective function as follows:

$$\begin{aligned} \min. \quad & \frac{1}{n_{max}^{out}} n_{ceil}^{out} \\ & - \frac{1}{2} \frac{1}{len(\mathcal{V})} \sum_{t \in \mathcal{D}_v, v \in \mathcal{V}} \frac{1}{len(\mathcal{D}_v)} \frac{1}{EV_{v,max}} EV_{v,t} \\ & - \frac{1}{2} \frac{1}{len(\mathcal{V})} \sum_{t=T, v \in \mathcal{V}} \frac{1}{EV_{v,max}} EV_{v,t} \quad (3.33) \end{aligned}$$

Looking at the above objective function it is clear that we will need to predict the time periods \mathcal{D}_v per vehicle in which it departs, along with all other data needed to populate a full 24 hour look ahead horizon, most notably the driving profiles of the vehicles as well as the PV production data. There is large body of research dealing with time series forecasting, ranging from traditional statistical methods like smoothing and auto-regression [40] to more advanced methods like basic machine learning [41] and neural networks [42]. The choice of the actual method is going to be highly dependent on the data available, the computing power one is willing to allocate as well as the quality expectations associated with the predictions.

3.2.4 Stochastic Charging

Unlike the deterministic predictive charging strategy, the stochastic charging strategy considers historic driving profiles (which we will refer to as scenarios in the following) as individual sub-problems instead of collapsing all these possibilities into one single prediction of the vehicles' behavior. Theory suggests that this approach should result in a more robust optimization result [28] that performs well for (almost) all possible scenarios [43], even for distribution-free problems such as ours [14] that depend on historic data as source of information.

To implement a stochastic optimization model, all decision variables and input data relating to the EVs gain an additional index s , denoting all the scenarios that are optimized against. As a result, we no longer need to predict the departure times \mathcal{D}_v of the EVs nor their power consumption.

As computation time is important, we use a two-stage stochastic modeling approach as discussed, for example, in [44], [14] and [43], defining the first time period as stage one and all periods thereafter as stage two. More specifically, stage one is the actual decision that has been made, considering all the

possible future scenarios considered in stage two. Decisions in stage two are themselves constrained by the decision made in stage one.

As for scenarios, again considering computation time, we follow the advice of Wu and Sioshansi [22] to use scenario reduction in order to reduce complexity and simply use the previous 8 days of data available sliced in 24 hour slices as scenarios, even though much more elaborate methods exist and are discussed in [45].

Thus, in analogy to Equation (3.33) we formulate the objective function as:

$$\begin{aligned} \min. \quad & \frac{1}{n_{max}^{out}} n_{ceil}^{out} \\ & - \frac{1}{2} \frac{1}{len(\mathcal{V})} \frac{1}{len(\mathcal{S})} \sum_{t \in \mathcal{D}, v \in \mathcal{V}, s \in \mathcal{S}} \frac{1}{len(\mathcal{D}_{v,s})} \frac{1}{EV_{v,max}} EV_{v,t,s} \\ & - \frac{1}{2} \frac{1}{len(\mathcal{V})} \frac{1}{len(\mathcal{S})} \sum_{t=T, v \in \mathcal{V}, s \in \mathcal{S}} \frac{1}{EV_{v,max}} EV_{v,t,s} \quad (3.34) \end{aligned}$$

Since only one decision can actually be made in stage one, we need to ensure that all scenarios collapse into one for the first period by adding additional constraints:

$$\forall t = 1, s \in \mathcal{S}, v \in \mathcal{V} : \quad (3.35)$$

$$\begin{aligned} n_{t,s}^{out} &= n_{t,0}^{out} \\ n_{t,s}^{in} &= n_{t,0}^{in} \\ \nu_{t,s}^{out} &= \nu_{t,0}^{out} \\ \nu_{t,s}^{in} &= \nu_{t,0}^{in} \\ b_{t,s}^{out} &= b_{t,0}^{out} \\ b_{t,s}^{in} &= b_{t,0}^{in} \\ \beta_{t,s}^{out} &= \beta_{t,0}^{out} \\ \beta_{t,s}^{in} &= \beta_{t,0}^{in} \\ B_{t,s} &= B_{t,0} \\ ev_{v,t,s}^{in} &= ev_{v,t,0}^{in} \end{aligned}$$

4 Field Test

To verify the methods discussed in section §3.2 and gather driving profiles, which include the the availability for charging and energy consumption during driving as well as PV production data, a field test was conducted in cooperation with Vlotte on their LiLa prototype facility.

The planning for this field test already started months in advance to ensure that it was possible to get the most out of it. It was decided to conduct the field test during the month of March 2022 (see Table 4.1), since the PV might be covered with snow during the earlier winter months otherwise. In addition, the planning of the phases was ordered from simple to most difficult, in order for the charging strategies involving optimization based on historic driving profiles to have enough data to go on in terms of prediction and/or selection of scenarios.

Phase	Starting Date	Charging Strategy
1	2022-03-07	Direct Charging
2	2022-03-14	Rule-based Charging
3	2022-03-21	Predictive Charging
4	2022-03-28	Stochastic Charging

Table 4.1: Planned field test phases

4.1 Hardware Setup

4.1.1 Components

Considering the possible system configurations discussed in section §3.1, the energy system for the field test can be classified as LVG+PV+BESS, meaning that it contains all the components desirable for a complete setup.

4.1.1.1 PV & BESS

The inverter used to convert DC power coming from the PV to AC also included a BMS to manage the BESS (see Figure 4.1). While various modes of operation exist according to the manufacturer's manual [46], the only useful option was 'self-use' mode, which basically stores energy from the PV in the BESS for later use by the EVs.

In terms of sizing, the PV generator on site was specified for p_{peak}^{out} of 14.28 kWp. The BESS (see Figure 4.2), a Neoom Kjuube H48074, was specified for B_{max} of 26.56 kWh, allowing energy flow at b_t^{in} & b_t^{out} of 12.78 kW respectively.

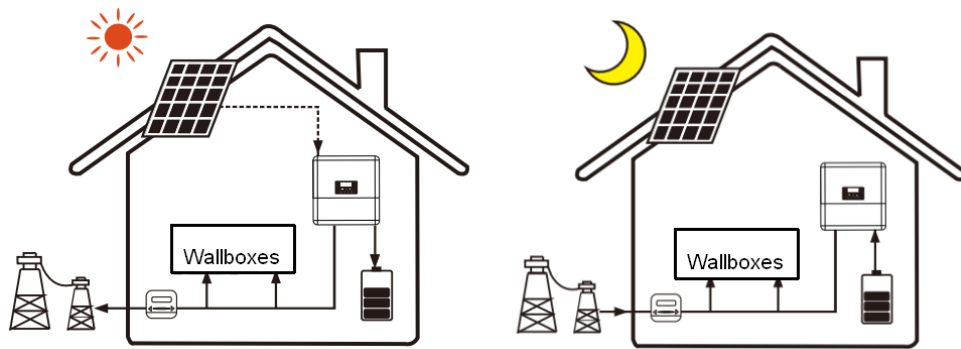


Figure 4.1: Inverter modes of operation
Source: Adapted from Solax Power [46]



Figure 4.2: BESS installed at LiLa site
Source: Vlotte

4.1.1.2 Wallboxes

To charge the EVs, wallboxes [47] that regulate the power delivery were installed at the LiLa prototype facility (see Figure 4.3). While the wallboxes themselves could have handled $e_{v,max}^{in}$ of 22 kW, they had to be limited to 11 kW due to electrical safety considerations.



Figure 4.3: Wallboxes installed at LiLa site
Source: Vlotte

4.1.1.3 Local Raspberry Pi

The LRP was installed in the power cabinet (see Figure 4.4) at the LiLa prototype facility, serving as local data acquisition device running NodeRed (see section 4.2.2.5).

4.1.1.4 Remote FHV Server

The RFS was used for running the optimization models in a reliable Linux environment hosted at FHV. A direct OpenVPN-tunnel [48] was configured to the LRP, in order to enable bi-directional data access.

4.1.1.5 Electric Vehicles

While originally six vehicles were planned for the field test, only five were available by the time the experiment was started (see Table 4.2).

Each of the vehicles was equipped with Evelix OBD2 data capturing devices [49]. Unfortunately, the manufacturer announced their going out of business just a few months prior (see Figure 4.5), unnoticed by the Vlotte team. A temporary solution was implemented using special firmware from the OEM of the DCDs, but not without loss of stability and data quality. As a result, it was not possible to retrieve the SOC of car #2, since the OEM firmware predated the release of this vehicle, rendering it incompatible for the duration of the field test.



Figure 4.4: Power cabinet installed at LiLa site
Source: Vlotte

ID	Model	Battery Capacity [kWh]
car1	Renault Zoe	52
car2	MG evLine	72
car3	Renault Zoe	52
car4	VW ID.3	62
car5	Renault Zoe	52

Table 4.2: Vehicles used in field test

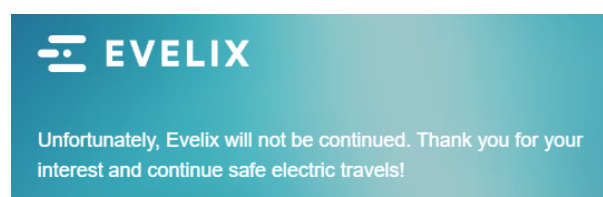


Figure 4.5: Evelix - End of Life
Source: Evelix [49]

4.1.2 Implementation

The components mentioned in section 4.1.1 were assembled and configured at the LiLa prototype facility by Vlotte engineers. The electric vehicles (see Table 4.2) were kindly provided by local car dealerships for the duration of the field test.

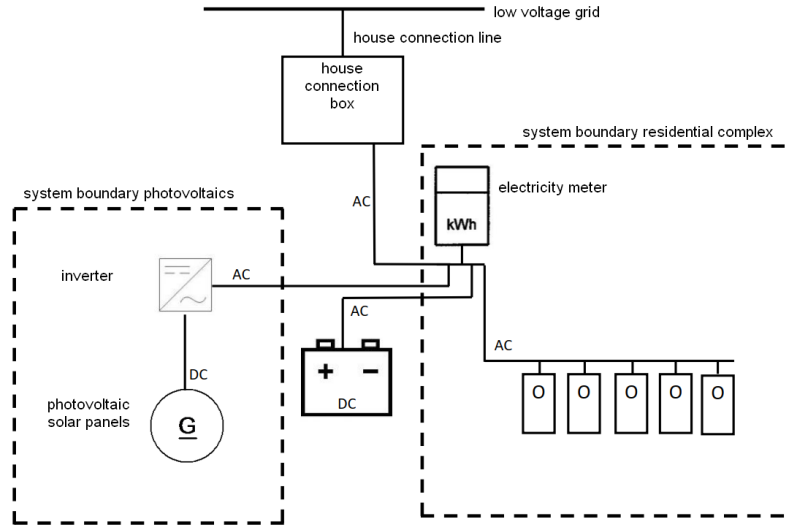


Figure 4.6: Planned LiLa system setup

Source: Vlotte original schematics, translated to English by Author

Deviating from the initially discussed system specifications (see Figure 4.6), the LiLa prototype facility was configured to only allow charging of the BESS with power coming from the PV (see Figure 4.7), due to the particular model of inverter used (see Figure 4.1).

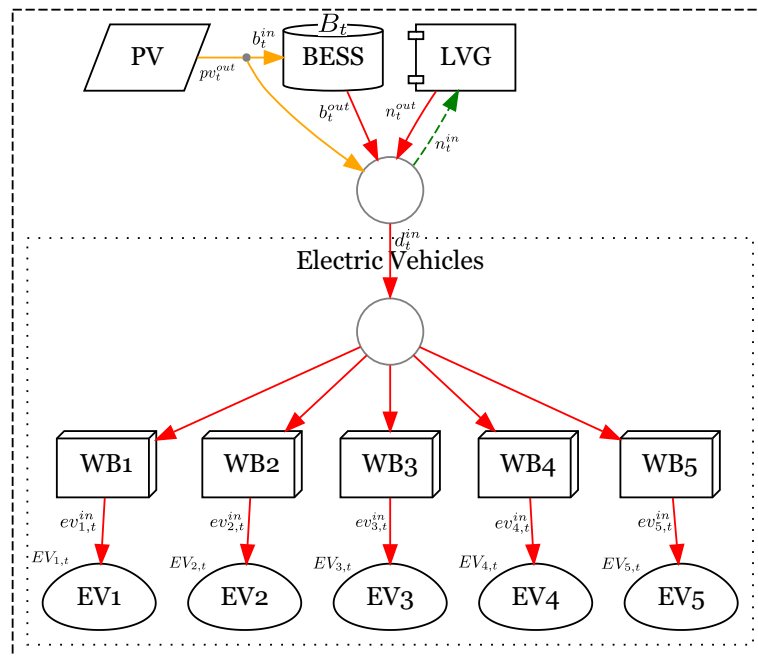


Figure 4.7: Energy System Model - LiLa setup

We model this deviation from the base model defined in section 3.1.1 by adding Equation (4.1)

and equation (4.2) as anti-concurrency constraints, which effectively prohibit charging the BESS with power from the LVG as well as feeding power to the LVG by discharging the BESS:

$$\forall t \in \mathcal{P} :$$

$$\nu_t^{out} + \beta_t^{in} \leq 1 \quad (4.1)$$

$$\nu_t^{in} + \beta_t^{out} \leq 1 \quad (4.2)$$

The system specific configuration parameters used in the software implementation are listed in Table 4.3 for quick reference. Note that while the values for the most relevant parameters (i. e. maximum power draw, battery capacities, etc.) could be quantified by the experts at Vlotte, assumptions had to be made for others (i. e. efficiency and self-discharging factors).

Symbol	Quantity	Unit	Value
Δt	time step	h	0.25
$e_{v,min}^{in}$	minimum allowable EV v charging power	kW	4.14
$e_{v,max}^{in}$	maximum allowable EV v charging power	kW	11.0
η_{EV}^{in}	efficiency factor for charging of EV		0.85
η_{EV}^{out}	efficiency factor for discharging of EV		0.85
ξ_{EV}	self-discharging factor of EV		0.9983
B_{max}	maximum SOC of BESS	kWh	26.56
b_{min}^{in}	minimum allowable BESS charging power	kW	0.0
b_{min}^{out}	minimum allowable BESS discharging power	kW	0.0
b_{max}^{in}	maximum allowable BESS charging power	kW	12.78
b_{max}^{out}	maximum allowable BESS discharging power	kW	12.78
η_B^{in}	efficiency factor for charging of BESS		0.95
η_B^{out}	efficiency factor for discharging of BESS		0.95
ξ_B	self-discharging factor of BESS		0.9986
n_{max}^{out}	maximum allowable power draw from LVG	kW	35.0
n_{max}^{in}	maximum allowable power feed into LVG	kW	35.0
pv_{peak}^{out}	peak power output of PV generator	kWp	14.28

Table 4.3: Configuration values used in the field test

4.2 Software Setup

4.2.1 Design Goals

In order to be able to choose the right software components and guide a successful implementation of the field test, a set of design goals was defined based on the author's experience as a professional software developer.

4.2.1.1 Open Source Software

The use of Open Source software has many advantages, the most important of which are availability, cost and documentation. Popular Open Source software typically is available for all relevant platforms and Operating Systems, licensed so that it can even be used in a commercial setting and - depending on popularity of the project - well documented and supported. We will therefore prefer solutions that are fully open source and well supported for our field test.

4.2.1.2 Time to market

Considering the ambitious time schedule for implementation of the field test, software components that reduce the amount of code that needs to be written clearly pose a big advantage when trying to meet fixed deadlines. We will therefore prefer components and frameworks that reduce the need to reimplement basic functionality.

4.2.1.3 Maintainability

Experienced software developers know that the context in which an application is run can change quickly, making it necessary to quickly develop new features, adapt to unexpected data or fix undiscovered bugs. At the same time, the running system needs to remain stable, while new software versions are deployed. We will therefore prefer software and development patterns that allow for proper testing and deployment procedures.

4.2.2 Components

4.2.2.1 Python

According to Van Rossum and Drake [50], Python 'is an easy to learn object-oriented programming language, which combines power with clear syntax'. Being developed since the 1990s, it has become one of the most important programming languages for data science and engineering. This is mainly due to its ubiquity and vast library of 3rd party packages to add a wide range of functionalities.

4.2.2.2 PuLP

Mitchell, O'Sullivan, and Dunning [51] introduce PuLP [52] as 'an open source package that allows mathematical programs to be described in the Python computer programming language'. A big advantage of this particular package is the fact that the models it generates can be solved with different solvers like Gurobi [53] and CBC [54], the latter of which is even included in the distribution due to its open source nature, making it a viable alternative to commercial solutions available [12].

4.2.2.3 Kedro

According to Alam, Bălan, Comym, *et al.* [55], Kedro 'is an open-source Python framework for creating reproducible, maintainable and modular data science code'. Compared to Python, it is a comparatively young project, having been donated to the Open Source community in 2019. Since then, it has received great praise from the data engineering community, because it helps developers focus on creating maintainable code by providing useful project structure templates, doing away with the usual mess of glue-code stuck in-between one-off scripts and Jupyter notebooks.

4.2.2.4 SQLite

SQLite is a 'a small, fast, self-contained, high-reliability, full-featured, SQL database engine' [56], which is freely available under an open-source license for all major platforms. Thus, it greatly helps in data management when dealing with large volumes of data that need to be processed efficiently.

4.2.2.5 NodeRed

The OpenJS Foundation [57] provides NodeRed as a 'programming tool for wiring together hardware devices, APIs and online services in new and interesting ways'.

4.2.3 Implementation

There are three main processes, all of which were implemented in Python within the aforementioned Kedro framework (see Figure 4.8, apologies for the very small font which unfortunately was beyond the control of the author):

- Data acquisition
- Data preprocessing
- Charging power calculation

We make the software implementation publicly available at [58].

All three subprocesses were implemented as pipelines in Kedro and scheduled to run every 15 minutes on the RFS.

4.2.3.1 Data acquisition

The process of data acquisition was handled on the remote side of the system described in the previous sections. The components of the energy system were polled for data which were written to the file system in CSV format (see algorithm 4.1).

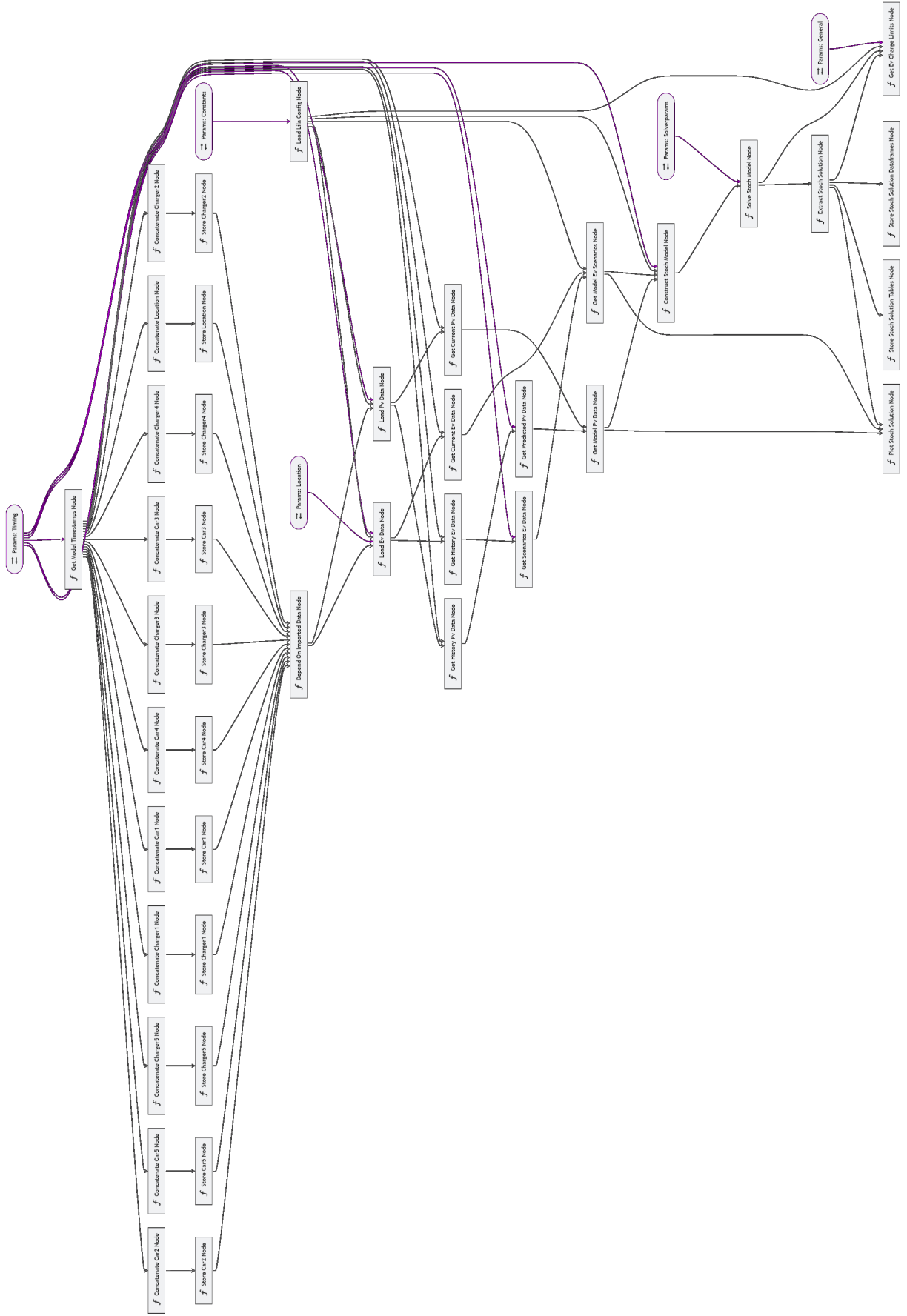


Figure 4.8: Kedro Pipeline

Algorithmus 4.1 Data acquisition

```

load config

get model timestamps

for all entities
    read new data from CSVs
    store new data to SQLite database

set latest processing timestamp

```

4.2.3.2 Data preprocessing

As in most real life scenarios, raw data is rarely ready for direct use in analytical processes. Therefore, the individual CSV files containing the acquired data were pulled from the remote system using SSH and stored in a SQLite database. This made it possible to resample and combine the data from all entities into one data table using SQL (see algorithm 4.2).

Algorithmus 4.2 Data preprocessing

```

load config

load PV data

for all vehicles
    load EV data

```

When resampling the data, we went with a Δt of 15 Minutes, effectively giving us a 96 period look ahead horizon for a full day.

4.2.3.3 Charging power calculation

With the preprocessed data available, we construct suitable model data from the most current value and the historic data. For the prediction of the PV profile, we simply use the average power per time period of the previous 8 days. For the EV driving profiles, we looked at various ways to predict driving profiles using methods of machine learning, but ended up using the same simple averaging method used for the PV to predict EV driving times and power consumption, the deciding factor being the much reduced calculation time combined with little to no loss of prediction quality compared to the more elaborate machine learning approaches.

We then proceed to solve the previously described charging strategy models to determine the optimal charging power limit for each of the cars connected to their wallboxes (see algorithm 4.3). The values to be set for each vehicle are stored on the LRP in a text file, which in turn is consumed by a monitoring process implemented in NodeRed in order to set the charging power limits on each of the wallboxes associated with a particular EV, thus completing a full optimization cycle.

Note: For the stochastic charging model, we construct the 8 scenarios per vehicle from the 8 preceding days instead of predicting an average profile of the look ahead period regarding EV power consumption and loadability from the same historic data.

Algorithmus 4.3 Charging power calculation

load config

get model timestamps

get current PV data

get current EV data

get history PV data

get history EV data

predict PV data for look ahead period

predict EV data for look ahead period

build model data using current and predicted PV & EV data

construct model

solve model

extract charging power from model solution

set charging power to wallboxes

4.3 Results

We will be examining the results of the field test in the following. Note that we make the software implementation publicly available at [59].

4.3.1 Data quality

Unfortunately, the field test was plagued by numerous data acquisition problems. A few days before the field test was scheduled to start, it was discovered during the installation of the equipment on-site that the data capturing devices (DCD) to be installed in the EVs were not fully compatible with the vehicles available. It was discovered, as we described earlier, that the service provider of the DCDs had gone out of business, which made obtaining software updates to make new vehicles work quite challenging. In case of car #2, it was not possible to capture the SOC during the course of the field test at all, while for the duration of the field test, the DCDs installed in the other cars were struggling to reliably report correct measurements (see Figure 4.9). A large number of these problems could be related to the design of the DCDs themselves, in that the OBD2 socket they had to be installed in usually is meant for connecting diagnostic equipment for short periods and not as a permanent installation that is subject to vibrations or other mechanical influences that are destined to impede connectivity.

During the field test, there also were numerous LRP outages causing further gaps in the data. In some cases, the VPN tunnel was unbearably slow (see Figure 4.10) or collapsed altogether, preventing timely control of the charging power allowed for the wallboxes, while data was still being collected locally.

```

/var/local/NodeRed/cars/car4/auto4_20220308_0500.csv
2022-03-08 05:29:16;862549041878888;idle;47.45396;0;100;41.7137563274772;56.08
2022-03-08 05:30:16;862549041878888;idle;47.45396;0;100;41.7137563274772;56.08
2022-03-08 05:31:16;862549041878888;idle;47.45396;0;100;41.7137563274772;56.08
2022-03-08 05:32:16;862549041878888;idle;47.45396;0;100;41.7137563274772;56.08
2022-03-08 05:33:16;862549041878888;idle;47.45396;0;100;41.7137563274772;56.08
2022-03-08 05:34:16;862549041878888;idle;47.45396;0;100;41.7137563274772;56.08
2022-03-08 05:35:16;862549041878888;idle;47.45396;0;100;41.7137563274772;56.08
2022-03-08 05:36:16;862549041878888;idle;47.45396;0;100;41.7137563274772;56.08
2022-03-08 05:37:16;862549041878888;idle;47.45396;0;100;41.7137563274772;56.08
2022-03-08 05:38:16;862549041878888;idle;47.45396;0;100;41.7137563274772;56.08
2022-03-08 05:39:16;862549041878888;idle;47.45396;0;100;41.7137563274772;56.08
2022-03-08 05:40:16;862549041878888;idle;47.45396;0;100;41.7137563274772;56.08
2022-03-08 05:41:16;862549041878888;idle;47.45396;0;100;41.7137563274772;56.08
2022-03-08 05:42:16;862549041878888;idle;47.45396;0;100;41.7137563274772;56.08
2022-03-08 05:43:16;862549041878888;idle;47.45396;0;100;41.7137563274772;56.08
2022-03-08 05:44:16;862549041878888;idle;47.45396;0;100;41.7137563274772;56.08
2022-03-08 05:45:16;862549041878888;idle;47.45396;0;100;41.7137563274772;56.08
2022-03-08 05:46:17;862549041878888;idle;47.45396;0;100;41.7137563274772;56.08
2022-03-08 05:47:17;862549041878888;idle;47.45396;0;100;41.7137563274772;56.08
2022-03-08 05:48:17;862549041878888;idle;47.45396;0;100;41.7137563274772;56.08
2022-03-08 05:49:17;862549041878888;idle;47.45396;0;100;41.7137563274772;56.08
2022-03-08 05:50:17;862549041878888;idle;47.45396;0;100;41.7137563274772;56.08
2022-03-08 05:51:17;862549041878888;ride;47.454304;0;null;null;87.06
2022-03-08 05:52:17;862549041878888;ride;47.454304;0;null;null;87.06
2022-03-08 05:53:17;862549041878888;ride;47.454304;0;null;null;87.06
2022-03-08 05:54:17;862549041878888;ride;47.454304;0;null;null;87.06

```

Figure 4.9: SOC measurement problems

```

PING 10.8.0.10 (10.8.0.10) 56(84) bytes of data.
64 bytes from 10.8.0.10: icmp_seq=1 ttl=64 time=2434 ms
64 bytes from 10.8.0.10: icmp_seq=2 ttl=64 time=1433 ms
64 bytes from 10.8.0.10: icmp_seq=3 ttl=64 time=420 ms
64 bytes from 10.8.0.10: icmp_seq=4 ttl=64 time=118 ms
64 bytes from 10.8.0.10: icmp_seq=5 ttl=64 time=74.0 ms
64 bytes from 10.8.0.10: icmp_seq=6 ttl=64 time=207 ms
64 bytes from 10.8.0.10: icmp_seq=7 ttl=64 time=76.1 ms
64 bytes from 10.8.0.10: icmp_seq=8 ttl=64 time=74.8 ms
64 bytes from 10.8.0.10: icmp_seq=9 ttl=64 time=584 ms
64 bytes from 10.8.0.10: icmp_seq=10 ttl=64 time=65.9 ms
64 bytes from 10.8.0.10: icmp_seq=11 ttl=64 time=238 ms
64 bytes from 10.8.0.10: icmp_seq=12 ttl=64 time=66.5 ms
64 bytes from 10.8.0.10: icmp_seq=13 ttl=64 time=6765 ms
64 bytes from 10.8.0.10: icmp_seq=14 ttl=64 time=6249 ms
64 bytes from 10.8.0.10: icmp_seq=15 ttl=64 time=5235 ms
64 bytes from 10.8.0.10: icmp_seq=16 ttl=64 time=4222 ms
64 bytes from 10.8.0.10: icmp_seq=17 ttl=64 time=3209 ms
64 bytes from 10.8.0.10: icmp_seq=18 ttl=64 time=2195 ms
64 bytes from 10.8.0.10: icmp_seq=19 ttl=64 time=1182 ms
64 bytes from 10.8.0.10: icmp_seq=20 ttl=64 time=182 ms
64 bytes from 10.8.0.10: icmp_seq=21 ttl=64 time=8680 ms
64 bytes from 10.8.0.10: icmp_seq=22 ttl=64 time=8570 ms
64 bytes from 10.8.0.10: icmp_seq=23 ttl=64 time=7556 ms
64 bytes from 10.8.0.10: icmp_seq=24 ttl=64 time=6543 ms

```

Figure 4.10: VPN tunnel problems

In other cases, the LRP stopped working altogether due to software and hardware issues (see Figure 4.11), leaving gaps of hours (and in rarer instances days) in the data collected. Unless the issue could be resolved remotely, a maintenance technician from Vlotte had to go onsite and solve the problem in order for the data collection to resume.

```

pi@RevPi12153:~$ df
Filesystem      1K-blocks    Used Available Use% Mounted on
/dev/root        3643560 3460372    0 100% /
devtmpfs         469908      0  469908   0% /dev
tmpfs            474516      0  474516   0% /dev/shm
tmpfs            474516    6372  468144   2% /run
tmpfs            5120         4    5116   1% /run/lock
tmpfs            474516      0  474516   0% /sys/fs/cgroup
/dev/mmcbblk0p1  42131    22139   19992  53% /boot
tmpfs            94900      0   94900   0% /run/user/1000
/dev/sdal        15319488 1462140 13079164 11% /var/local/NodeRed
pi@RevPi12153:~$
    
```

Figure 4.11: LRP downtime due to running out of storage

To make matters worse, the BESS was not tested prior to the field test and despite all optimism turned out to be defective, not accepting any charge at all (see column “Kreisel-SOC” in Figure 4.12). Sadly, it was not possible to obtain a replacement from the manufacturer during the course of the field test.

TimeDate	PV-W	Kreisel	Arbeitsmodus	Kreisel-Ladeleistung	Kreisel-Entladeleistung	Kreisel-SOC
2022-03-04 09:13:07	2210		self use mode	0	0	0
2022-03-04 09:13:22	2208		self use mode	0	0	0
2022-03-04 09:13:37	2200		self use mode	0	0	0
2022-03-04 09:13:52	2224		self use mode	0	0	0
2022-03-04 09:14:07	2219		self use mode	0	0	0
2022-03-04 09:14:22	2212		self use mode	0	0	0
2022-03-04 09:14:37	2219		self use mode	0	0	0
2022-03-04 09:14:52	2216		self use mode	0	0	0

Figure 4.12: BESS not accepting charge despite PV power availability

4.3.2 Driving Profiles

4.3.2.1 Vehicle Departure Times

Since one of the most interesting metrics for DSM is the deadline, by which the electric vehicle needs to be charged as much as possible, we first look at the departure times of the five vehicles in the field test.

In Figure 4.13, we plot the vehicles' departure times and immediately see that there seems to have been a problem with car #2. Indeed, car #2 was largely incompatible with the DCD and therefore hardly any usable data was gathered. While the median of the departure time ranges between 7 and 11 a.m. for the remaining cars, car #4 has minima of leaving as early as 4 a.m. while car #3 has maxima of leaving as late as midnight.

4.3.2.2 Driving & Charging Periods

In order to create meaningful predictions or scenarios for the charging strategy models, there needs to be a minimum of event data available. Considering all the problems during the field test, a certain amount of skepticism about the data quality was in order.

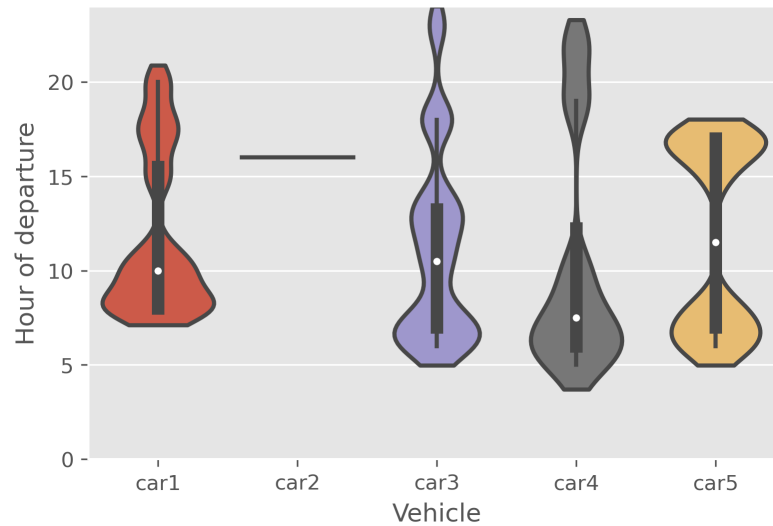


Figure 4.13: Vehicle Departure Times

As can be seen in the heatmap depicted in Figure 4.14, there are actually no events of driving recorded for car #2. Moreover, during the 2nd week of the field test, the data recorded say that car #3 was only driving, while the other cars were only charging. Week 4 also shows a strange picture, in that the vehicles were more driving than charging, with car #5 seemingly driving non-stop without charging at all.

All in all, due to the problems in data acquisition on the LRP side of things, hardly any reliable driving profiles could be obtained.

4.3.3 Optimization Runs

Despite the aforementioned issues with data acquisition, we will inspect select examples of the documented optimization runs, since they still give us insight into the operation of the various charging strategies.

4.3.3.1 Direct Charging

As expected, the direct charging strategy causes the vehicles to draw power at maximum rate (see Figure 4.15), hitting the maximum allowable combined grid draw for the first few periods until the respective SOC of the EVs has reached maximum levels. We can also see that there is hardly any driving activity predicted for the look ahead horizon, due to the aforementioned lack of overall driving activity.

Looking at the curves for PV production (yellow in the top plot) and the BESS SOC (black in the bottom plot), it becomes obvious that the sizing of either is far too small to make any difference, even considering the time of year (March) where PV output is not at its maximum.

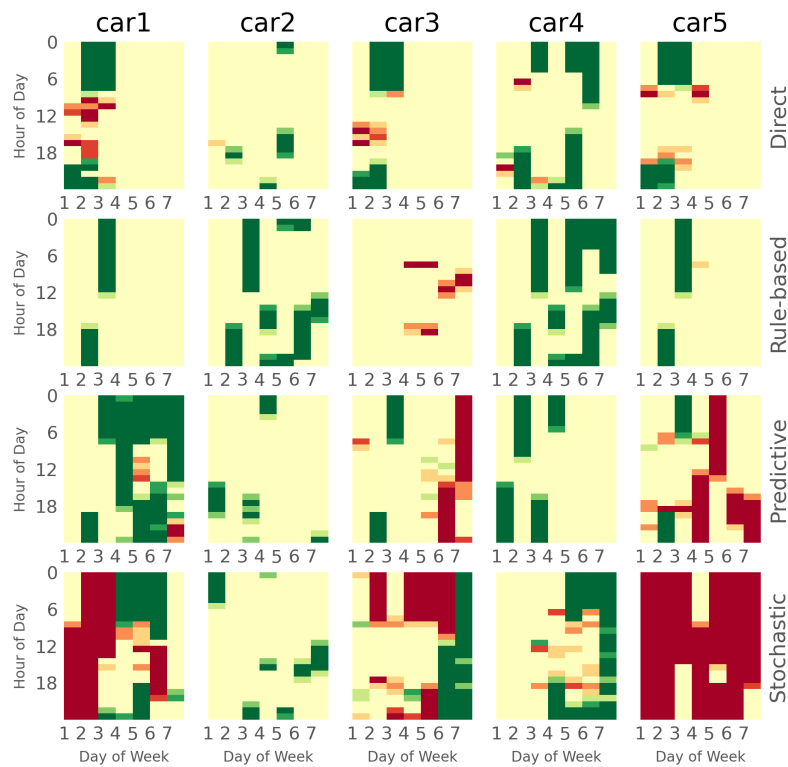


Figure 4.14: Charging & Driving Periods
(red = driving, green = charging)

4.3.3.2 Rule-based Charging

Similar to the direct charging strategy, we can see in Figure 4.16 that the grid draw ceiling hits the maximum allowable grid draw at the beginning of the observation period. At the same time, when comparing the combined grid draw of both strategies, it becomes clear that the rule-based charging strategy helps to more quickly reduced the maximum grid draw as the SOC of the EVs increases.

4.3.3.3 Predictive Charging

The predictive charging strategy is the first approach that actually tries to optimize peak power consumption by shifting loads throughout the look ahead horizon. Comparing the maximum grid draw to the two previous examples shows a big difference: Where the non-peak shaving models hit the maximum allowable power limit, predictive charging spreads out the charging power demand across the look ahead horizon (see Figure 4.17), taking down the maximum value from 35 to just 5.7 kW. In addition, we can see that the model tries to take advantage of the PV power by not only charging the EVs, but also storing energy in the BESS for later use in the day.

Note that since the BESS didn't really work during the field test, the starting value is always going to be zero and the model being unaware of this thinks it can use the BESS for energy storage, which in fact will not be the case.

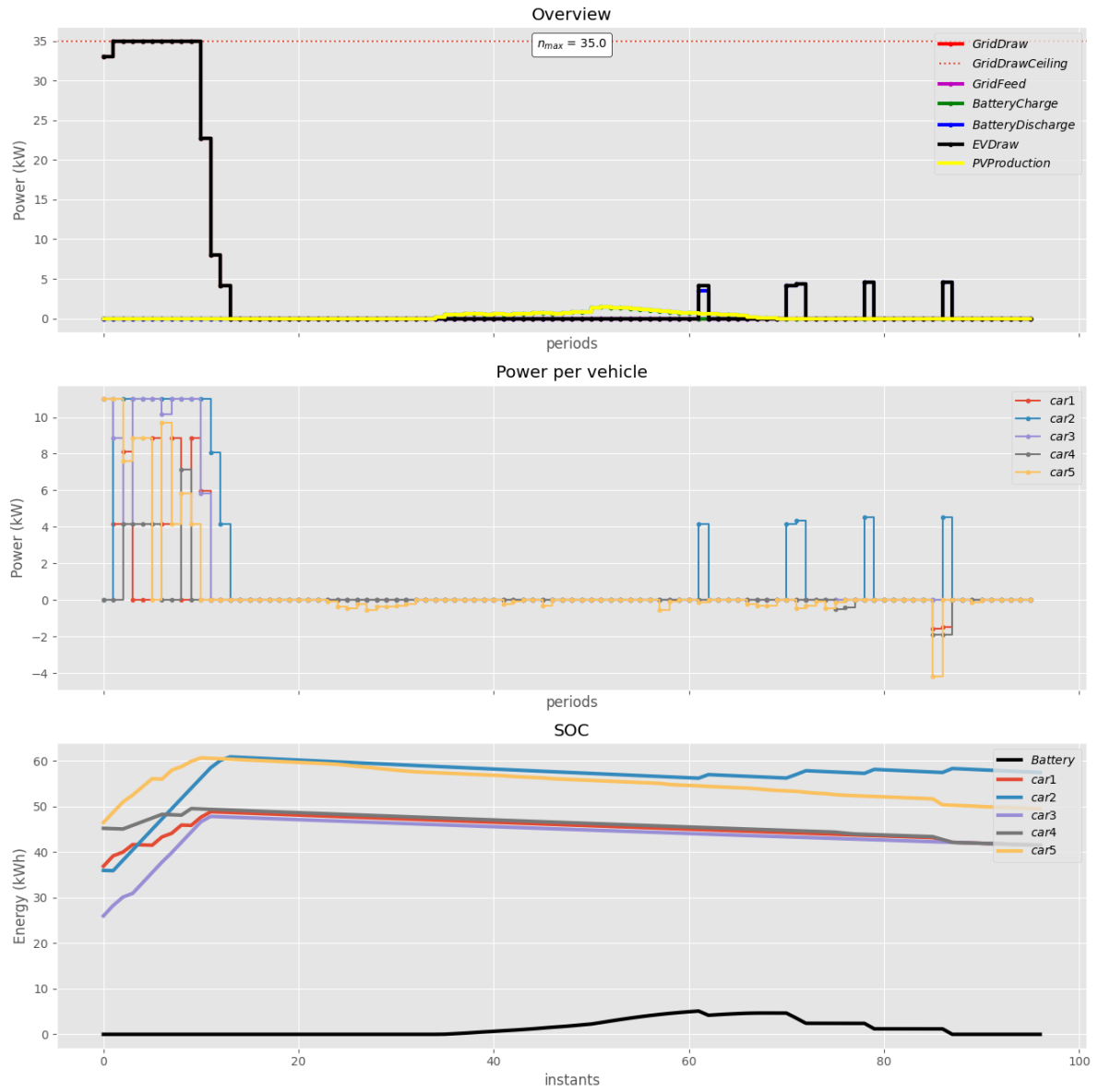


Figure 4.15: Direct Charging - Solution Timeseries example from 2022-03-13 00:10:54

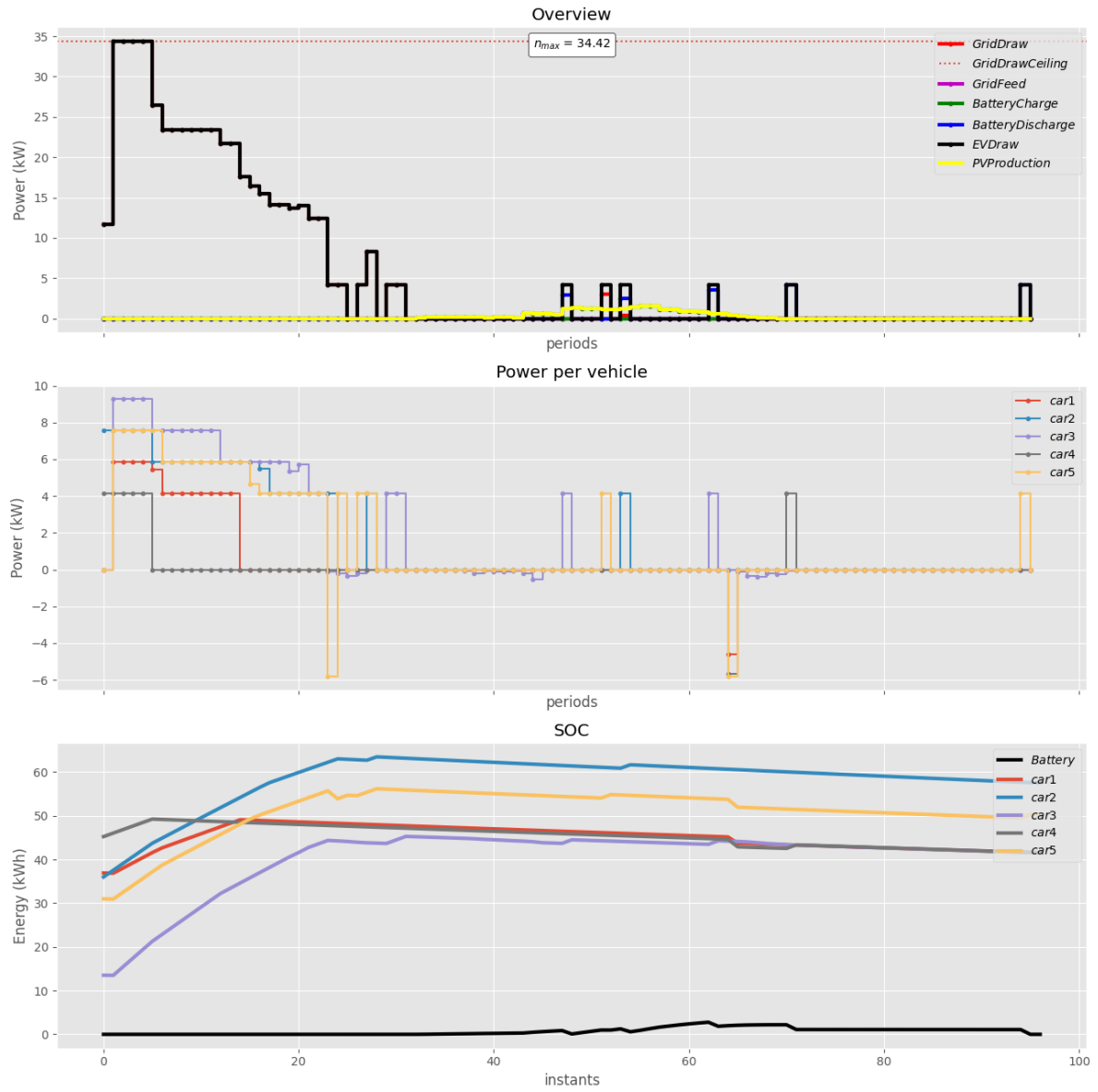


Figure 4.16: Rule-based Charging - Solution Timeseries example from 2022-03-20 00:10:23

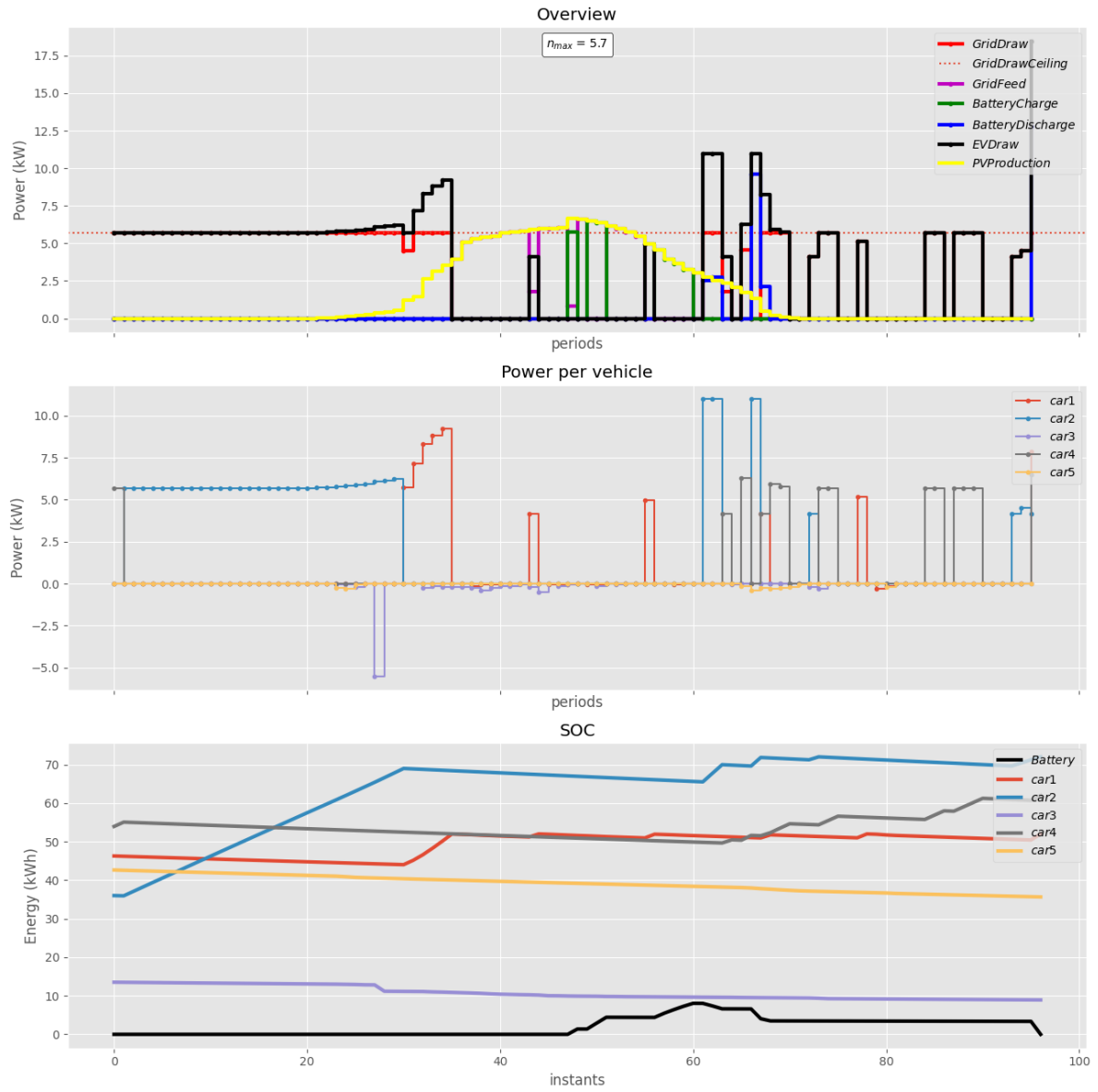


Figure 4.17: Predictive Charging - Solution Timeseries example from 2022-03-27 00:10:26

4.3.3.4 Stochastic Charging

As described earlier, the stochastic charging strategy is an extension of the deterministic charging strategy model where the prediction of the future periods of the look ahead horizon are replaced with numerous scenarios from historic data, thus optimizing the expected value against a much broader set of possible future developments.

Note that the first period resembles stage one in our stochastic model, meaning that these values represent what is happening now (see Figure 4.18), while all future values in the plot denote possible future scenarios or stage two. These future scenarios are plotted in lighter colors, while their expected value is plotted with a more solid color. To highlight the range of the values, the standard deviation is plotted and the areas between are hatched to show the most likely range of values within the scenarios considered.

Comparing the time series of the stochastic solution, we see that the maximum grid draw could be reduced even further, from 5.7 to 4.14 kW, which is also the minimum allowable EV charging power in our field test setup.

4.3.4 Peak Shaving

As outlined in section 2.3.1, we evaluate the effectiveness of a charging strategy in terms of peak shaving by four key metrics applied to the power draw from the LVG: Maximum, average, standard deviation and PAPR. Inspecting Figure 4.19 confirms what we already saw section 4.3.3, namely that the direct charging strategy has the highest maximum grid draw, with the average not being far below the peak. Introducing additional rules that reduce the grid draw the higher the EV SOC improves the situation already considerably, reducing the average power draw to slightly below 12 kW, while still having peaks at the maximum allowable grid draw. As expected, the maximum grid draw is greatly reduced to below 13 kW with strategies that minimize the maximum grid draw, like in the case of the predictive and stochastic charging strategies.

A closer look at the same metrics in Table 4.4 reveals that the standard deviation is inversely related to the sophistication of the charging strategy used, as we expected. As somewhat of a surprise, however, the PAPR metric actually increased the more the maximum grid draw was reduced. This means that while actually reducing maximum and average grid draw values alike, which is the effect desired for peak shaving, the PAPR metric looks worse and thus might lead to wrong conclusions, which confirms our initial conjecture that the standard deviation might be the more practical metric to use for evaluating peak shaving effectiveness in situations where not only the maximum is lowered, but the average grid draw as well.

	Maximum [kW]	Average [kW]	Std. Deviation [kW]	PAPR
Direct	35.00	21.65	14.64	1.62
Rule-based	35.00	12.81	7.34	2.73
Predictive	12.42	4.98	2.81	2.49
Stochastic	10.94	3.10	2.47	3.53

Table 4.4: Grid Draw per Strategy

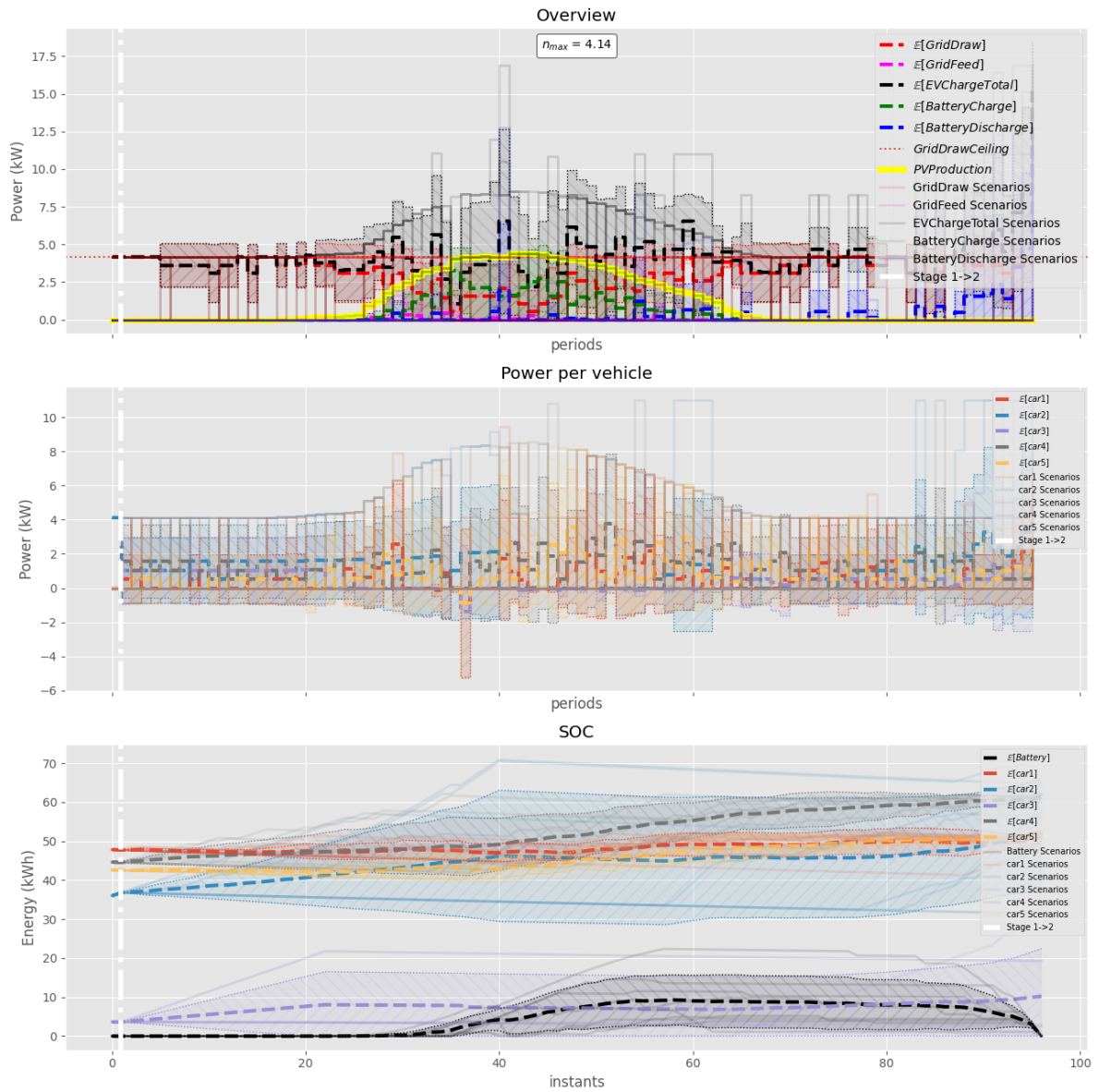


Figure 4.18: Stochastic Charging - Solution Timeseries example from 2022-03-31 00:10:40

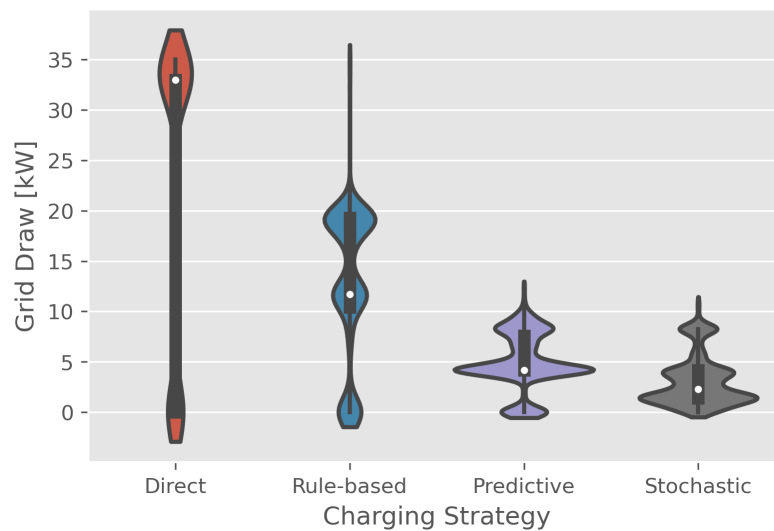


Figure 4.19: Grid Draw per Strategy

4.3.5 Charging Comfort

As we already pointed out in section 4.3.1, due to the absence of SOC data from car #2 we will not be able to evaluate the charging comfort experienced by drivers of that particular electric vehicle. For the remaining four vehicles, however, we were able to extract some of the average EV SOC_s at the time of departure, grouped by the respective charging strategy in Figure 4.20, with gray squares resembling missing data.

Judging from the heatmap, charging comfort never fell below the critical value of 50 %, meaning that the drivers were probably mostly happy about the charging level at the time of departure. For the direct charging strategy, however, we would have expected much higher values, but the issues with data quality already mentioned numerous times probably prevented a more complete measurement.

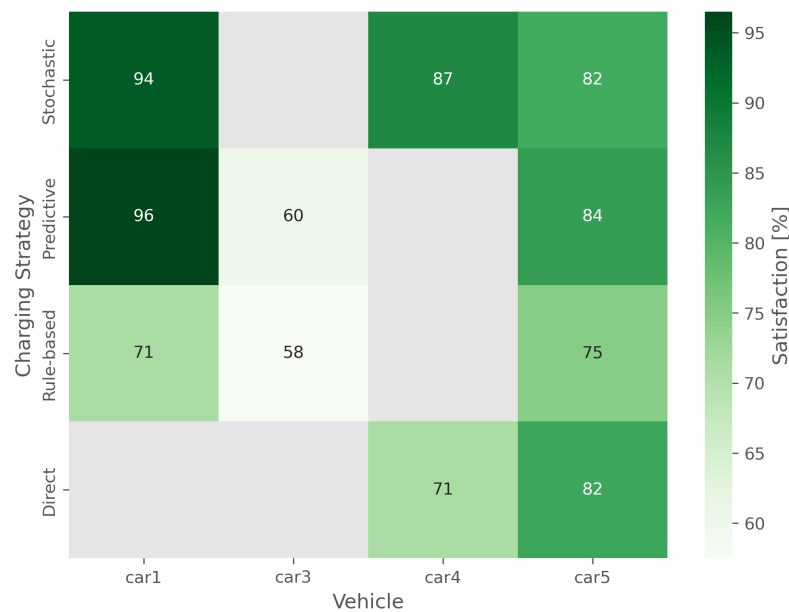


Figure 4.20: Charging Comfort per Vehicle

If we leave the individual vehicles out of the picture and aggregate the data on charging strategy level as depicted in Figure 4.21, we can see that the direct charging strategy did indeed yield maximum values of 90 % satisfaction, while also dipping below 60 % in some cases. Surprisingly, the rule-based charging strategy did considerably worse, both in maximum and average satisfaction, which might partially be explained by the aforementioned data acquisition problems. With predictive and stochastic charging strategies, it was possible to achieve over 86 % median satisfaction, with a outlier in case of the former dipping into 30 % territory.

Looking more closely at the numbers in Table 4.5, we can see that - had it not been for the outlier in case of the predictive charging strategy - the standard deviation of the charging comfort levels achieved by predictive and stochastic charging are greatly improved, suggesting consistently high satisfaction levels on the part of the vehicles' drivers.

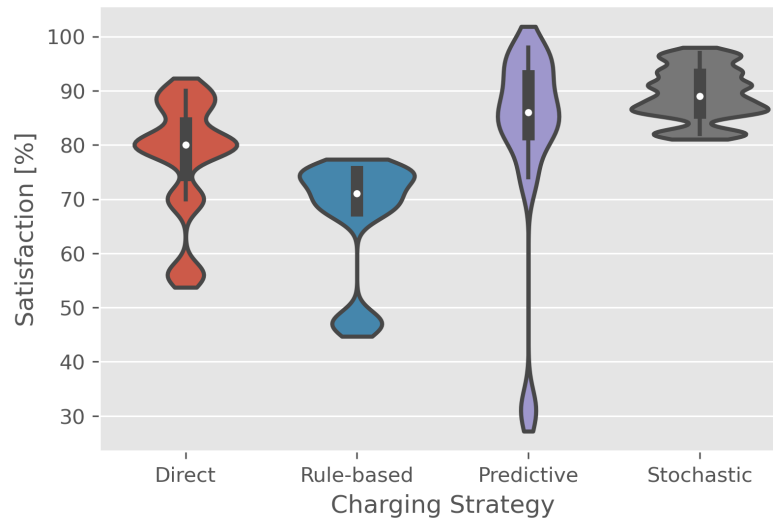


Figure 4.21: Charging Comfort per Strategy

	Maximum Satisfaction [%]	Minimum Satisfaction [%]	Std. Deviation Satisfaction [%]	Median Satisfaction [%]
Direct	90.0	56.0	11.44	80.0
Rule-based	75.0	47.0	11.67	71.0
Predictive	98.0	31.0	19.20	86.0
Stochastic	97.0	82.0	4.84	89.0

Table 4.5: Charging Comfort per Strategy

4.3.6 Computation Time

The actual optimization runs were executed on the RFS, which contained an Intel i7-3770 CPU (4 cores, 8 threads, 16 GB RAM) running a Linux operating system.

Considering that the charging process of electric vehicles is usually measured in hours and not seconds, we designed the system for near real-time operation, scheduling the computation of new maximum charging power values every 15 minutes. Looking at Figure 4.22, we can see that the rather simple direct charging strategy usually ran quite quickly, averaging at six seconds per optimization run, with some outliers taking as long as over 200 seconds to complete. Surprisingly, the rule-based strategy took considerably longer, averaging at over 160 seconds per optimization run with lots of variance between the individual runs. The predictive charging strategy ran quite quickly, averaging only slightly above the simpler direct charging strategy. Lastly, with the stochastic charging strategy we can see the reason why this plot had to be log-scaled on the y-axis: Not only is the average well above 600 seconds, but the optimization runs also hit the time limit of 1200 seconds quite often, resulting in a non-optimal solution of the optimization problem.

Inspecting the numbers in Table 4.6, we conclude that from a computation time standpoint, the direct and predictive charging strategies are good choices to calculate new maximum charging power values as often as possible, while stochastic charging clearly was too demanding for the configuration and settings of this field test.

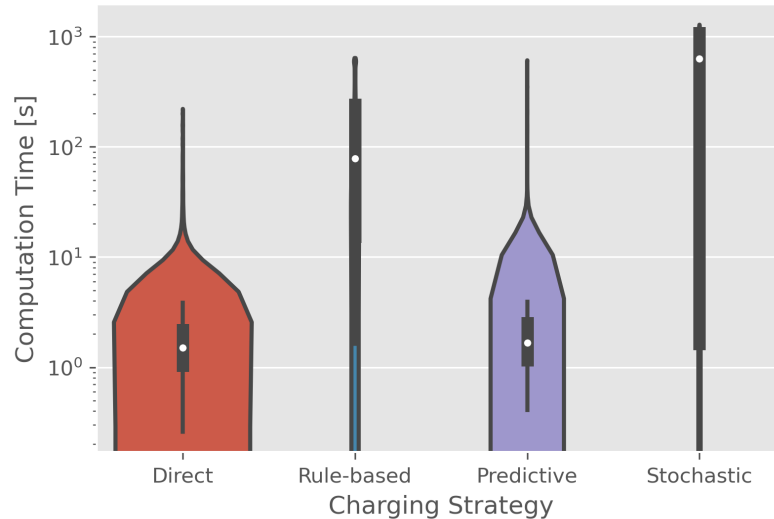


Figure 4.22: Computation Time per Strategy

	Maximum Computation Time [s]	Minimum Computation Time [s]	Std. Deviation Computation Time [s]	Average Computation Time [s]
Direct	216.26	0.26	22.58	6.09
Rule-based	600.44	1.64	198.01	167.48
Predictive	601.00	0.41	43.46	7.87
Stochastic	1197.99	1.02	422.96	617.54

Table 4.6: Computation Time per Strategy

4.4 Discussion

Despite the planning for the field test already having started well in advance of its execution, the high number of problems clearly shows that not enough time can be spent on preparation and testing. While chance will always introduce some problems into real world implementations, in hindsight we feel that many issues could have been avoided had more time been spent on testing the hardware side of the implementation, unfortunately outside of the author's influence. Nonetheless, we did our utmost to prevent the field test from failing entirely, capturing the data that was available and analyzing it. A big part in saving the field test from failing entirely was the use of a best-of-breed data pipelining framework like Kedro, which allowed for quick fixes in the code to address the numerous issues as they came up.

Being a complete LVG + PV + BESS configuration, the sizing of the components at the LiLa prototype facility clearly shows its age (apart from the BESS failing altogether). With the advent of electric vehicles sporting 50 kWh batteries and above in the mainstream market, a BESS half that size for more than five EVs clearly is no longer sufficient for serious DSM efforts. In addition, allowing it to only be charged by equally under-sized PV also hampered more impactful load shifting, especially considering that the most important charging periods do not coincide with peak PV generation.

It could be shown that advanced charging strategies can make a huge difference in reducing the peak power draw from the grid, greatly improving grid friendliness from the point of view of the grid operators. At the same time, the shifting of the loads did not impede charging comfort from the point of view of the vehicles' drivers, with satisfaction levels always remaining in the non-critical

range of above 50 %. In addition, it appears that the computation time for the optimization can be brought down to sub-minute level, well supporting the idea of near real-time operation.

By means of the field test, we were able to verify hypothesis #1, in that our - admittedly sparse - historical data is suitable for the prediction of future loads, which can clearly be seen by comparing the results of the direct and rule-based charging and the predictive and stochastic charging strategies side by side. Considering all the data acquisition issues during the field test, we have to defer evaluating hypothesis #3 to the simulation studies. Inspecting Figure 4.20 and Figure 4.21 we see hypothesis #4 confirmed in that predictive and stochastic charging actually even raised the charging comfort experienced by the vehicles' drivers. Lastly, hypothesis #5 is also verified, with the predictive charging strategy well within the defined 15 minute time window of charging power updates to the LRP.

Looking at Table 4.4, we can also verify hypothesis #2, in that stochastic charging yielded a lower maximum and average grid draw as well as the lowest standard deviation out of all strategies applied. Moreover, we are also able to partially answer the main research question of this thesis as follows: Predictive charging reduced the peak load in our field test by 64.5 %, stochastic charging by a slightly higher 68.7 %.

5 Simulation Studies

Since the insights generated by the field test were rather limited by the data acquisition issues described in the last chapter, we proceed to study the ESM in more detail by simulating various combinations of configurations and charging strategies using better quality data. In general, we will be reusing most of the definitions and models introduced in the previous chapters, exploring a wider range of configurations regarding PV and BESS sizings to test the sensitivity on the main metrics. In addition, we will inspect additional metrics like the PV self-sufficiency- and self-consumption-rate, as well as compute key optimization metrics like the VSS and the EVPI.

5.1 Setup

5.1.1 Data

For our simulation studies, we use data of much better quality, kindly put together by Rheinberger [60] for researchers trying to apply DSM principles to real world data [61]. In essence, this repository provides programs that will process raw data from various sources and preprocess them for maximum consistency, resulting in a dataset that offers a whole year worth of data in quarter-hourly resolution. In our case, that parts of highest interest are the photovoltaic production as well as the electric vehicle driving patterns.

5.1.1.1 Electric vehicles

The vehicles in this dataset have a maximum battery capacity of 40 kWh, which is what we will be using as the upper bound for the optimization runs. For starting conditions, we assume all EVs to have 50 % SOC.

5.1.1.2 PV generation

The PV generation data in this dataset will be scaled to reasonable peak value, based on the simulation plan.

5.1.2 Simulation planning

In essence, we want to apply the charging strategies described in section §3.2 and already used in the field test (see Table 4.1) to higher quality data. In terms of factors, we want to understand the effects of various system configurations, as already described in section §3.1, giving us 20 base scenarios to simulate (see Table 5.1).

System Configuration	Charging Strategy				
	Direct charging	Rule-based charging	Predictive charging	Stochastic charging	Perfect Information
LVG only	#01	#02	#03	#04	#05
LVG + PV	#06	#07	#08	#09	#10
LVG + BESS	#11	#12	#13	#14	#15
LVG + PV + BESS	#16	#17	#18	#19	#20

Table 5.1: Combinations of base scenarios to be examined

However, we also want to more clearly understand the sensitivities of the key metrics described in section §2.3, which is why we not only simulate the extreme configuration options described in Table 3.1, but take a more fine-grained approach by exploring the values in between. This is done by redefining the binary features ‘PV’ and ‘BESS’ into linear space ranging from 0 to 100 % of the respective nominal capacity value. In order to get a reasonable amount of supporting data points for later analysis, we propose values of 0, 25, 50, 75 and 100 % of the maximum size for both PV and BESS each, resulting in 25 combinations to simulate for each of the 5 charging strategies.

$$pv_{peak}^{out} = \{0, .25, .50, .75, 1\} * pv_{max}^{out} \quad (5.1)$$

$$B_{max} = \{0, .25, .50, .75, 1\} * B_{max,sys} \quad (5.2)$$

Thus, we are going to simulate 125 different configuration combinations (see Table 5.2), which allows us to see the sensitivities between the maximum and minimum settings as well as the values at the extremes.

System Configuration		Charging Strategy				
PV [%]	BESS [%]	Direct charging	Rule-based charging	Predictive charging	Stochastic charging	Perfect Information
0	0	#001	#002	#003	#004	#005
0	25	#006	#007	#008	#009	#010
⋮	⋮	⋮	⋮	⋮	⋮	⋮
100	75	#116	#117	#118	#119	#120
100	100	#121	#122	#123	#124	#125

Table 5.2: Combinations of sensitivity scenarios to be examined

With the relative values and step sizes determined, the question still remains which values to choose for pv_{max}^{out} and $B_{max,sys}$. For the latter, we choose to set the maximum value to the capacity of the

batteries in the electric vehicles - in our case 40 kWh - in order to be able to theoretically fully charge at least one EV with the BESS alone.

Since the focus of this thesis is not one of economic optimization, we dispense with the sizing guidelines put forward by [62], recommending to minimize BESS sizing for maximum economic efficiency, and instead follow the analysis of [63], which recommends a ratio of PV to BESS size of roughly $\frac{3}{4}$. For sake of simplicity and following the findings of R uf [3], we will extend the explored parameter space to a ratio of 1, giving us maximum boundary values of 40 kWp and 40 kWh for PV and BESS respectively.

In order to further reduce the problem size in favor of a larger parameter space, we reduce - without loss of generality - the resolution of the data from quarter-hourly to hourly by resampling. In addition, we simulate a single 24 hour day from the dataset (namely the 22nd of June 2016), using the 8 previous days of data for profile and scenario building and the day after for the perfect information model run.

The system specific configuration parameters used in the software implementation are listed in Table 5.3 for quick reference.

Symbol	Quantity	Unit	Value
Δt	time step	h	1.0
$ev_{v,min}^{in}$	minimum allowable EV v charging power	kW	4.14
$ev_{v,max}^{in}$	maximum allowable EV v charging power	kW	22.0
η_{EV}^{in}	efficiency factor for charging of EV		0.85
η_{EV}^{out}	efficiency factor for discharging of EV		0.85
ξ_{EV}	self-discharging factor of EV		0.9983
b_{min}^{in}	minimum allowable BESS charging power	kW	0.0
b_{min}^{out}	minimum allowable BESS discharging power	kW	0.0
b_{max}^{in}	maximum allowable BESS charging power	kW	12.78
b_{max}^{out}	maximum allowable BESS discharging power	kW	12.78
η_B^{in}	efficiency factor for charging of BESS		0.95
η_B^{out}	efficiency factor for discharging of BESS		0.95
ξ_B	self-discharging factor of BESS		0.9986
n_{max}^{out}	maximum allowable power draw from LVG	kW	35.0
n_{max}^{in}	maximum allowable power feed into LVG	kW	35.0
EV_{max}	maximum SOC of EVs	kWh	40.0
pv_{max}^{out}	maximum power of PV	kWp	40.0
$B_{max,sys}$	maximum SOC of BESS	kWh	40.0

Table 5.3: Configuration values used in the simulation studies

Finally, we initialize the BESS with an SOC of 50 %, while mandating it to end the 24 hour period with the same value it had at the beginning.

5.2 Results

We will be examining the results of the simulation runs in the following. We make the code for both simulation and analysis available publicly at [64].

5.2.1 Optimization Runs

5.2.1.1 Direct Charging

Looking at Figure 5.1, we can see a similar picture as in the field test, insofar as the electric vehicles immediately start to charge, causing a peak in the grid draw right at the beginning. Since the simulation initializes the BESS with 50 % SOC, we can see that the power drawn by the electric vehicles even exceeds the maximum grid draw by tapping into the BESS' power. Unlike the field test, the model makes good use of the available PV power to recharge the BESS without affecting maximum grid draw at all.

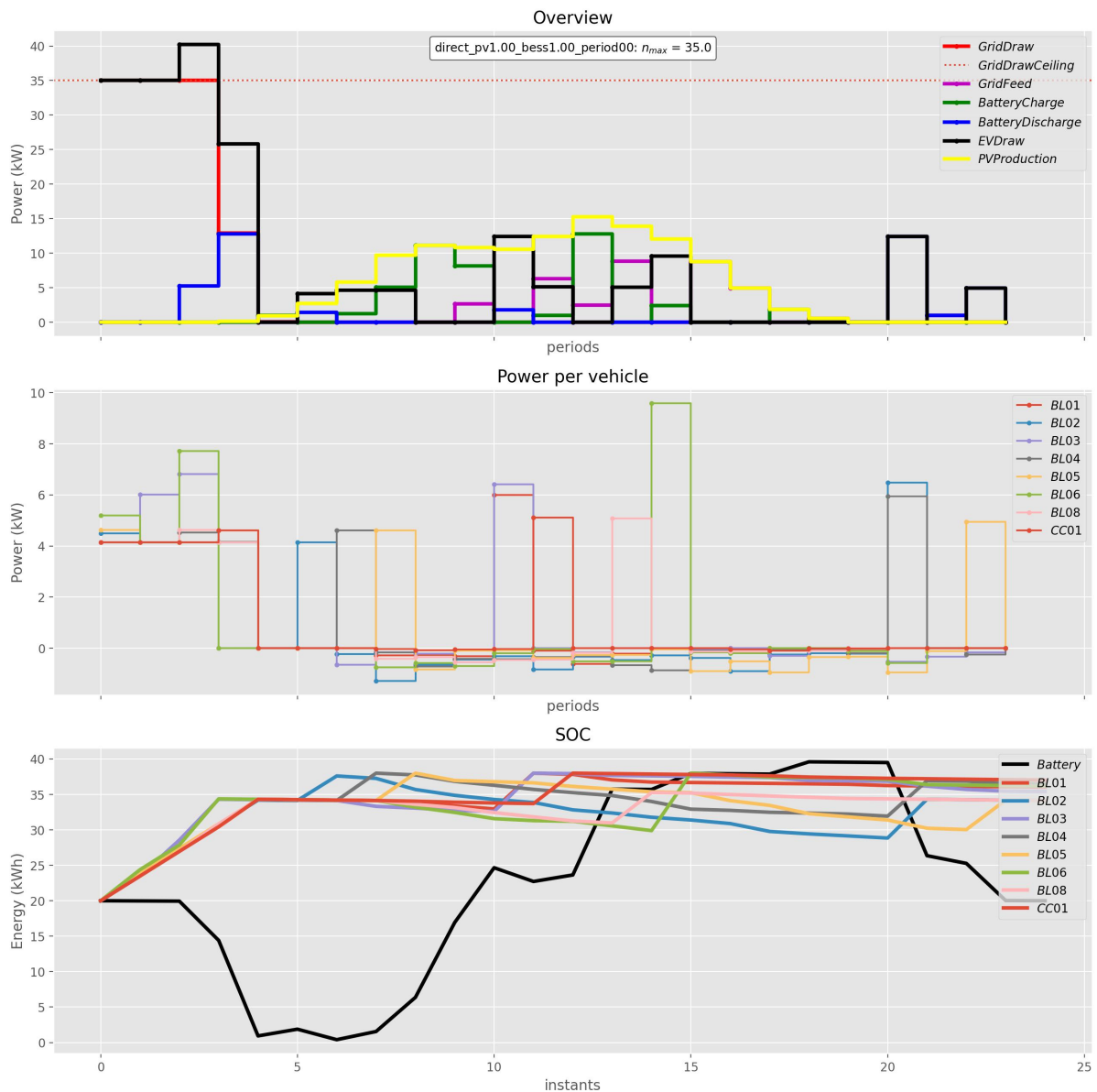


Figure 5.1: Direct Charging - Solution Timeseries example with 100 % PV & BESS

5.2.1.2 Rule-based Charging

In Figure 5.2, we can see that the initial conditions chosen result in an almost identical result compared to the direct charging strategy. This is caused by the fact that the 8 electric vehicles are already competing for power due to the constraint of the maximum power draw, leaving the rules depicted in Figure 3.5 without effect on the charging behavior.

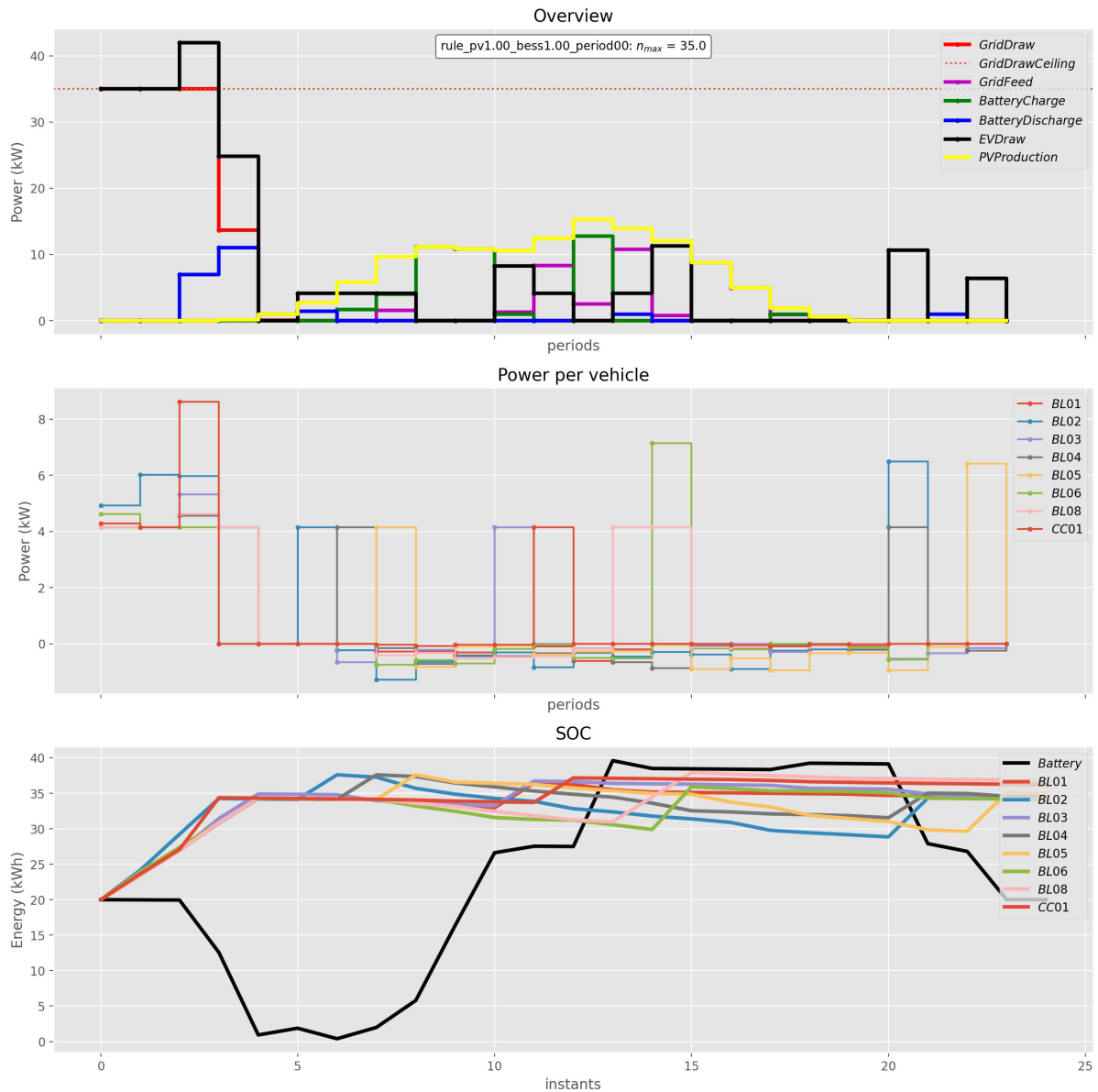


Figure 5.2: Rule-based Charging - Solution Timeseries example with 100 % PV & BESS

5.2.1.3 Predictive Charging

As expected considering theory and field test, the predictive charging strategy attempts to postpone charging some of the electric vehicles to later periods, greatly reducing peak power draw from the grid (see Figure 5.3). In this particular example we can also see how the model makes good use of the available PV and BESS, by using stored energy in the morning to quickly charge some of the available vehicles and recharging the BESS with excess PV energy for later use in the afternoon and evening.

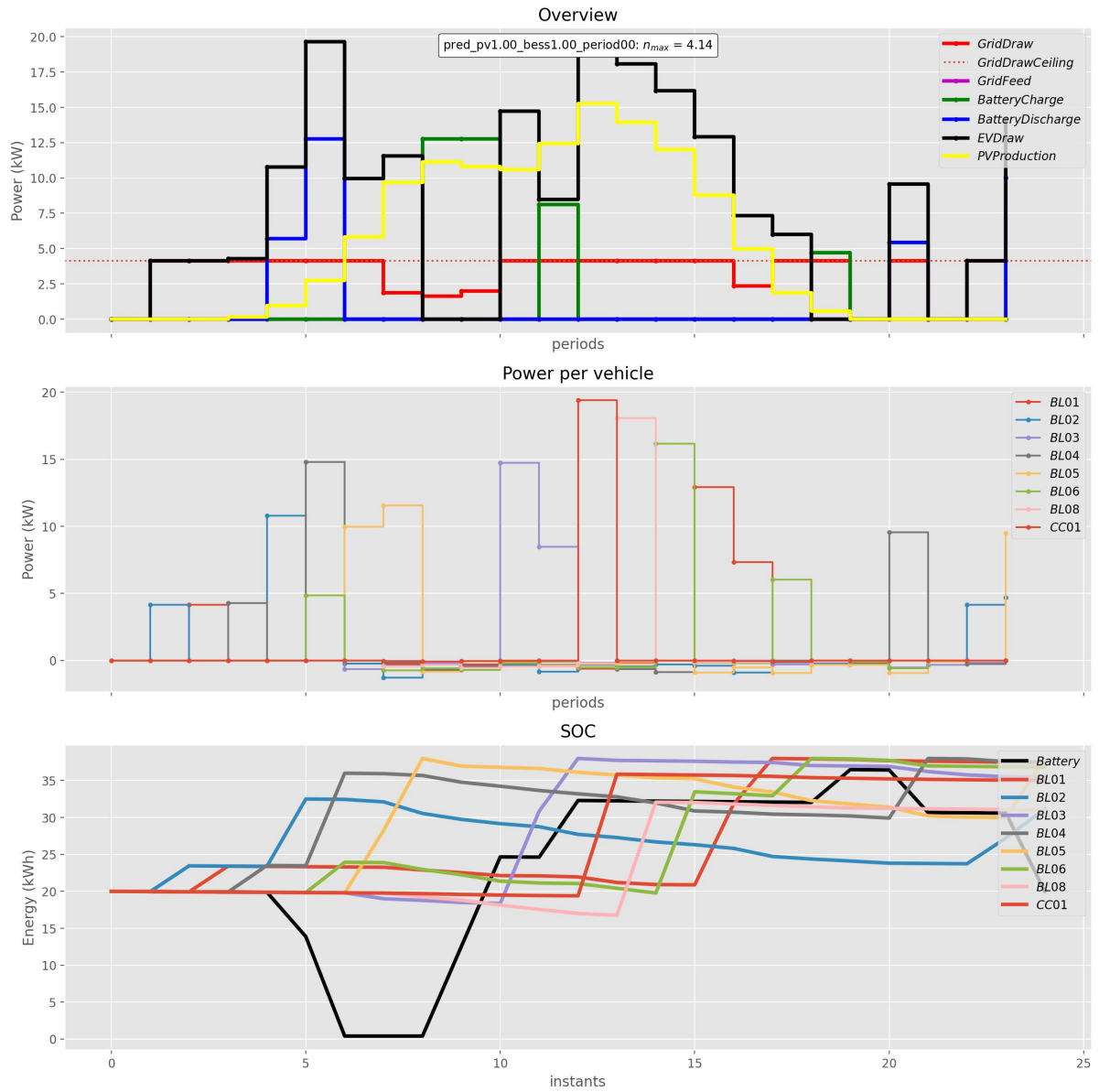


Figure 5.3: Predictive Charging - Solution Timeseries example with 100 % PV & BESS

5.2.1.4 Stochastic Charging

Inspecting Figure 5.4, we see how the stochastic charging strategy considers all future scenarios in (stage two) to make the optimal choice in the first period (stage one). More than in the field test, where predictive and stochastic charging were run at different times and thus on different data, we can see the subtle differences between the average-based prediction and the expected value of the scenarios. Where outliers in the historic data probably were flattened out by averaging over the values, their retention in the individual scenarios causes the model to arrive at a potentially more conservative solution, reducing the peak power draw from the grid less than in the predictive charging strategy.

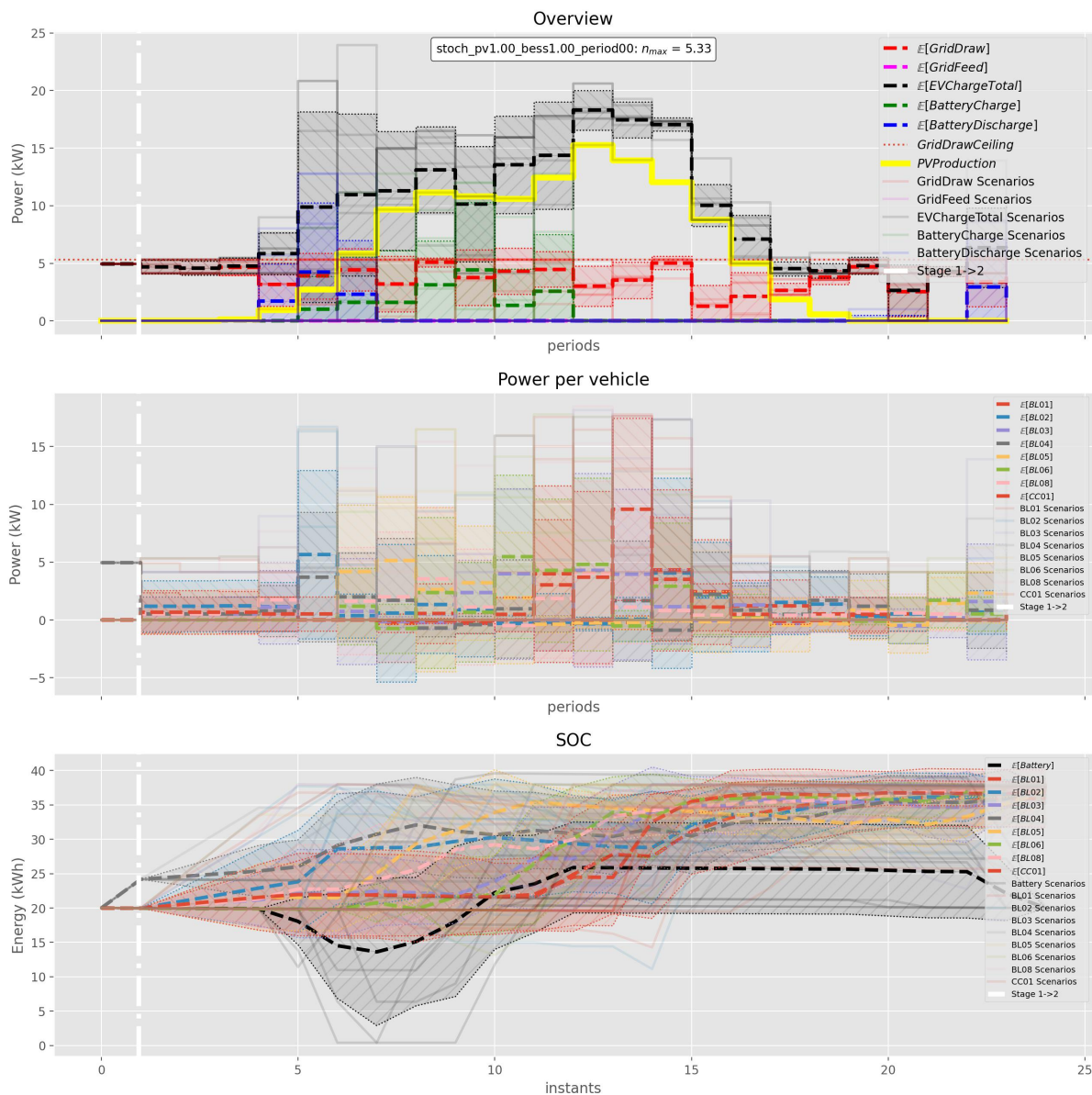


Figure 5.4: Stochastic Charging - Solution Timeseries example with 100 % PV & BESS

5.2.1.5 Perfect Information

Unlike in the live-run of the field test, we can compare all the previous charging strategies against a situation in which we have perfect information. Instead of making predictions or using scenarios to fill the look ahead horizon, this time we optimize against data that has actually happened. Not only was there more power from the PV, but the driving behavior of the vehicles themselves was also different from the prediction as well as the scenarios used in the previous models (see Figure 5.5). Since the model is the same as the one used for the predictive charging strategy, it is no surprise that they look quite similar.

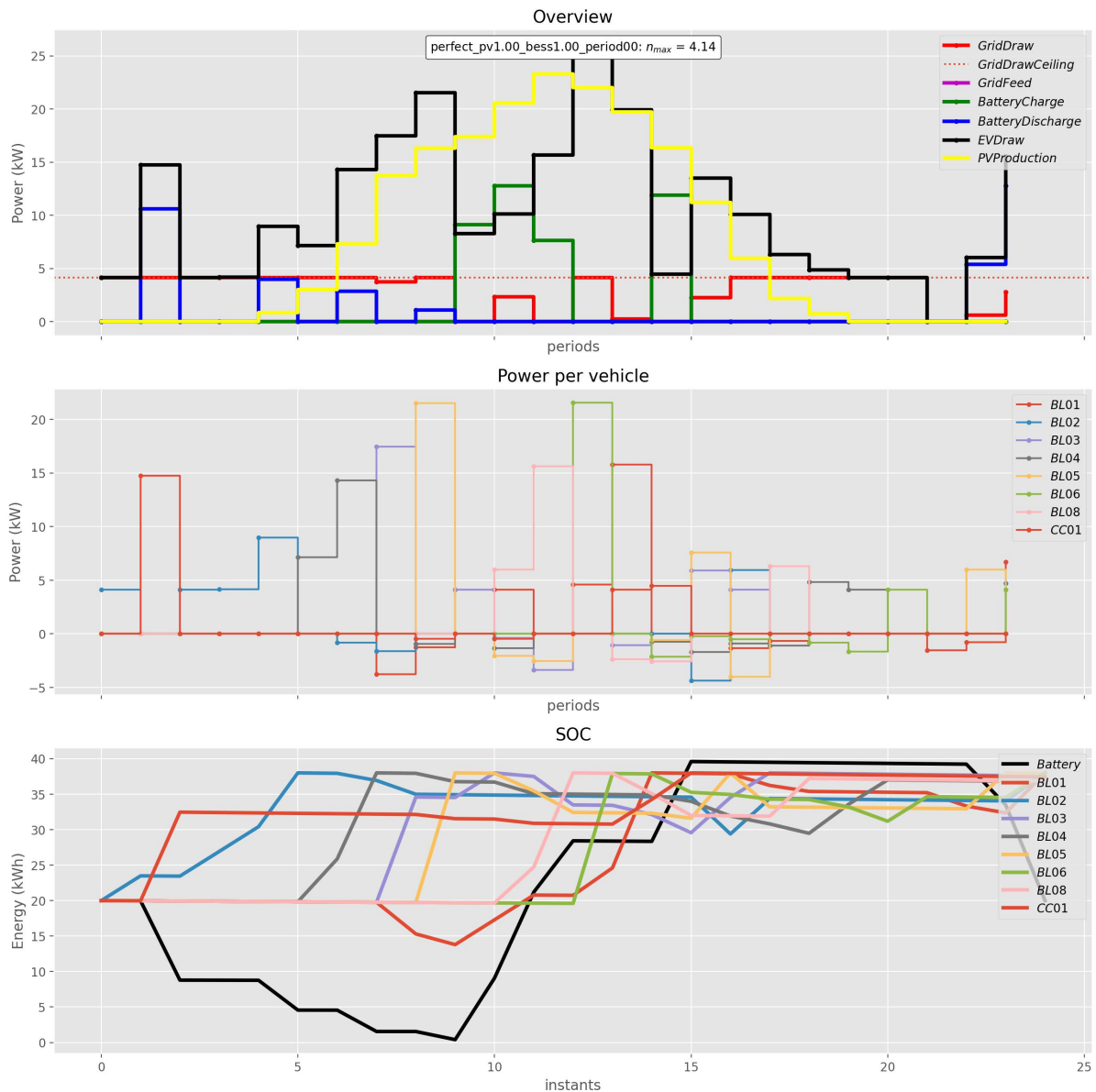


Figure 5.5: Perfect Information - Solution Timeseries example with 100 % PV & BESS

5.2.2 Peak Shaving

In order to see the influence of the PV and BESS configuration as factors on the individual metrics, we present the data using contour plots, applying a 2nd order least-squares model **Scipy2022** to the

raw data beforehand to make the effects easier to interpret.

5.2.2.1 Direct Charging

Looking at Figure 5.6, it is probably no surprise that regardless of the sizing of either PV and BESS, the maximum grid draw peaks at the allowable 35 kW mark. Adding PV to the configuration lowers the average grid draw from 11 to 7 kW, while the sizing of the BESS seems to have only a slightly positive effect. Without little to no PV power, adding more BESS capacity increases the standard deviation due to the fact that all charging activities have to come from the power grid. As explained in the analysis of the field test, we can see the PAPR increase with the amount of PV power added to the system, while the sizing of the BESS having a slightly negative (if any) effect in this charging strategy.

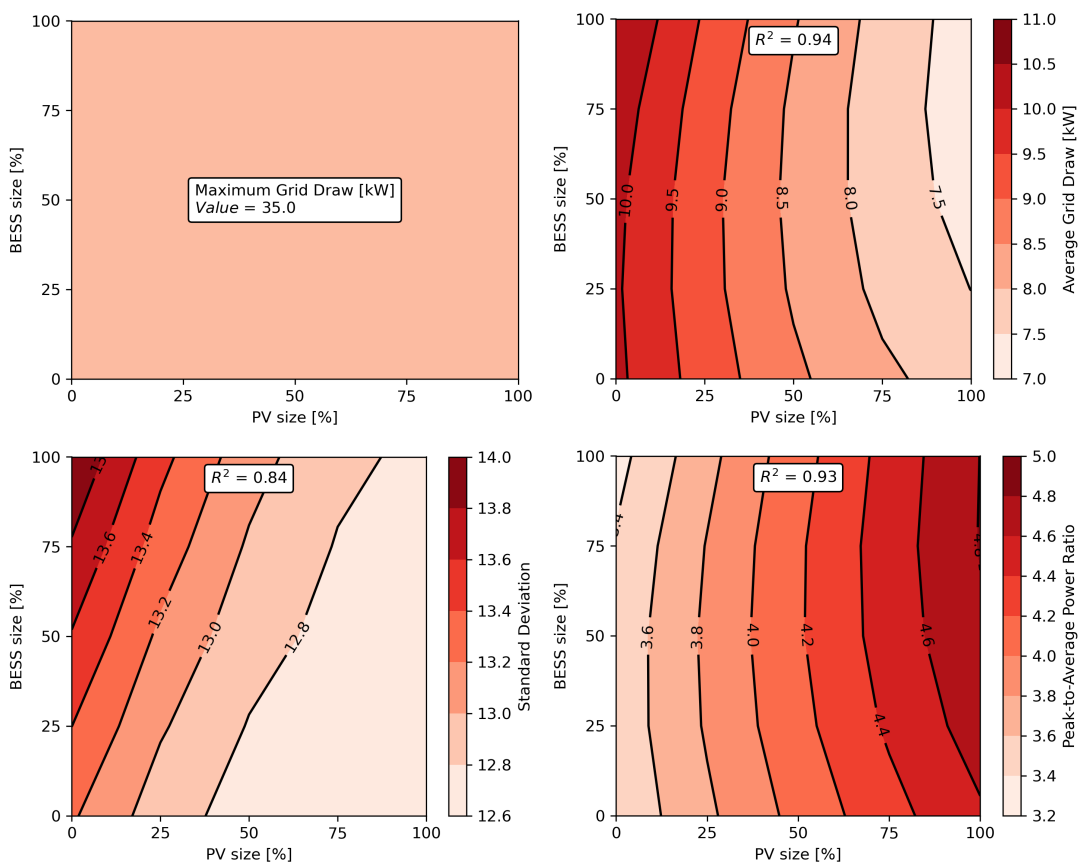


Figure 5.6: Direct Charging - Grid Draw sensitivity to variations in PV & BESS sizing

5.2.2.2 Rule-based Charging

While the example time series we inspected in the analysis of the optimization runs looked quite similar to the one obtained using direct charging, in Figure 5.7 we can see PV and BESS sizing have a stronger effect, with the exception of the maximum grid draw, which also peaks at the maximum allowable value of 35 kW. The average grid draw is lowered by about 1 kW, while the advantage of increasing both PV and BESS capacity is more pronounced. In contrast to the otherwise similar

direct charging strategy, the power limiting rules in this model seem to favor adding BESS capacity past 50 % sizing of the PV capacity, as far as the standard deviation is concerned.

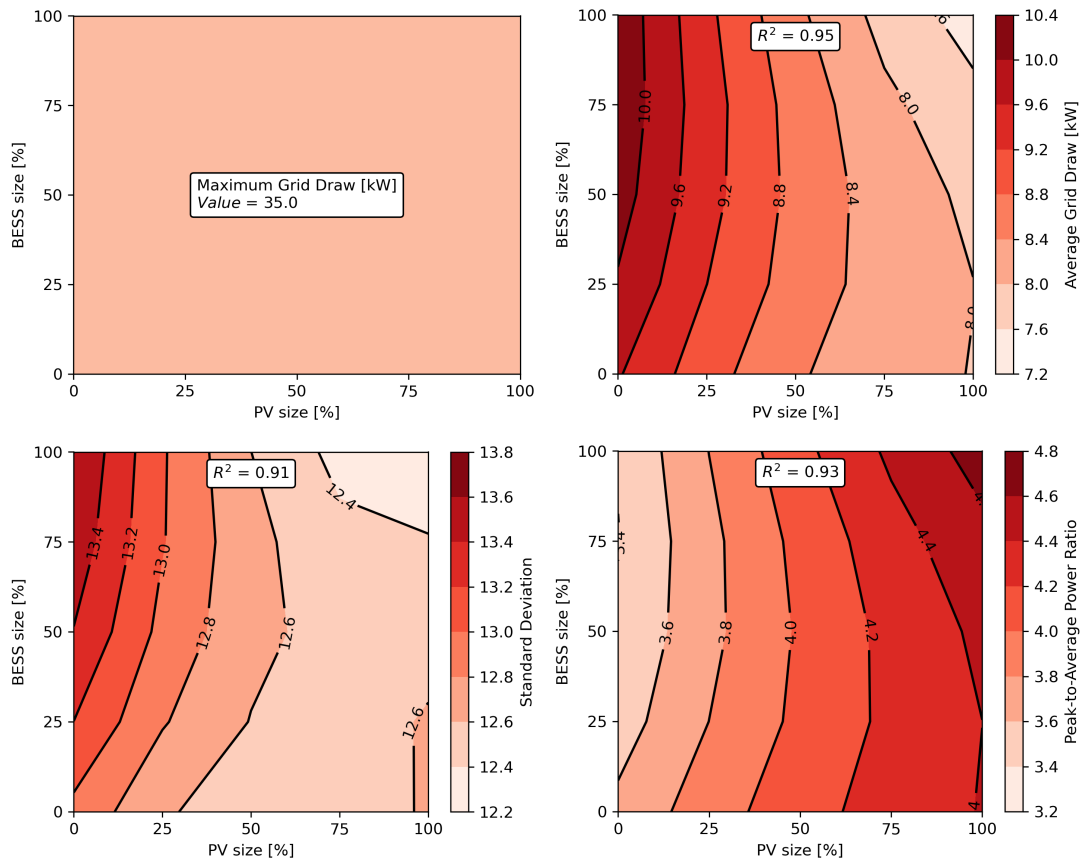


Figure 5.7: Rule-based Charging - Grid Draw sensitivity to variations in PV & BESS sizing

5.2.2.3 Predictive Charging

As we can see in Figure 5.8, the predictive charging strategy manages to lower the maximum power draw from the grid considerably, with an optimal value of less than 5 kW when both PV and BESS are maximized in capacity. As for the average grid draw, adding more PV has the strongest influence, lowering the average value from 7 to below 2 kW, while the BESS capacity only has a slightly positive effect. Looking at the standard deviation, we see an interesting non-linear relationship between PV and BESS, where the optimal values are those with maximum BESS capacity and either no or maximum PV, while the standard deviation is worst at 50 % PV capacity. The PAPR on the other hand, as we have seen in previous plots, gets worse as we add more PV, while adding more BESS capacity just narrows the spread of this metric.

5.2.2.4 Stochastic Charging

Gathering from Figure 5.9, we can see that results of the main metrics are quite similar to those we obtained using predictive charging. However, in this model we observe an overall lower standard deviation regarding grid draw, in addition to the non-linear relationship between PV and BESS capacity being even more pronounced around the 50 % PV capacity mark than in the previous model.

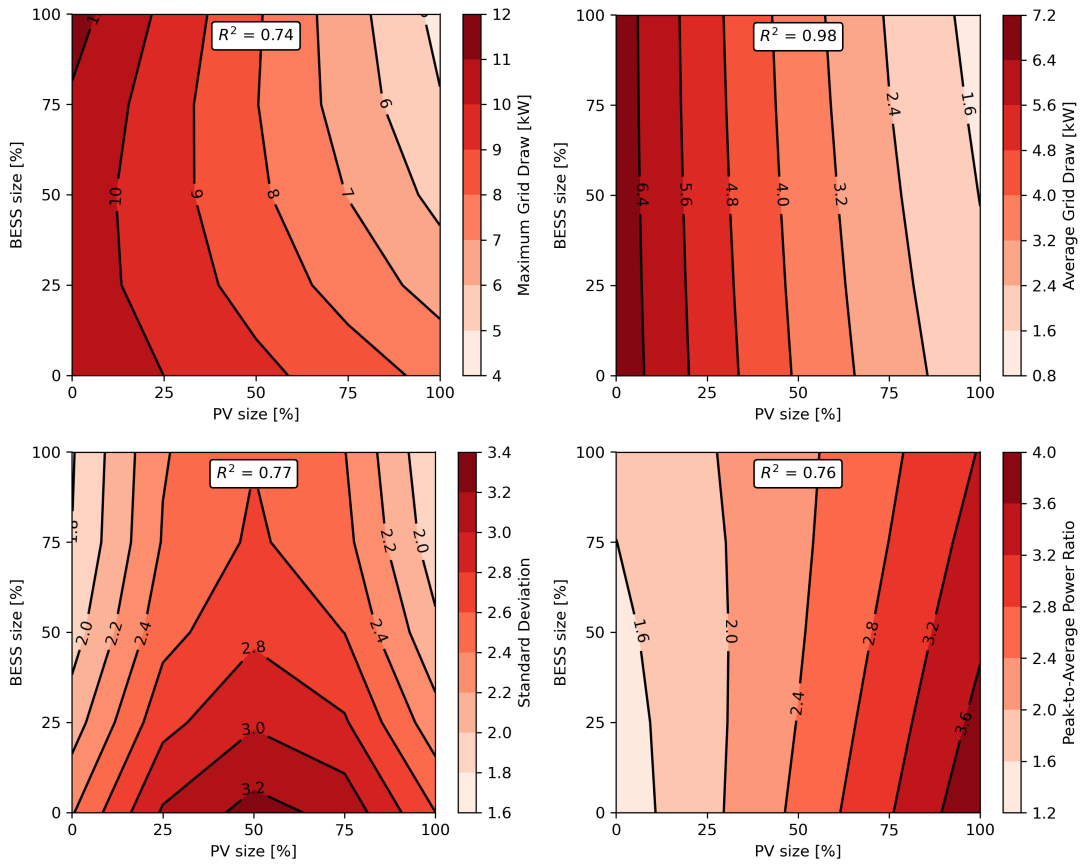


Figure 5.8: Predictive Charging - Grid Draw sensitivity to variations in PV & BESS sizing

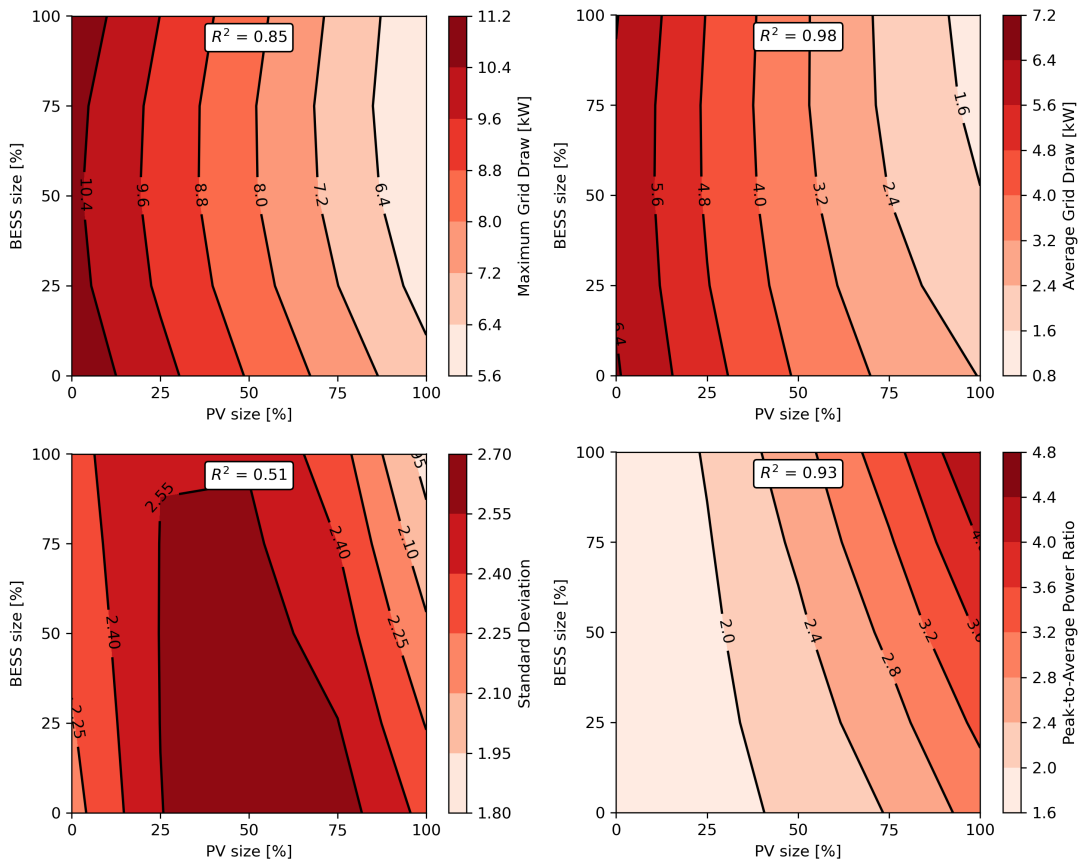


Figure 5.9: Stochastic Charging - Grid Draw sensitivity to variations in PV & BESS sizing

5.2.2.5 Perfect Information

As expected, we can see the theoretically optimal values in Figure 5.10, where the simulation was run using actual data instead of predictions or scenarios based on historic data. As such, it is no surprise that overall, we see the lowest maximum and average grid draw. The standard deviation is the lowest we have seen so far, albeit expanding the area of highest standard deviation to 25 % PV capacity. We also see an interesting new relation between PV and BESS in the PAGR metric, where finally adding more BESS capacity actually lowers the metric instead of increasing it like with the previous models.

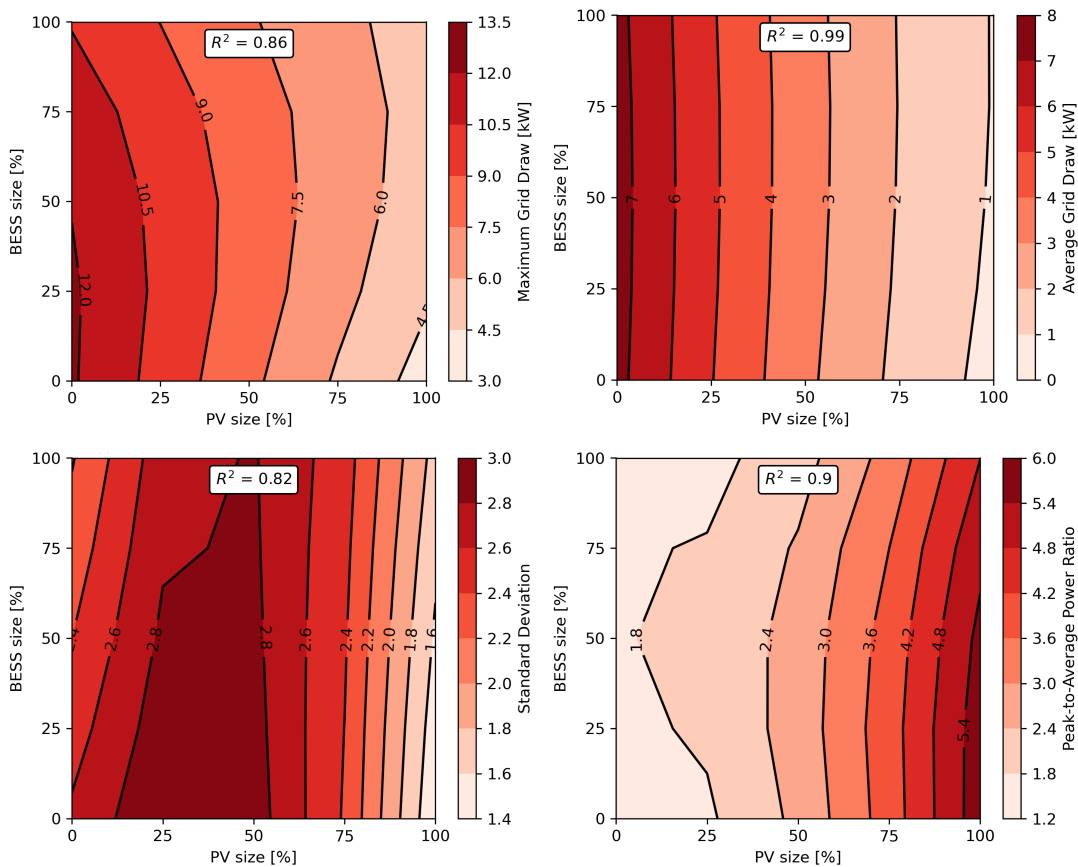


Figure 5.10: Perfect Information - Grid Draw sensitivity to variations in PV & BESS sizing

5.2.2.6 Summary

In essence, we could see that predictive and stochastic charging strategies greatly contribute to lowering the maximum power draw from the grid. In contrast to direct and rule-based charging, they also are the only ones that really benefit from adding BESS capacity to the system, while adding PV makes sense in most cases, given that some vehicles are loadable during the times of day when PV power is available.

Looking at Figure 5.11 leaves no doubt regarding the effectiveness of advanced optimization techniques when it comes to reducing grid draw. At the same time, it is remarkable, how close the predictive and stochastic charging strategies come to the theoretically optimal results obtained with perfect information.

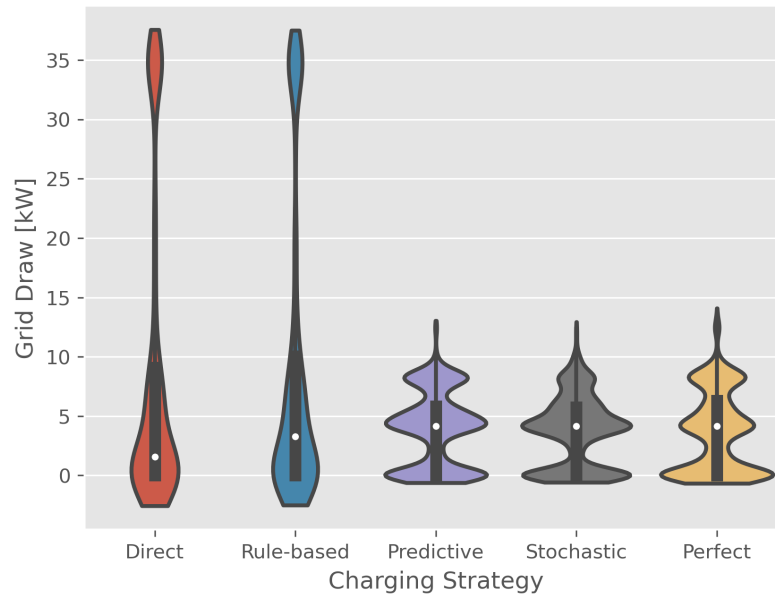


Figure 5.11: Peak shaving - Summary

5.2.3 Charging Comfort

5.2.3.1 Direct Charging

Considering that the direct charging strategy attempts to maximize the SOC of the electric vehicles at all times, it comes at little surprise that the satisfaction values all are well above 93 % (see Figure 5.12). For all practical purposes, PV and BESS sizing has little to no influence with this model.

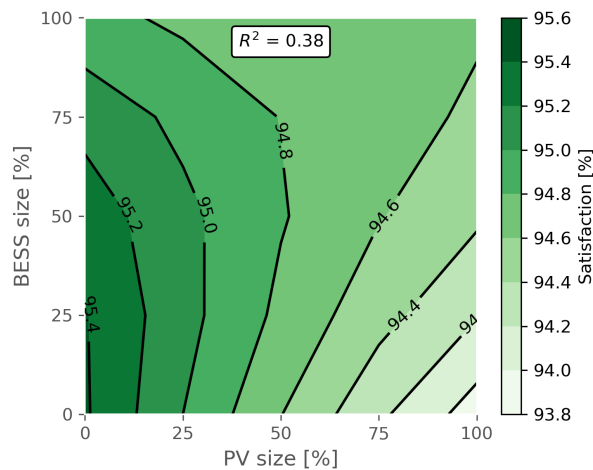


Figure 5.12: Direct Charging - Charging Comfort sensitivity to variations in PV & BESS sizing

5.2.3.2 Rule-based Charging

As can be seen in Figure 5.13, satisfaction values with the SOC of the electric vehicles are equally high as in the case of direct charging. While the lowest satisfaction value is found with 0 % PV and 100 % BESS capacity, it is still above 93 % and not far at all from the overall maximum of 95 %.

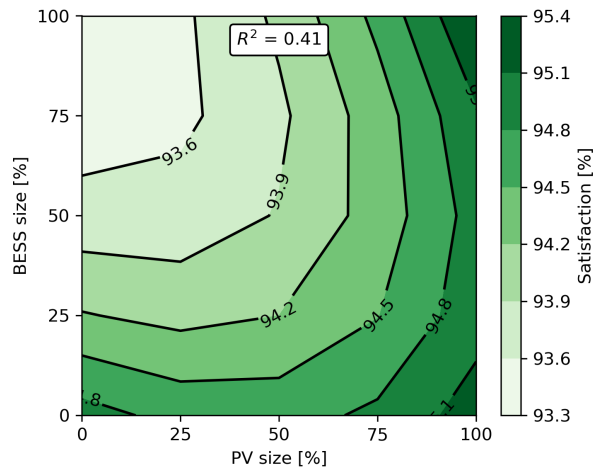


Figure 5.13: Rule-based Charging - Charging Comfort sensitivity to variations in PV & BESS sizing

5.2.3.3 Predictive Charging

In contrast to the previous two charging strategies, overall we observe somewhat lower satisfaction values with the predictive charging strategy (see Figure 5.14), ranging between 72 and 80 %, while there is a positive correlation between the satisfaction and higher PV and BESS capacity values. The overall lower satisfaction values can be explained by the conflicting goals of minimizing maximum grid draw and maximizing each vehicle's SOC at the time of departure. While we deem these satisfaction levels to be totally acceptable, changing the weights of the conflicting objectives in the objective function of the optimization model in favor of the vehicles' SOC might help in achieving higher values, albeit at the cost of potentially worsening the grid draw side of things.

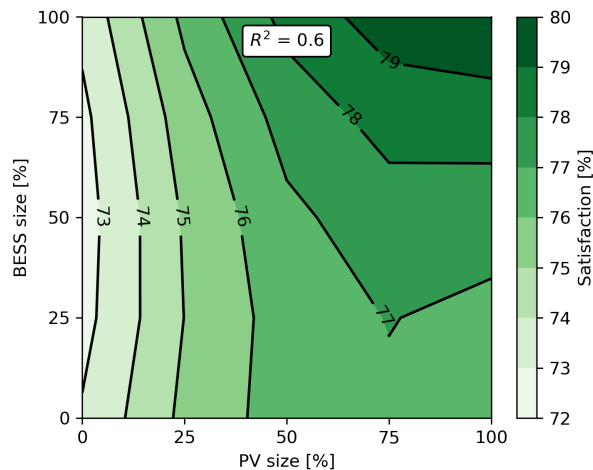


Figure 5.14: Predictive Charging - Charging Comfort sensitivity to variations in PV & BESS sizing

5.2.3.4 Stochastic Charging

Looking at Figure 5.15, we observe slightly lower satisfaction levels compared to the predictive charging strategy. While the BESS seems to have little influence on the result, the optimal values regarding charging comfort are obtained when the PV capacity is at 50 to 75 % of the defined maximum.

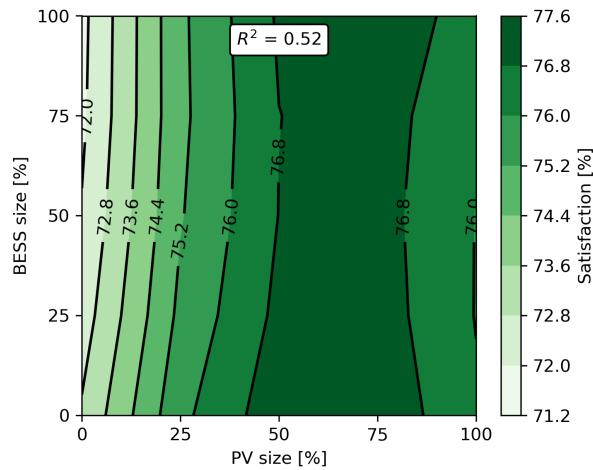


Figure 5.15: Stochastic Charging - Charging Comfort sensitivity to variations in PV & BESS sizing

5.2.3.5 Perfect Information

Using perfect information, we get satisfaction levels ranging between 80 and 88 % (see Figure 5.16) with the BESS capacity having a clearly positive influence on the result, while adding more PV capacity actually decreases satisfaction levels slightly. As with the predictive charging strategy model, the lower maximum satisfaction compared to the direct and rule-based models can be explained by the conflict in objectives, thus having to compromise on SOC somewhat in favor of peak shaving. Nonetheless, drivers will probably agree that 80 % is usually more than enough in most real world situations.

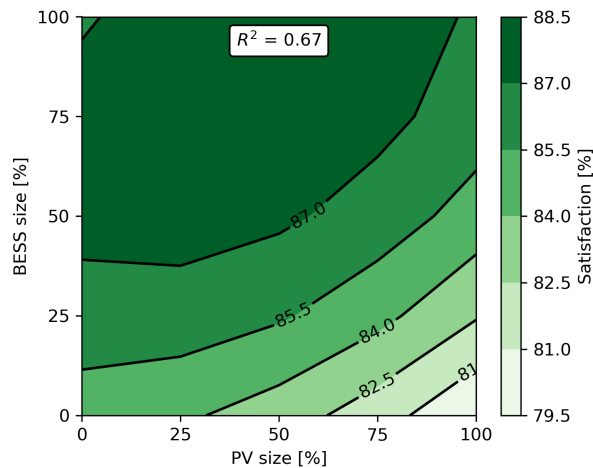


Figure 5.16: Perfect Information - Charging Comfort sensitivity to variations in PV & BESS sizing

5.2.3.6 Summary

As we have seen in the detailed discussion of the sensitivities, charging comfort using either of the charging strategies ranges well above 70 % in all cases. It was no surprise, that simple strategies that only focus on maximizing the vehicles' SOC will have higher satisfaction levels (see Figure 5.17), while the models having to strike a balance with the competing objective of minimizing maximum

grid draw are clearly at a disadvantage here. As pointed out earlier, this can be improved by adjusting the weights in the objective function accordingly (see Equation (3.33) and Equation (3.34)).

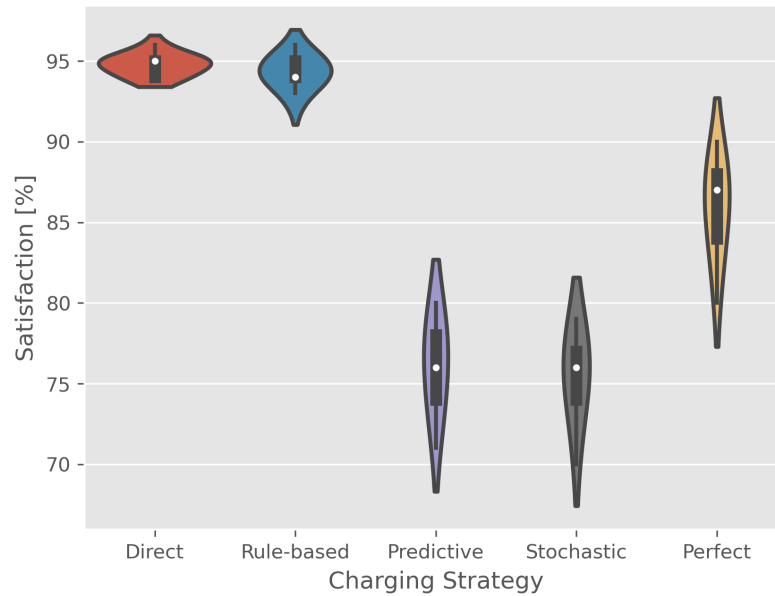


Figure 5.17: Charging Comfort - Summary

5.2.4 Computation Time

One of the goals of this thesis is to verify that implementing peak shaving DSM algorithms is actually feasible on comparatively low powered computing hardware all while using open source solvers like CBC instead of commercial offerings like Gurobi.

To do this, we ran our simulations on an Intel i7-6700 CPU (4 cores, 8 threads, 32 GB RAM) using Gurobi as a solver (see Figure 5.18) and repeated the process using CBC instead (see Figure 5.19). Finally, we ran the simulation on a low-end AMD Ryzen 3200U CPU (2 cores, 4 threads, 16 GB RAM) using CBC as a solver (see Figure 5.20) to find out whether any of the methods discussed previously were actually feasible on lower end hardware.

Inspecting Figure 5.18, we can see that the most optimization runs were complete on the i7 using Gurobi in less than 0.1 seconds on average and that like in the field test, the stochastic charging strategy generally took over an order of magnitude longer.

Figure 5.19 shows a similar picture, with the stochastic charging strategy taking much longer than any other, but we can also see that Gurobi is vastly superior to CBC when it comes to solving efficiency on identical problems and hardware.

Lastly, Figure 5.20 shows the computation times when using CBC on lower end hardware to execute the various charging strategies. Quite surprisingly, execution times did not increase despite using much slower hardware. Since all simulations were run on Windows systems, we suspect that this can at least partially be explained by the fact that CBC is by default compiled without support for multi threading on this platform, thus being unable to utilize the extra cores despite their availability.

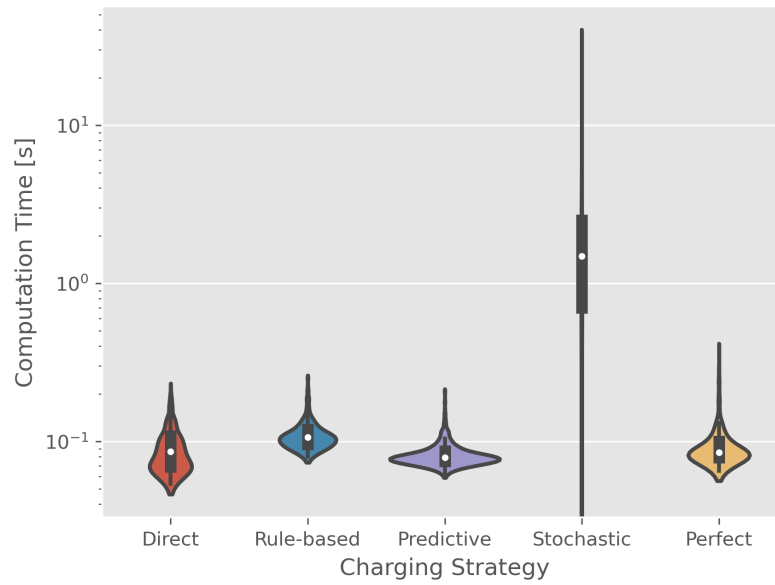


Figure 5.18: Computation Time - Gurobi Solver on Intel i7

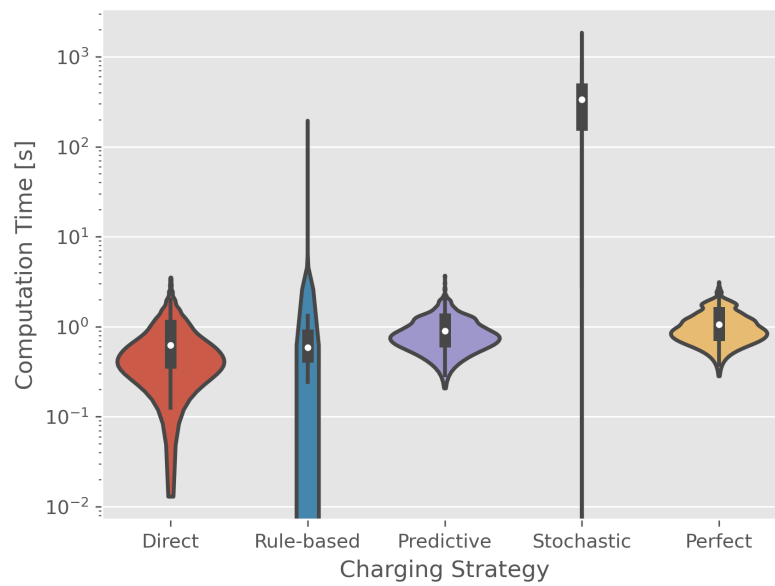


Figure 5.19: Computation Time - CBC Solver on Intel i7

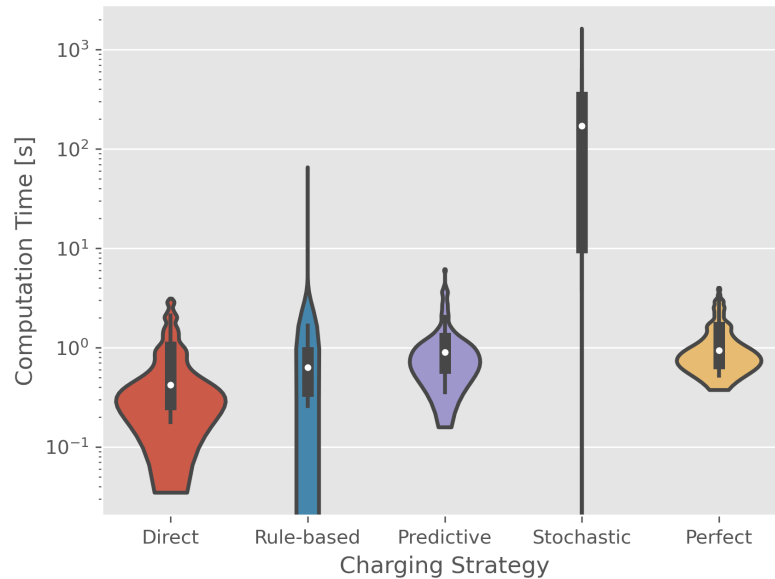


Figure 5.20: Computation Time - CBC Solver on AMD Ryzen 3 3200U

Looking at Table 5.4, with the exception of the stochastic charging strategy, it appears entirely feasible to run advanced optimization models even on modest hardware.

Metric CPU Strategy	mean			std			max		
	CBC on 3200U	CBC on i7	Gurobi on i7	CBC on 3200U	CBC on i7	Gurobi on i7	CBC on 3200U	CBC on i7	Gurobi on i7
Direct	0.782	0.803	0.094	0.716	0.560	0.031	2.982	3.425	0.225
Perfect	1.235	1.160	0.096	0.737	0.455	0.035	3.864	3.051	0.407
Predictive	1.211	0.987	0.084	0.984	0.418	0.017	5.982	3.623	0.210
Rule-based	1.404	1.078	0.112	6.465	8.005	0.026	63.909	192.697	0.255
Stochastic	229.478	319.005	1.775	281.612	219.651	1.912	1568.841	1803.512	39.710

Table 5.4: Computation Time per Strategy & Environment

5.2.5 Self-Sufficiency- & Self-Consumption-Rate

For the evaluation of the SSR and SCR, we consider the results of the simulations where a PV component was present only.

5.2.5.1 Direct Charging

As we already have seen in the analyses above, by design the direct charging strategy immediately draws maximum power to charge the non-fully charged electric vehicles, which in our case means that the biggest draw happens at times where PV power is not yet available and thus has to be drawn from the grid (see Figure 5.1), limiting the Self-sufficiency rate to a maximum of 44 % (see Figure 5.21). In general, adding more PV and BESS capacity will increase the SSR here. As for the Self-consumption rate, we observe that adding more PV power requires adding more BESS capacity in order to maintain the same SCR.

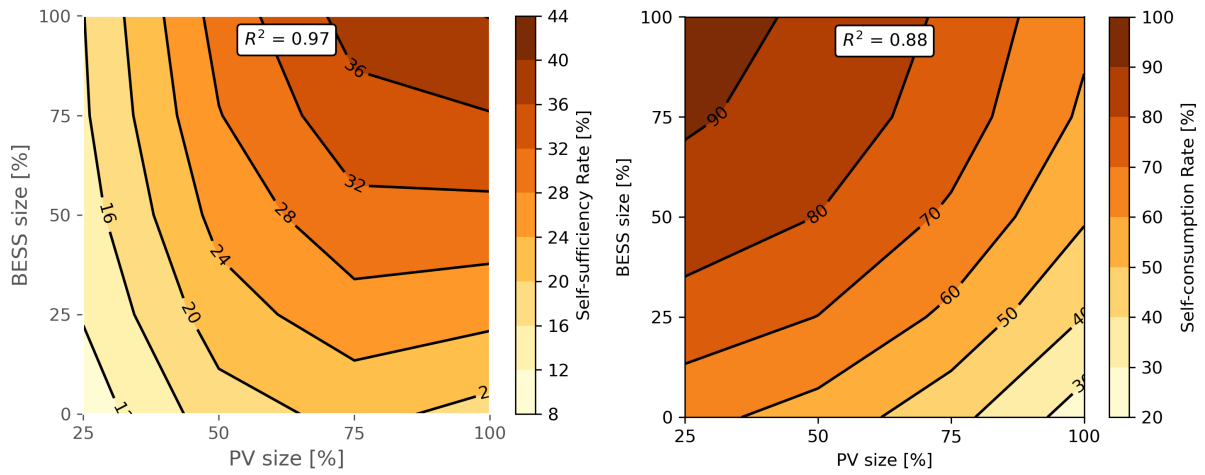


Figure 5.21: Direct Charging - SSR & SCR sensitivity to variations in PV & BESS sizing

5.2.5.2 Rule-based Charging

Similar to the analyses above, there is again little difference in the results of the rule-based charging strategy regarding SSR and SCR compared to the direct one (see Figure 5.22).

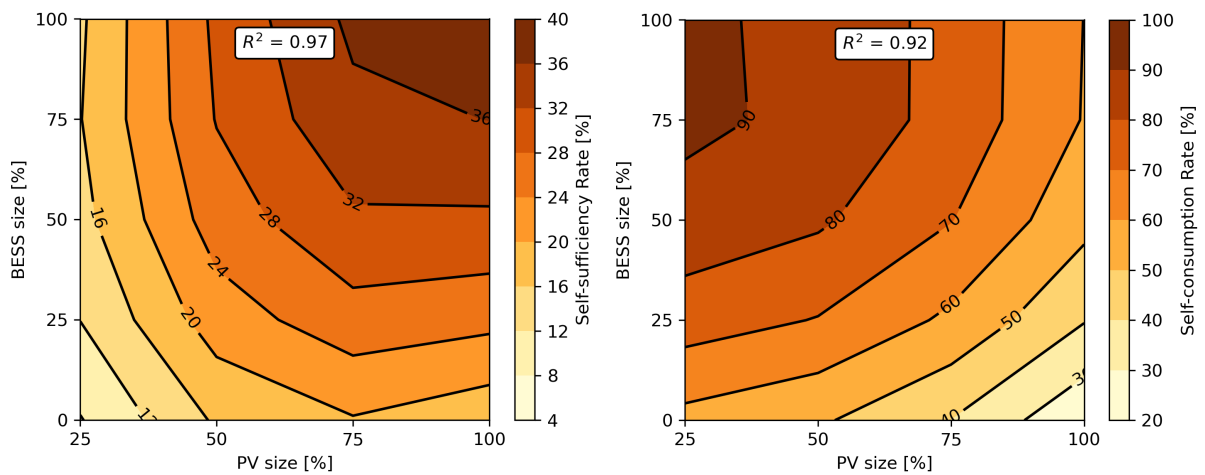


Figure 5.22: Rule-based Charging - SSR & SCR sensitivity to variations in PV & BESS sizing

5.2.5.3 Predictive Charging

Looking at Figure 5.23, we can clearly see a big difference to the previous two charging strategies. First of all, the maximum SSR now reaches 64 %. This is mostly due to model's objective of minimizing grid draw, thus directly increasing the value of the nominator in Equation (2.5). While overall the SSR increases with adding more PV power, the maximum value require upwards of 75 % BESS sizing. In the same vein, the predictive charging strategy yields the highest self-consumption rate provided with maximum PV and BESS capacities. However, even without a BESS, this charging strategy manages to use 75 % of PV energy by cleverly shifting the loading times of the electric vehicles alone.

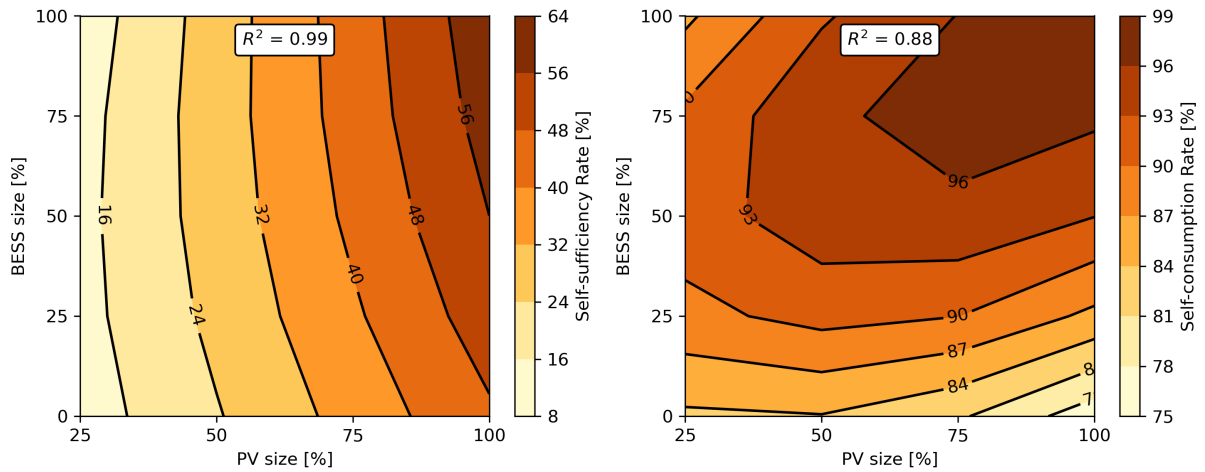


Figure 5.23: Predictive Charging - SSR & SCR sensitivity to variations in PV & BESS sizing

5.2.5.4 Stochastic Charging

Compared to predictive charging, the sizing of the BESS hardly seems to have any influence on the Self-sufficiency rate in case of the stochastic charging strategy (see Figure 5.24), while the range of achievable SSR values themselves are in the same range. In case of the SCR, on the other hand, we see an entirely different picture in that all values are between 96 and 100 %, more or less regardless of PV and BESS sizing.

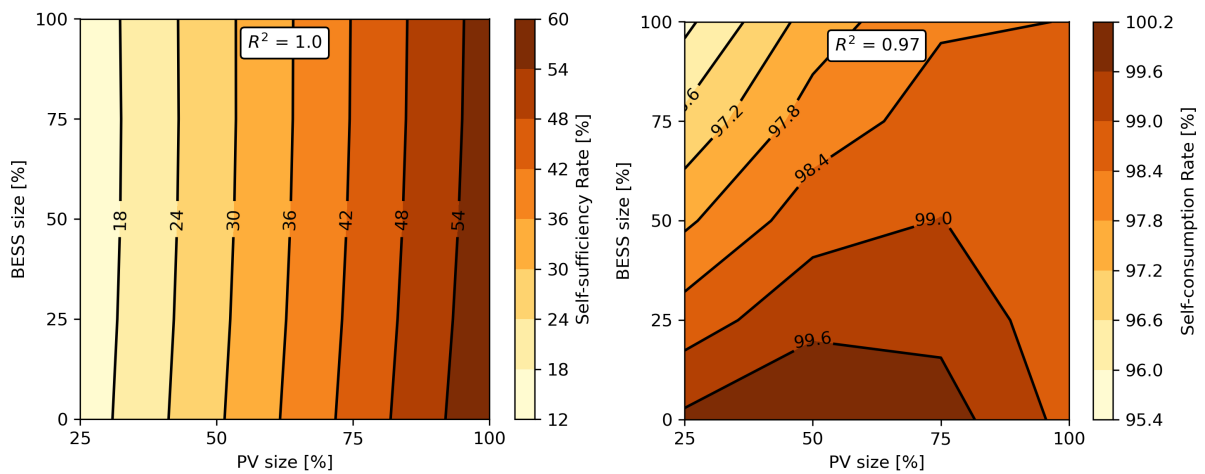


Figure 5.24: Stochastic Charging - SSR & SCR sensitivity to variations in PV & BESS sizing

5.2.5.5 Perfect Information

While in previous analyses, the results with perfect information were always rather similar to the ones obtained by the predictive charging strategy, we can see subtle differences in Figure 5.25. For starters, the SSR can be brought up to almost 90 % using perfect information, while the influence of the BESS sizing remains small for this metric. Having perfect information also seems to help achieving higher self-consumption rates, in our case ranging between 90 and 100 % as compared with the 75 % to 100 % we saw in the model using predicted data.

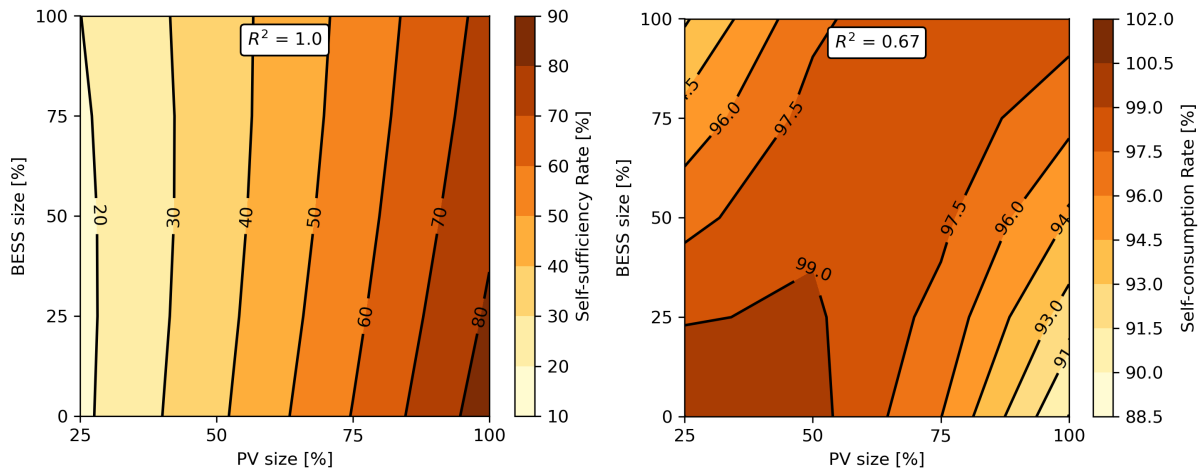


Figure 5.25: Perfect Information - SSR & SCR sensitivity to variations in PV & BESS sizing

5.3 Discussion

Our simulation studies explored the parameter space defined by PV size, BESS size and charging strategy for the metrics grid draw, charging comfort, computation time and SSR/SCR using 3000 optimization runs.

Looking at Table 5.5, we get the same vast improvement of the maximum grid draw when moving from the rule-based to the predictive charging strategy as we saw in the field test previously, thus hypothesis #1 stands confirmed also in the simulation studies. While certainly not perfect, even the most basic prediction based on simple averages of the historic data enables our linear and stochastic optimization models to improve the metrics considerably.

Configuration Strategy	LVG only	LVG + PV	LVG + BESS	LVG + PV + BESS
Direct	35.00	35.00	35.00	35.00
Rule-based	35.00	35.00	35.00	35.00
Predictive	12.42	8.14	12.42	4.14
Stochastic	12.35	7.33	11.62	5.14
Perfect	12.42	4.14	9.84	4.14

Table 5.5: Charging Strategies vs. Configurations - Maximum Grid Draw [kW]

This leads us to hypothesis #2, which states that more sophisticated optimization algorithms create higher added value, which in our case means lowering maximum and average grid draw as well as standard deviation and PAPR. As we can see in Table 5.5, the maximum values generally decrease with the sophistication of the charging strategy, usually having the lowest value in case of perfect information. The same is true for the average values (see Table 5.6), the standard deviation (see Table 5.7) and even the PAPR (see Table 5.8). While there are some minor outliers, the general direction holds true, thus confirming hypothesis #2.

Regarding hypothesis #3, stating that using additional data for predictions of load and PV production, we are a bit more skeptical, considering the data we have seen. On the one hand, having perfect

Configuration Strategy	LVG only	LVG + PV	LVG + BESS	LVG + PV + BESS
Direct	9.99	7.49	10.63	7.43
Rule-based	9.56	7.63	10.48	7.77
Predictive	6.94	1.83	6.69	1.41
Stochastic	6.38	2.37	6.61	1.05
Perfect	7.24	0.74	6.96	1.01

Table 5.6: Charging Strategies vs. Configurations - Average Grid Draw [kW]

information yields the best results for configuration and strategies, but not all. On the other hand, we see how well our predictive charging strategy performs using really simple aggregation of historic data. Overall, we feel that hypothesis #3 is confirmed, but at the same time we have serious doubts regarding diminishing marginal gains possible with additional data.

Configuration Strategy	LVG only	LVG + PV	LVG + BESS	LVG + PV + BESS
Direct	13.19	12.61	13.81	12.67
Rule-based	12.82	12.51	13.62	12.38
Predictive	2.18	2.35	2.02	1.88
Stochastic	2.34	2.66	2.03	1.89
Perfect	2.86	1.53	2.58	1.68

Table 5.7: Charging Strategies vs. Configurations - Standard Deviation [kW]

As for hypothesis #4, stating that peak shaving and charging comfort can be addressed in a single optimization model, we are glad to report that this hypothesis holds true as well. As we have seen in Figure 5.11 and Figure 5.17, the objective functions as formulated in Equation (3.33) and Equation (3.34) served their purpose of unifying the potentially diverging interests of peak shaving and charging comfort very well.

Configuration Strategy	LVG only	LVG + PV	LVG + BESS	LVG + PV + BESS
Direct	3.51	4.67	3.29	4.71
Rule-based	3.66	4.58	3.34	4.50
Predictive	1.79	4.46	1.86	2.93
Stochastic	1.94	3.09	1.76	4.91
Perfect	1.72	5.60	1.41	4.10

Table 5.8: Charging Strategies vs. Configurations - PAPR

Similar to our observations during the field test, the simulation studies have revealed that in general, advanced charging strategies can be successfully run on lower end hardware like single-board computers. Looking at the computation times needed in Table 5.4, however, hypothesis #5 can only be verified for reasonably compact problems like the predictive charging strategy and not for the obviously too overwhelmingly large problems resulting from a stochastic formulation.

In general, we saw that adding a BESS to an existing LVG only or LVG + PV configuration has positive effects. For configurations containing PV, we saw in Figure 5.23 that a BESS greatly helps

in leveraging the additional power for peak shaving as well as maximizing SSR and SCR alike.

Finally, we are able to evaluate the benefits of the deterministic and stochastic optimization approaches by calculating the VSS and EVPI metrics as described in Section §2.2. As we can gather from Table 5.9, there is a clear progression of added value (in our case decreasing values) moving from predictive to stochastic charging and finally having perfect information. However, considering the high computational effort combined with the comparatively low VSS value in our setting, we doubt that stochastic optimization will be adopted by the mainstream in these kinds of scenarios in the near future.

Strategy	Predictive	Stochastic	Perfect	VSS	EVPI
Grid Draw Maximum [kW]	10.28	9.48	6.99	0.8	2.49

Table 5.9: VSS & EVPI of Charging Strategies

6 Conclusion

In this thesis, an optimization framework for near-realtime demand-side management of battery-electric vehicle charging stations in residential complexes of Vorarlberg was developed using methods of linear and stochastic optimization techniques. With the basic concepts briefly explained in chapter 2, we proceeded to formulate an energy system model suitable to the problem at hand, including possible system configurations and charging strategies as summarized in chapter 3. A first verification of the outlined concepts was attempted in a field test, documented in chapter 4, yielding only partially satisfactory results due to operational issues during execution. To more deeply explore the effects of the system components in a setting of quality data, we proceeded to clarify the effects by performing a simulation study in chapter 5.

Judging by all the efforts to promote electromobility and phase out combustion engines within the next ten years, there is no doubt that demand-side management is going to have to be a key feature in any electric vehicle charging infrastructure going forward. This is especially true for the context we placed our thesis in, namely the residential complexes of Vorarlberg, where despite the broad availability of renewable energies neither the production capacities nor the power transmission capabilities are limitless. With that in mind, it is clear that making the most efficient use of the energy available in a decentralized fashion is going to be important.

As we have seen in both the field test as well as the simulation studies with little surprise, the traditional charging strategies we currently know (referred to as direct charging in this thesis) from public charging stations are entirely unsuitable for existing residential complexes, since on the one hand the power peaks of the combined charging load of multiple vehicles are a great burden for the power grid while on the other hand power still has to be divided among all vehicles, not yielding the maximum possible charging speeds anyway. While some manufacturers of wallboxes try to optimize this power distribution problem by allocating power dependent on the SOC of each individual vehicle (referred to as rule-based charging in this thesis), we saw in both the field test as well as the simulation studies that this only adds some amount of fairness among the individual vehicles, but does nothing to address the main problem of power consumption peaks.

An original contribution of this thesis is the empirical quantification of the effects of using advanced optimization algorithms on such kinds of systems, measured by key metrics as maximum grid draw, charging comfort and computation time as described in section §2.3. We employed deterministic and stochastic optimization techniques (referred to as predictive and stochastic charging in this thesis) to optimize the outlined energy system, reducing the maximum grid draw by over 64 and the standard deviation by over 80 % in the field test, thus answering the primary research question of this thesis as well as the first secondary one.

Moreover, both the field test as well as the simulation studies confirmed that it is entirely possible to peak-shave the load generated by electrical vehicle charging processes while maintaining high charging comfort on the part of the vehicles' drivers, with satisfaction levels typically well above 80 % in most configurations and scenarios. This was achieved by predicting the typical departure times of each vehicle and formulating the objective function such that the SOC at those times is maximized. By combining this objective with the minimization of the maximum grid draw through adjustable weights, we were able to answer the second secondary research question of this thesis as well.

When comparing the field test with the simulation studies, it became apparent that the importance of reliability and quality of the data being used can not be over-emphasized. Combined with the excellent results obtained by using simple predictions of driving profiles and PV production, we conclude that given a choice, emphasis should be put on obtaining good historic data rather than adding additional data sources. To be clear, more data is usually always better, but it fails to add value unless the essential data is not sound, which is the answer to the third of the secondary research questions.

Taking the deterministic optimization result from the discussion of the simulation studies as a baseline, we saw that the more sophisticated stochastic optimization only improved the result by 7.8 % in terms of the VSS, while at the same time increasing the computational effort by at least an order of magnitude, making this approach non-viable in the context of the intended usage scenario. Having perfect information would improve the obtainable result by another 26.3 % in terms of the EVPI. In answering the fourth of the secondary research questions, we see great potential in obtaining more data from the vehicles' drivers themselves, especially in terms of their typical coming home and departure times which could further close the gap in striving for perfect information.

In the simulation studies, we took the opportunity of exhaustively exploring the sensitivities regarding PV and BESS sizing on each of the metrics discussed in order to answer the fifth and final of our secondary research questions. Overall, we saw that while adding PV to a system already helps reduce maximum grid draw in some scenarios (like figure 5.8 for example), there can be no doubt that the addition of a BESS is needed to achieve optimal results, especially in the context of residential complexes which are unique in that the primary charging times are assumed to be over night where there is no PV production.

7 Outlook

With the advent of the European energy crisis in March 2022, it has become painfully obvious that the efforts to break the dependence from fossil energy sources need to be pursued with top priority going forward. While in Vorarlberg we are lucky to have a sizable amount of renewable energy sources available, the necessity of employing the latest in demand-side management methodology if we want to successfully manage the transition to electromobility is only slowly beginning to dawn on us.

We have become accustomed to being surrounded by technology that makes our lives more mobile and smart. The trend towards smarter devices has also found its way into our vehicles, electric or otherwise. Mandated by EU safety regulations, modern vehicles are equipped with a plethora of sensors that capture data about the vehicle itself as well as its whereabouts, the idea being that in case of emergency, vehicles are able to call for help autonomously using existing mobile cell infrastructure. With this data already being available in their (cloud) data centers, car manufacturers have proceeded to make it available to their customers also, so they can stay informed about the status of their vehicles using apps on their smartphones, for example. From a technological point of view, the communication between those apps and the vehicle itself is orchestrated using so-called APIs, which - after proper authentication and authorization - could also be used by other information systems such as a smart home controller.

At this point it is undeniably obvious that the equipment used in the field test, specifically the cumbersome and unreliable data acquisition devices, needs to be replaced and upgraded with something more adequate and up-to-date. Instead of relying on in-vehicle add-on devices, modern demand-side management of the charging process in a residential complex should tap into the new smart capabilities of current electric vehicles, immediately gaining access to all the data we have been struggling to reliably obtain in our field test. While there are attempts being made to make vehicle data available to enthusiasts' home automation systems (see Heck [65] and TA2k [66] for examples), to the best of our knowledge, there still are no commercial systems available to the mass market that would allow residential complexes to manage their charging efforts based on historical driving profiles while applying the predictive charging strategies outlined in this thesis.

It appears that local energy providers as well as grid operators should (and will) be heavily investing in systems such as this, since otherwise the market will be dominated by the solutions put forward by car manufacturers, hardly known for being overly concerned with peak-shaving, but rather charging vehicles in the shortest possible time.

References

- [1] Amt der Vorarlberger Landesregierung, "Elektromobilitätsstrategie Vorarlberg 2015-2020", Tech. Rep., 2015. [Online]. Available: <https://vorarlberg.at/at.gv.wien.vlbg.portal/documents/21336/122370/elektromobilitaetsstrategie1.pdf/a72130d2-01ac-4f3e-b482-6e1d624d2a81?version=1.0>.
- [2] Illwerke VKW AG, *Strom Business Basis*, 2022. [Online]. Available: <https://www.vkw.at/vkw-business-24-geschaeftskunden.htm> (visited on 01/05/2022).
- [3] M. RUF, "Analyse von Optimierungspotentialen von elektrischen Prosumer-Haushalten mit E-Auto Nutzung, stationärem Batteriespeicher und exogener PV-Erzeugungs- und Lastprofile", Master Thesis, FH Vorarlberg, 2020. [Online]. Available: <https://opus.fhv.at/frontdoor/deliver/index/docId/3651/file/Ruef.pdf>.
- [4] K. Papendick, U. Brennecke, J. Marquez, and B. Deml, "Nutzerverhalten beim Laden von Elektrofahrzeugen", *Forsch. und ...*, vol. 10, pp. 1–9, 2011. [Online]. Available: http://www.iaf-ag.ovgu.de/iniafag%7B%5C_%7Dmedia/Downloads/publikationen/Nutzerverhalten+beim+Laden+von+Elektrofahrzeugen.pdf.
- [5] S. Nojavan and K. Zare, Eds., *Demand Response Application in Smart Grids: Concepts and Planning Issue - Volume 1*. Cham: Springer International Publishing, 2020, ISBN: 978-3-030-31398-2. DOI: 10.1007/978-3-030-31399-9.
- [6] VDE Forum Netztechnik/Netzbetrieb, *VDE FNN Hinweis - Netzintegration Elektromobilität*, Berlin, 2019. [Online]. Available: <https://www.vde.com/resource/blob/1896388/8dc2a98adff3baa259dbe98ec2800bd4/netz-als-backbone-fnn-hinweis-e-mobilitaet-download-data.pdf>.
- [7] PowerDrive Europe, *Experteninterview – E-Mobilität: Die wichtigsten Fragen zum Aufbau eines Ladeparks*, 2021. [Online]. Available: <https://www.powertodrive.de/neuigkeiten/experteninterview/e-mobilitaet-die-wichtigsten-fragen-zum-aufbau-eines-ladeparks> (visited on 01/06/2022).
- [8] C. Grimme and J. Bossek, *Einführung in die Optimierung*. Wiesbaden: Springer Fachmedien Wiesbaden, 2018, ISBN: 978-3-658-21150-9. DOI: 10.1007/978-3-658-21151-6.
- [9] P. Kall and J. Mayer, *Stochastic Linear Programming* (International Series in Operations Research & Management Science). Boston, MA: Springer US, 2011, vol. 156, ISBN: 978-1-4419-7728-1. DOI: 10.1007/978-1-4419-7729-8.
- [10] W. Schellong, *Analyse und Optimierung von Energieverbundsystemen*. Berlin, Heidelberg: Springer Berlin Heidelberg, 2016, ISBN: 978-3-662-48527-9. DOI: 10.1007/978-3-662-49463-9.

- [11] U. M. Diwekar, *Introduction to Applied Optimization* (Springer Optimization and Its Applications), 3rd ed. Cham: Springer International Publishing, 2020, vol. 22, ISBN: 978-3-030-55403-3. DOI: 10.1007/978-3-030-55404-0.
- [12] J. Kallrath, *Gemischt-ganzzahlige Optimierung: Modellierung in der Praxis*, 2nd ed. Wiesbaden: Springer Fachmedien Wiesbaden, 2013, ISBN: 978-3-658-00689-1. DOI: 10.1007/978-3-658-00690-7.
- [13] K. Marti, *Optimization Under Stochastic Uncertainty* (International Series in Operations Research & Management Science). Cham: Springer International Publishing, 2020, vol. 296, ISBN: 978-3-030-55661-7. DOI: 10.1007/978-3-030-55662-4.
- [14] W. B. Powell, *Stochastic Optimization and Learning. A Unified Framework*, March 2019. Hoboken, New Jersey: Wiley-Interscience, 2019, ISBN: 3175723993.
- [15] P. Richardson, D. Flynn, and A. Keane, "Optimal Charging of Electric Vehicles in Low-Voltage Distribution Systems", *IEEE Trans. Power Syst.*, vol. 27, no. 1, pp. 268–279, Feb. 2012, ISSN: 0885-8950. DOI: 10.1109/TPWRS.2011.2158247.
- [16] W. E. Elamin and M. F. Shaaban, "New real-time demand-side management approach for energy management systems", *IET Smart Grid*, vol. 2, no. 2, pp. 183–191, 2019, ISSN: 25152947. DOI: 10.1049/iet-stg.2018.0033.
- [17] Z. Yang, K. Li, A. Foley, and C. Zhang, "Optimal Scheduling Methods to Integrate Plug-in Electric Vehicles with the Power System: A Review", *IFAC Proc. Vol.*, vol. 47, no. 3, 2014, ISSN: 1474-6670. DOI: 10.3182/20140824-6-ZA-1003.01804.
- [18] V. L. Nguyen, T. Tran-Quoc, S. Bacha, and B. Nguyen, "Charging strategies to minimize the peak load for an electric vehicle fleet", *IECON Proc. (Industrial Electron. Conf.)*, pp. 3522–3528, 2014. DOI: 10.1109/IECON.2014.7049022.
- [19] M. Amoasi Acquah, D. Kodaira, and S. Han, "Real-Time Demand Side Management Algorithm Using Stochastic Optimization", *Energies*, vol. 11, no. 5, p. 1166, May 2018, ISSN: 1996-1073. DOI: 10.3390/en11051166.
- [20] D. van der Meer, G. R. Chandra Mouli, G. Morales-Espana Mouli, L. R. Elizondo, and P. Bauer, "Energy Management System With PV Power Forecast to Optimally Charge EVs at the Workplace", *IEEE Trans. Ind. Informatics*, vol. 14, no. 1, pp. 311–320, Jan. 2018, ISSN: 1551-3203. DOI: 10.1109/TII.2016.2634624.
- [21] O. Sundstrom and C. Binding, "Planning electric-drive vehicle charging under constrained grid conditions", in *2010 Int. Conf. Power Syst. Technol.*, IEEE, Oct. 2010, pp. 1–6, ISBN: 978-1-4244-5938-4. DOI: 10.1109/POWERCON.2010.5666620.
- [22] F. Wu and R. Sioshansi, "A two-stage stochastic optimization model for scheduling electric vehicle charging loads to relieve distribution-system constraints", *Transp. Res. Part B Methodol.*, vol. 102, pp. 55–82, Aug. 2017, ISSN: 01912615. DOI: 10.1016/j.trb.2017.05.002.
- [23] L. Gong, W. Cao, K. Liu, and J. Zhao, "Optimal charging strategy for electric vehicles in residential charging station under dynamic spike pricing policy", *Sustain. Cities Soc.*, vol. 63, no. 2, p. 102474, Dec. 2020, ISSN: 22106707. DOI: 10.1016/j.scs.2020.102474.

- [24] R. Mehta, D. Srinivasan, A. M. Khambadkone, J. Yang, and A. Trivedi, "Smart Charging Strategies for Optimal Integration of Plug-In Electric Vehicles Within Existing Distribution System Infrastructure", *IEEE Trans. Smart Grid*, vol. 9, no. 1, pp. 299–312, Jan. 2018, ISSN: 1949-3053. DOI: 10.1109/TSG.2016.2550559.
- [25] G. Chrysanidis, D. Kosmanos, A. Argyriou, and L. Maglaras, "Stochastic Optimization of Electric Vehicle Charging Stations", in *2019 IEEE SmartWorld, Ubiquitous Intell. Comput. Adv. Trust. Comput. Scalable Comput. Commun. Cloud Big Data Comput. Internet People Smart City Innov.*, IEEE, Aug. 2019, pp. 1–7, ISBN: 978-1-7281-4034-6. DOI: 10.1109/SmartWorld-UIC-ATC-SCALCOM-IOP-SCI.2019.00046.
- [26] A. Arteconi, N. Hewitt, and F. Polonara, "State of the art of thermal storage for demand-side management", *Appl. Energy*, vol. 93, pp. 371–389, May 2012, ISSN: 0306-2619. DOI: 10.1016/j.apenergy.2011.12.045.
- [27] A. Shewale, A. Mokhade, N. Funde, and N. D. Bokde, "An Overview of Demand Response in Smart Grid and Optimization Techniques for Efficient Residential Appliance Scheduling Problem", *Energies*, vol. 13, no. 16, p. 4266, Aug. 2020, ISSN: 1996-1073. DOI: 10.3390/en13164266.
- [28] M. Cavazzuti, *Optimization Methods*. Berlin, Heidelberg: Springer Berlin Heidelberg, 2013, ISBN: 978-3-642-31186-4. DOI: 10.1007/978-3-642-31187-1.
- [29] J. R. Birge and F. Louveaux, *Introduction to Stochastic Programming* (Springer Series in Operations Research and Financial Engineering). New York, NY: Springer New York, 2011, p. 510, ISBN: 978-1-4614-0236-7. DOI: 10.1007/978-1-4614-0237-4.
- [30] B. Martin, B. Feron, E. De Jaeger, F. Glineur, and A. Monti, "Peak shaving: A planning alternative to reduce investment costs in distribution systems?", *Energy Syst.*, vol. 10, no. 4, pp. 871–887, Nov. 2019, ISSN: 1868-3967. DOI: 10.1007/s12667-018-0299-3.
- [31] Next Kraftwerke, *What does Peak shaving mean?*, 2022. [Online]. Available: <https://www.next-kraftwerke.com/knowledge/what-is-peak-shaving> (visited on 05/04/2022).
- [32] M. A. S. T. Ireshika, K. Rheinberger, R. Lliuyacc-Blas, M. L. Kolhe, M. PreiBinger, and P. Kepplinger, "Optimal power tracking for autonomous demand side management of electric vehicles", *J. Energy Storage*, vol. 52, no. May, Aug. 2022, ISSN: 2352152X. DOI: 10.1016/j.est.2022.104917.
- [33] P. Kepplinger, B. Fässler, G. Huber, M. A. S. T. Ireshika, K. Rheinberger, and M. PreiBinger, "Autonomes Demand Side Management verteilter Energiespeicher", *e i Elektrotechnik und Informationstechnik*, vol. 137, no. 1, pp. 52–58, Feb. 2020, ISSN: 0932-383X. DOI: 10.1007/s00502-019-00782-9.
- [34] R. Ahuja, "Minimax linear programming problem", *Oper. Res. Lett.*, vol. 4, no. 3, pp. 131–134, Oct. 1985, ISSN: 0167-6377. DOI: 10.1016/0167-6377(85)90017-3.
- [35] J. Bisschop, *AIMMS - Optimization Modeling*. Haarlem: AIMMS B.B., 2021. DOI: 10.2139/ssrn.1423288. [Online]. Available: https://manual.aimms.com/%7B%5C_%7Ddownloads/AIMMS%7B%5C_%7Dmodeling.pdf.
- [36] S. Rajakaruna, F. Shahnian, and A. Ghosh, Eds., *Plug In Electric Vehicles in Smart Grids - Charging Strategies*. Singapore: Springer Science+Business Media, 2015, vol. 89, ISBN: 978-981-287-316-3.

- [37] M. Markstaler, *Photovoltaik für Ingenieure - Theorie und Anwendung für dezentrale Energiesystemberechnung mit Python*. Norderstedt: Books on Demand, 2020, ISBN: 978-3-739-24715-1.
- [38] P. M. van de Ven, N. Hegde, L. Massoulié, and T. Salonidis, "Optimal Control of End-User Energy Storage", *IEEE Trans. Smart Grid*, vol. 4, no. 2, pp. 789–797, Jun. 2013, ISSN: 1949-3053. DOI: 10.1109/TSG.2012.2232943.
- [39] H. Song, C. Liu, M. Jalili, X. Yu, and P. McTaggart, "Multi-Objective Optimization of Electric Vehicle Charging Schedule with Time of Use Tariff", pp. 1–11, 2021. arXiv: 2108.05062. [Online]. Available: <http://arxiv.org/abs/2108.05062>.
- [40] B. V. Vishwas and A. Patel, *Hands-on Time Series Analysis with Python: From Basics to Bleeding Edge Techniques*. Berkeley: Apress, 2020, ISBN: 978-1-4842-5992-4. DOI: 10.1007/978-1-4842-5992-4.
- [41] F. Lazzeri, *Machine Learning for Time Series Forecasting with Python*. Indianapolis: John Wiley & Sons, 2021, ISBN: 978-1-119-68237-0.
- [42] J. Brownlee, *Deep Learning for Time Series Forecasting: Predict the Future with MLPs, CNNs and LSTMs in Python*, v1.4. Melbourne: Machine Learning Mastery, 2018. [Online]. Available: <https://machinelearningmastery.com/deep-learning-for-time-series-forecasting/>.
- [43] A. Shapiro and A. Philpott, "A tutorial on stochastic programming", 2007. [Online]. Available: https://www.researchgate.net/publication/228381968%7B%5C_%7DA%7B%5C_%7Dtutorial%7B%5C_%7Don%7B%5C_%7Dstochastic%7B%5C_%7Dprogramming.
- [44] D. B. Shmoys and C. Swamy, "An approximation scheme for stochastic linear programming and its application to stochastic integer programs", *J. ACM*, vol. 53, no. 6, pp. 978–1012, 2006, ISSN: 0004-5411. DOI: 10.1145/1217856.1217860.
- [45] M. Kaut, "Scenario generation by selection from historical data", *Comput. Manag. Sci.*, vol. 18, no. 3, pp. 411–429, Jul. 2021, ISSN: 1619-697X. DOI: 10.1007/s10287-021-00399-4.
- [46] Solax Power, *X3-Hybrid User Manual*, 2017. [Online]. Available: <https://www.solaxpower.com/wp-content/uploads/2017/10/X3-Hybrid-User-Manual.pdf> (visited on 05/03/2022).
- [47] KEBA AG, *KeContact P30 Charging Station Modbus TCP Programmiers Guid v1.03*, 2020. [Online]. Available: https://www.keba.com/download/x/dea7ae6b84/kecontactp30modbustcp%7B%5C_%7Dpgen.pdf (visited on 05/03/2022).
- [48] OpenVPN Inc., *OpenVPN*, Pleasanton, 2021. [Online]. Available: <https://openvpn.net/> (visited on 02/02/2021).
- [49] Evelix, *Evelix EX2 Connector (OBD2)*, 2022. [Online]. Available: <https://www.evelix.app/> (visited on 03/01/2022).
- [50] G. Van Rossum and F. L. Drake, *Python 3 Reference Manual*. Scotts Valley, CA: CreateSpace, 2009, ISBN: 978-1-4414-1269-0. DOI: 10.5555/1593511.
- [51] S. Mitchell, M. O'Sullivan, and I. Dunning, "PuLP: A Linear Programming Toolkit for Python", University of Auckland, Auckland, Tech. Rep. September, 2011. [Online]. Available: http://www.optimization-online.org/DB%7B%5C_%7DHTML/2011/09/3178.html.

- [52] COIN-OR Foundation, *PuLP: A Python library for modeling linear and integer programs*, 2021. [Online]. Available: <https://github.com/coin-or/PuLP> (visited on 09/26/2021).
- [53] Gurobi Optimization, *Yield Management*, 2020. [Online]. Available: https://gurobi.github.io/modeling-examples/yield%7B%5C_%7Dmanagement/yield%7B%5C_%7Dmanagement.html (visited on 11/29/2021).
- [54] COIN-OR Foundation, *CBC: An LP-based branch-and-cut library*, 2021. DOI: 10.5281/zenodo.3700700. [Online]. Available: <https://github.com/coin-or/Cbc> (visited on 09/26/2021).
- [55] S. Alam, L. Bălan, G. Comym, *et al.*, *Kedro*, 2022. [Online]. Available: <https://github.com/kedro-org/kedro>.
- [56] R. D. Hipp, *SQLite*, 2022. [Online]. Available: <https://www.sqlite.org> (visited on 05/04/2022).
- [57] OpenJS Foundation, *Node-RED*, 2022. [Online]. Available: <https://nodered.org>.
- [58] A. Ulmer, *Purple Controller*, 2022. [Online]. Available: <https://github.com/drdebian/purple-controller> (visited on 06/25/2022).
- [59] A. Ulmer, *Purple Analysis*, 2022. [Online]. Available: <https://github.com/drdebian/purple-analysis> (visited on 06/22/2022).
- [60] K. Rheinberger, *Demand Side Management data*, Dornbirn, 2020. [Online]. Available: <https://github.com/klaus-rheinberger/DSM-data> (visited on 07/12/2021).
- [61] K. Rheinberger and P. Kepplinger, *Special Issue: Demand Side Management of Distributed and Uncertain Flexibilities*, 2021. [Online]. Available: https://www.mdpi.com/journal/energies/special%7B%5C_%7Dissues/demand%7B%5C_%7Dside%7B%5C_%7Dmanagement%7B%5C_%7Ddistributed%7B%5C_%7Duncertain%7B%5C_%7Dflexibilities (visited on 07/12/2021).
- [62] J. Bergner and V. Quaschnig, “Kurzstudie: Sinnvolle Dimensionierung von Photovoltaikanlagen für Prosumer”, Hochschule für Technik und Wirtschaft Berlin, Berlin, Tech. Rep., 2019. [Online]. Available: <http://pvspeicher.htw-berlin.de>.
- [63] Y. Khawaja, D. Giaouris, H. Patsios, and M. Dahidah, “Optimal cost-based model for sizing grid-connected PV and battery energy system”, in *2017 IEEE Jordan Conf. Appl. Electr. Eng. Comput. Technol.*, vol. 2018-Janua, IEEE, Oct. 2017, pp. 1–6, ISBN: 978-1-5090-5969-0. DOI: 10.1109/AEECT.2017.8257779.
- [64] A. Ulmer, *DSM-Data Simulation*, 2022. [Online]. Available: <https://github.com/drdebian/dsmdata-simulation> (visited on 06/22/2022).
- [65] M. Heck, *Renault Zoe im Smarthome (neue API 2020)*, 2022. [Online]. Available: <https://michael-heck.net/index.php/elektromobilitaet/renault-zoe-im-smarthome-neue-api-2020> (visited on 03/01/2022).
- [66] TA2k, *Test Adapter VW Connect für VW, ID, Audi, Seat, Skoda*, 2022. [Online]. Available: <https://github.com/TA2k/ioBroker.vw-connect> (visited on 03/01/2022).

List of Abbreviations and Symbols

BESS Battery-electric Storage System

DCD Data Capturing Device

DSC Degree of Self-Consumption

DSM Demand-Side Management

DSS Degree of Self-Sufficiency

ESM Energy System Model

EV Electric Vehicle

LP Linear Programming

LRP Local Raspberry Pi

LVG Low-Voltage Grid

MILP Mixed Integer Linear Programming

PAPR Peak to Average Power Ratio

PAR Peak to Average Ratio

PV Photovoltaics

RFS Remote FHV Server

SCR Self-consumption Rate

SOC State of Charge

SSR Self-sufficiency Rate

WB Wallbox

List of Figures

2.1	Load shifting vs. Peak shaving	8
3.1	Energy System Model consisting of LVG, PV, BESS, EV & WB	11
3.2	Energy System Model consisting of LVG, PV, EV & WB	15
3.3	Energy System Model consisting of LVG, BESS, EV & WB	16
3.4	Energy System Model consisting of LVG, EV & WB	17
3.5	Charging power limit based on EV SOC	18
4.1	Inverter modes of operation	23
4.2	BESS installed at LiLa site	23
4.3	Wallboxes installed at LiLa site	24
4.4	Power cabinet installed at LiLa site	25
4.5	Evelix - End of Life	25
4.6	Planned LiLa system setup	26
4.7	Energy System Model - LiLa setup	26
4.8	Kedro Pipeline	30
4.9	SOC measurement problems	33
4.10	VPN tunnel problems	33
4.11	LRP downtime due to running out of storage	34
4.12	BESS not accepting charge despite PV power availability	34
4.13	Vehicle Departure Times	35
4.14	Charging & Driving Periods	36
4.15	Direct Charging - Solution Timeseries example from 2022-03-13 00:10:54	37
4.16	Rule-based Charging - Solution Timeseries example from 2022-03-20 00:10:23	38
4.17	Predictive Charging - Solution Timeseries example from 2022-03-27 00:10:26	39
4.18	Stochastic Charging - Solution Timeseries example from 2022-03-31 00:10:40	41
4.19	Grid Draw per Strategy	41
4.20	Charging Comfort per Vehicle	42
4.21	Charging Comfort per Strategy	43
4.22	Computation Time per Strategy	44
5.1	Direct Charging - Solution Timeseries example with 100 % PV & BESS	49
5.2	Rule-based Charging - Solution Timeseries example with 100 % PV & BESS	50
5.3	Predictive Charging - Solution Timeseries example with 100 % PV & BESS	51
5.4	Stochastic Charging - Solution Timeseries example with 100 % PV & BESS	52
5.5	Perfect Information - Solution Timeseries example with 100 % PV & BESS	53
5.6	Direct Charging - Grid Draw sensitivity to variations in PV & BESS sizing	54

5.7	Rule-based Charging - Grid Draw sensitivity to variations in PV & BESS sizing . . .	55
5.8	Predictive Charging - Grid Draw sensitivity to variations in PV & BESS sizing	56
5.9	Stochastic Charging - Grid Draw sensitivity to variations in PV & BESS sizing	56
5.10	Perfect Information - Grid Draw sensitivity to variations in PV & BESS sizing	57
5.11	Peak shaving - Summary	58
5.12	Direct Charging - Charging Comfort sensitivity to variations in PV & BESS sizing . .	58
5.13	Rule-based Charging - Charging Comfort sensitivity to variations in PV & BESS sizing	59
5.14	Predictive Charging - Charging Comfort sensitivity to variations in PV & BESS sizing	59
5.15	Stochastic Charging - Charging Comfort sensitivity to variations in PV & BESS sizing	60
5.16	Perfect Information - Charging Comfort sensitivity to variations in PV & BESS sizing	60
5.17	Charging Comfort - Summary	61
5.18	Computation Time - Gurobi Solver on Intel i7	62
5.19	Computation Time - CBC Solver on Intel i7	62
5.20	Computation Time - CBC Solver on AMD Ryzen 3 3200U	63
5.21	Direct Charging - SSR & SCR sensitivity to variations in PV & BESS sizing	64
5.22	Rule-based Charging - SSR & SCR sensitivity to variations in PV & BESS sizing . .	64
5.23	Predictive Charging - SSR & SCR sensitivity to variations in PV & BESS sizing . . .	65
5.24	Stochastic Charging - SSR & SCR sensitivity to variations in PV & BESS sizing . . .	65
5.25	Perfect Information - SSR & SCR sensitivity to variations in PV & BESS sizing . . .	66

List of Tables

3.1	Possible System Configurations Overview	10
3.2	Symbols and units used to describe the energy system model	14
4.1	Planned field test phases	22
4.2	Vehicles used in field test	25
4.3	Configuration values used in the field test	27
4.4	Grid Draw per Strategy	40
4.5	Charging Comfort per Strategy	43
4.6	Computation Time per Strategy	44
5.1	Combinations of base scenarios to be examined	47
5.2	Combinations of sensitivity scenarios to be examined	47
5.3	Configuration values used in the simulation studies	48
5.4	Computation Time per Strategy & Environment	63
5.5	Charging Strategies vs. Configurations - Maximum Grid Draw [kW]	66
5.6	Charging Strategies vs. Configurations - Average Grid Draw [kW]	67
5.7	Charging Strategies vs. Configurations - Standard Deviation [kW]	67
5.8	Charging Strategies vs. Configurations - PAPR	67
5.9	VSS & EVPI of Charging Strategies	68